Assessment of microglia influence in synaptic transmission and early amyloid-β plaque deposition in knock-in mouse models for Alzheimer`s disease

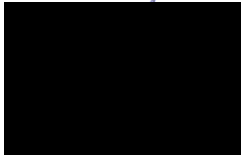**Diana Pamela Benitez Jimenez**

University College London

Thesis submitted for the degree of Doctor of Philosophy

June 2021

Declaration

I, Diana Pamela Benitez Jimenez confirm that the work presented in this thesis is my own. Where information has been derived from other sources, I confirm that this has been indicated in the thesis.

Diana P. Benitez

Acknowledgements

Firstly, I would like to thank Prof. Frances Edwards for providing me with the opportunity to work at her lab. I am extremely thankful for her support and guidance during the writing of this thesis.

My immense and endless gratitude goes to Dr Damian Cummings, without whom I really could not have been able to complete this project. The whole lab would not work without him. His support and brilliant scientific inputs were always helpful. Thank you Damian, for welcoming and helping me from my very first day at the lab until today; learning electrophysiology was challenging, but you were always there to answer all my questions.

I also want to thank Dr Dervis Salih, Prof. Alasdair Gibb and Prof. Kate Jeffery for not just supporting me academically but also personally, in particular at the beginning of my PhD. You always had the door open for discussing my PhD journey and made me believe I could do it, even when I could not believe in myself.

A huge amount of thanks goes to all my fellow lab mates. Especially, I was so lucky on meeting great female scientists: Carlijn, Chloe, Katie, Kari, Rui, Natalie, Mila and Tashu, it was always a pleasure to work with you in the lab and office every day. Katie, Kari and Carlijn: I know our friendships will continue beyond this PhD.

Thanks to Omar who has always been by my side in the worst and best moments of this PhD. Thank you for encouraging me every day and for being "my home" here in London. Meeting you at the beginning of this PhD was one of the best things that could have happened to me.

I dedicate this work to my family for their support throughout this experience. Everything I am and have is because of you. Thank you all for believing in me.

ABSTRACT

Alzheimer´s disease (AD) is the most common type of dementia representing an estimated 60-80% of all cases, and no cure or successful therapy has been found. Two main hallmarks have been identified in AD histopathology: senile plaques, composed of amyloid-β protein (Aβ), and neurofibrillary tangles, composed of phosphorylated TAU protein. Additionally, genetic studies have shown that immune processes play important roles in AD. Microglial gene expression and function are closely correlated to amyloid pathology and are therefore potential targets for altering the progression of AD. Recently an Amyloid Precursor Protein knock-in line was generated, which, in contrast to transgenic AD mice shows an Aβ pathology without overexpression. This project aims to analyse if microglial cells are active modulators of Aβ plaques and synaptic changes in APP knock-in mice at early stages of the pathology. Initial characterisation of electrophysiological phenotypes for APP^{NL-G-F} and APP^{NL-F} were studied. Also, dose- and time-dependent effects of the drug PLX5622, which has been shown to specifically deplete microglia, were analysed. APP^{NL-G-F} mice exhibited unaltered synaptic transmission at 3.5 months of age regardless a clear accumulation of hippocampal Aβ plaques. APP^{NL-F} mice showed increased glutamate release probability, unchanged spontaneous excitatory activity and little accumulation of Aβ plaques at 10 months of age. After PLX5622 treatments, surviving microglia tended to be $CD68^+$ in both APP knock-in models. Partial microglia ablation led to aged but not young wild type animals mimicking the increased glutamate release probability and exacerbated the APP knock-in phenotype. Complete ablation was less effective in altering synaptic function, while neither treatment altered plaque load. It is suggested that alteration of surviving microglia towards a phagocytic phenotype, rather than microglial loss, drives age dependent effects on glutamate release that become exacerbated in AD.

IMPACT STATEMENT

It is projected that by next year, 2022, about one million people in the UK will have developed dementia. Improvements in medicine in the past century have contributed to people living longer and healthier lives and as the world's population ages, the prevalence of dementia rise. Alzheimer's disease is the most common type of dementia and its increasing incidence, together with a current lack of treatments, makes this disease a public health priority. According to the World Health Organisation, dementia leads to increased costs for governments, communities and families which significantly impacts economic productivity. My research is directly contributing to the understanding of the mechanisms involved with the progression of the disease; such understanding could help to identify methods of early detection, test drug targets, develop therapies to alleviate the symptoms and ultimately save the lives of patients.

It is now widely accepted that immune system-mediated actions contribute to Alzheimer's disease pathogenesis. My project suggests that microglia is an important modulator of the brain's inflammatory response which is contributing to eventful cognitive decline. Selective modulation of the immune response through the elimination of microglia could be a promising therapeutic approach to delay the progression of neurodegeneration. This is the first study focused on comparing electrophysiological phenotypes of the APP knock-in mouse models at an early stage of the pathology, and also one of the first studies analysing microglia depletion in non-transgenic models. Novel insights arising from this thesis regarding the modelling of the disease and microglial manipulation are improving our conception of such devastating disorder.

The findings from the present study recently published as a journal paper in Molecular Neurodegeneration (Benitez et al., 2021); this will enable the research community to access and benefit from the results found. Additionally, this work has been disseminated through 8 poster/oral presentations and 3 training workshops; valuable scientific discussions arisen those events with

peers increased the communication of my results and gathered interest for research into APP knock-in models and microglia depletion approaches. I was actively involved in public engagement events to communicate the importance of my study, such as the Biology of Reproduction Research Unit seminars UNAM (2017, 2019, Mexico City), UCL Mexican Society Talk About (2018), Soap Box Science UK (2019) and the Faculty of Higher Studies Zaragoza Research Forum (2020). As a member of the Federation of European Neurosciences Society, I was selected to become a Social Media Ambassador for their biannual event (2020) to contribute to the dissemination of information through social media networks. Finally, thanks to one of those oral presentations I gave in my home country, Mexico, I gained interest from researchers at the Biology of Reproduction Unit (UNAM) to develop a project focused on microglia depletion and circadian rhythms using aged rats as models.

Table of Contents

List of figures

List of Tables

Chapter 1

INTRODUCTION

1.1 Alzheimer's disease

Dementia is defined as a chronic or progressive syndrome characterised by deterioration in memory, thinking and behaviour that causes an inability to perform everyday activities. Currently, there is an estimate of 50 million people with dementia worldwide and numbers still increasing due to the anticipated rise in life expectancy; by 2030 it is projected to reach 82 million people affected and 152 million by 2050 (World Health Organisation, 2020). The most common type form of dementia is Alzheimer´s disease (AD), a neurodegenerative disease that contributes with 60-80% of all dementia cases (Alzheimer`s Association Report, 2021); it affects about 50% of the population aged 75-84 years and up to 20% of people aged around 65. Given these numbers the World Health Organization (WHO) has recognized the complexity and impact of AD as a critical public health priority that demands urgent and severe focus in order to find effective treatments, earlier detection and diagnosis, as well as prevention methods and cures (Prince et al., 2016; WHO 2020).

AD is defined as the impossibility to remember new and old information, difficulty completing everyday tasks, confusions with time and place, misunderstanding of visual images and spatial relationships, poor judgment, depression and behaviour changes. Eventually, patients will develop complications with swallowing, speaking and walking (Jucker et al., 2006a ; Alzheimer`s Association Report, 2021). This disease was identified more than 100 years ago by Dr Alois Alzheimer in Germany. He described the first patient´s behaviour and mental degeneration until death. Additionally, he gave details of pathological abnormalities in the autopsied brain, like the presence of agglomerations of dense deposits outside the neurons, tangles within brain

cells and unusual ameboid glial cells (Blennow et al., 2006; Jucker et al., 2006a). AD has been intensely studied during the last decades and the field keeps gaining scientific interest considering that the precise pathogenesis process and progression mechanisms are still unknown

AD brain pathology is characterised by two main hallmarks: neuritic plaques and neurofibrillary tangles. Although these hallmarks were described more than a century ago, it was not until the mid-1980s that the proteins responsible for this pathology were found. The AD plaques are composed of extracellular accumulation of insoluble amyloid β-peptide (Aβ), a protein of mostly about 40 amino acids in length (Aβ$_{40}$, Aβ$_{42}$) (Masters et al., 1985), and tangles are formed from abnormally hyperphosphorylated Tau protein that affects proper intracellular assembly of microtubules in axons (Grundke-Iqbal et al., 1986). Both hallmarks are found in brain regions involved in learning and memory, such as the transentorhinal region, hippocampus, basal forebrain, amygdala and cortical areas (Braak et al., 1999; Mattson, 2004). In addition, neuroinflammation is also present in AD brains which can include reactive microglia and astrocytes. Eventually, neuronal populations degenerate, cerebral atrophy develops, and the brain is seen to have enlarged ventricles, prominent sulci and shrunken cortex (Blennow et al., 2006). All these cellular processes converge over time and are unnoticeable to the people affected until problems with memory manifest (**Figure 1.1**).
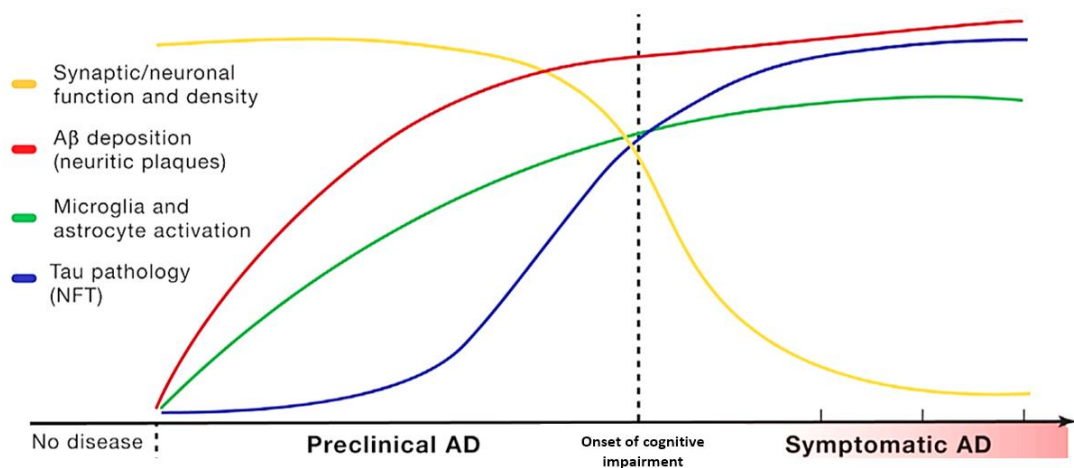
Figure 1.1 Timeline of major Alzheimer´s disease pathophysiological events in relation to clinical course. Aβ amyloidosis, tauopathy and neuroinflammation are the three essential phases leading to neurodegeneration and eventual onset of clinical AD (Long and Holtzman, 2019).

AD can be divided into two groups according to the age of onset: the most common type is defined as 'late-onset AD' (LOAD), which is later than 65 years, and only 1-5% of all AD cases are defined as 'early' (EOAD), which has an onset from 30-65 years. Genetically, AD is divided in familial (FAD) or sporadic (SAD), both types share the same phenotype, but it is suggested that they reach the clinical stage triggered by different processes (Piaceri et al., 2013; Dorszewska et al., 2016). FAD, which cover much of the EOAD cases, is linked to mutations in amyloid precursor protein (APP), presenilin 1 (PSEN1) and presenilin 2 (PSEN2) genes; SAD is more complicated and it is related to a mixture of genetic and environmental factors, the major gene associated to date is the Apolipoprotein E-ε4 (ApoE4) (Blennow et al., 2006; Ballard et al., 2011; De Strooper and Karran, 2016).

Over the last three decades, thanks to the knowledge of the main hallmarks of the disease and to the findings of the genes implicated, several hypotheses have been proposed to explain the cause for neurodegeneration in AD. Today, the amyloid cascade hypothesis proposed by Hardy and Selkoe is the most discussed and accepted in the field for describing the disease (Dorszewska et al., 2016). This hypothesis states that AD is a result of an imbalance in Aβ production and a failure in its clearance, this central event triggers an abnormal accumulation and oligomerisation of Aβ which evolve into plaques and synapses/neurons start being affected. In response to such abnormal changes in the brain environment, an inflammatory reaction is triggered by microglia and astrocytes. Eventually, tangle formation is displayed, synaptic functions are impaired, and finally, dementia is manifested (Hardy and Selkoe, 2002; Selkoe and Hardy, 2016). Relying on this hypothesis, it is suggested that the AD pathology begins at least 20 years before noticeable symptoms in patients and for this reason, AD research has been driven towards preventive treatments or therapeutics instead of a cure development (Sasaguri et al., 2017). Most of the AD drug therapies designed target Aβ pathways to reduce its production or remove it, and consequently, ameliorate AD symptoms; several pharmacological agents have reached phase 3 of clinical trials (Azeliragon, BAN2401, CAD106, Gantenerumab, Solanezumab), most of them are estimated to end by 2023 (Cummings et al.,

2020). Aducanumab was just approved by the U.S. Food and Drug Administration (FDA) and it is the first AD targeted therapy that moves further from phase 3.It is worth considering that, apart from Aducanumab, historically all trials have failed in the clinic until now, potentially because such trials have been performed on people who have already been diagnosed, and hence present tangles and neurodegeneration, or because they target only one mechanism, such as Aβ aggregation, which may not be sufficient to modify the progression of a multifactorial disease like AD.

1.2 Amyloid pathology and APP processing

The Amyloid Precursor Protein (APP) is an endogenous transmembrane protein with ~770 amino acids that comprises a long extracellular N-terminal domain and a shorter intracellular C-domain. Under physiological conditions, APP is mostly located at synapses and it is believed to contribute to neuronal differentiation, development, branching, synapse formation and synaptic transmission (Priller et al., 2006). It is produced in large amounts by neurons and is cleaved by α-secretase and γ-secretase. Normal physiological α-secretase enzymatic cleavage generates an N-terminal fragment sAPP$_α$, that is extracellularly released, and a C-terminal fragment C$_{83}$, that remains membrane-bound. Then C$_{83}$ is cleaved by γ-secretase to produce p3 (Aβ$_{17-40}$ and Aβ$_{17-42/43}$) and intracellular domain AICD that is released into the cytoplasm for degradation. This pathway is called the physiological or non-amyloidgenic pathway since no Aβ$_{40}$ or Aβ$_{42}$ is produced (Spies et al., 2012). On the other hand, the pathological or amyloidogenic pathway involves cleavage of APP by β-secretase that generates the sAPP$_β$ and C$_{99}$ fragments. C$_{99}$ is subsequently cleaved by γ-secretase to produce Aβ$_{40}$ or Aβ$_{42}$ and AICD (**Figure 1.2**) (Murphy and LeVine, 2010; Chasseigneaux and Allinquant, 2012). Aβ$_{42}$ is more prevalent than Aβ$_{40}$ in AD plaques as it is more fibrillogenic and hydrophobic, therefore more prone to aggregate (Zhang et al., 2010).

Knowledge about how Aβ led scientists to start manipulating the APP gene to evaluate how the abnormal progression of the peptide occurs until the deposition of amyloid plaques and eventually decipher which factors play

essential roles in that process. A variety of animal models with APP gene mutations have been generated to understand amyloid pathology development, and although no animal model that encapsulates all AD hallmarks is available, mouse models are currently the most manipulated and studied (Van Dam and De Deyn, 2011; Jankowsky and Zheng, 2017).
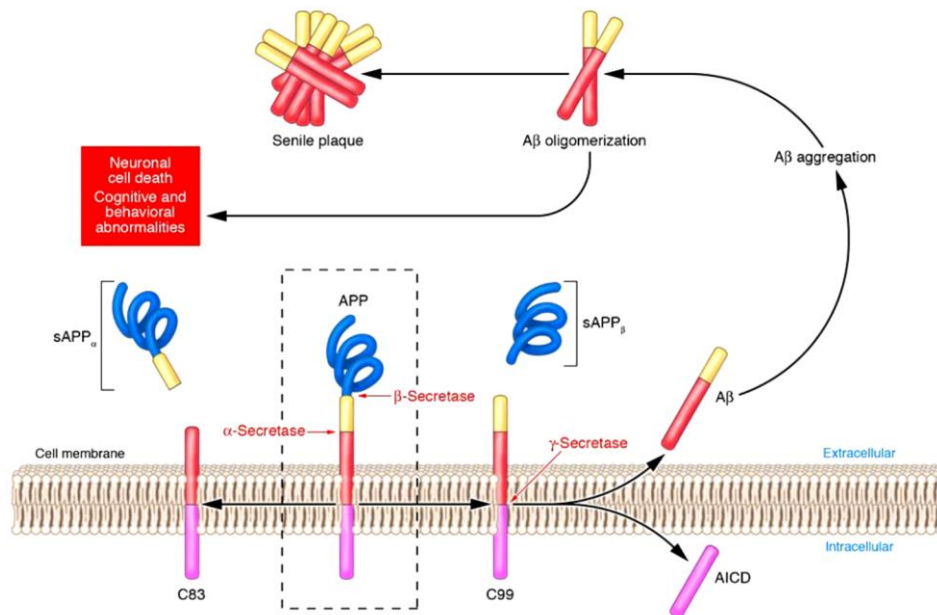
Figure 1.2 The non-amyloidogenic and amyloidogenic pathways of APP processing. Non-amyloidogenic cleavage by α-secretase generates sAPP$_\alpha$ and C83; γ-secretase generates AICD and p3 (not shown) (left). Amyloidogenic cleavage by β-secretase generates sAPP$_\beta$ and C$_{99}$; γ-secretase generates Aβ and abnormal AICD (Taken from Spies et al., 2012).

1.2.1 Mouse models

Genetic findings of AD led to the development of transgenic mice with similar pathology shown in patients. Current AD modelling studies have the primary purpose of finding a strategy to either block or delay the accelerated degeneration of this disease (Jucker et al., 2006b; Jankowsky and Zheng, 2017). The transgenic mouse models aim to recapitulate AD pathology through the overexpression of protein variants related to AD, such as APP, PSEN1, PSEN2, APOE and recently, TREM2. Targeting this disease is challenging due to the fact that mice do not develop neuronal degeneration, therefore scientists have mainly focused only on either amyloid or Tau

pathology, in some cases both. There are at least 204 models available for studying AD and 96 have a mutation in the APP gene that can cause FAD (Alzforum, 2020).

The *APP* gene is allocated on chromosome 21 and each mutation reported is associated with a different condition related to the aggregation of the Aβ peptide. The first mutation described was by Goate et al. who showed that the substitution of a base in the APP gene position 717 (Val→Ile; Val→Gly) led to an increased pathological $Aβ_{42}/Aβ_{40}$ ratio (Chartier-Harlin et al., 1991; Goate et al., 1991), Since then, several mutations linked to FAD were found and based on that, more mouse models started being designed. The now extinct NSE-APP751 model was the first transgenic mouse produced by expressing wild type human APP751 isoform under the control of the rat neural-specific enolase (NSE) promoter (Alzforum, 2020); Aβ extracellular deposits were mainly present in the hippocampus and cortex (Quon et al., 1991). The Swedish K670N/M671L double mutation at the β-secretase cleavage site results in increased BACE cleavage and consequent increased Aβ production. The London (V717I), Indiana (V717F) and other mutations at the γ- secretase site tend to produce more toxic $Aβ_{42}$. Other *APP* mutations within Aβ, increase fibrillogenesis such as the Dutch (E693Q) and Arctic (E693G) mutations (Hall and Roberson, 2012). In general, all the lines available have strengths and limitations, but the most relevant complication is that all the transgenic mice overexpress APP. This results in overproduction of APP fragments additional to the Aβ aggregation seen in humans. This condition can trigger secondary abnormal phenotypes incomparable with AD which makes results difficult to interpret (Jankowsky and Zheng, 2017; Sasaguri et al., 2017).

To avoid overexpression of APP, in 2014 it was generated a new approach of a mouse model with an APP knock-in strategy that developed amyloid pathology. These mice presented minor behavioural changes and an endogenous APP promoter-driven gene expression. This novel model improved the amyloid pathology by increasing mainly $Aβ_{42}$ levels without affecting other APP products, which makes them more similar to what is seen in AD patients. The murine Aβ sequence was humanised by changing three

amino acids that are different from human (G601R, F696Y and R609H), and three mouse lines were generated by inserting FAD mutations in that APP sequence (Nilsson et al., 2014; Saito et al., 2014; Sasaguri et al., 2017).

This new generation of models harbour one, two or three mutations in the APP gene. One of the lines developed is a model referred as APP^{NL-F}, which uses the Swedish (KM670/671<u>NL</u>) and Beyreuther/Iberian (I716<u>F</u>) modifications. The former triggers an increase in the total amount of Aβ_{40} and Aβ_{42}, the latter one enhances the ratio of Aβ_{42} to Aβ_{40}. These effects are age-progressive and, according to the authors, Aβ plaques are initially seen at 6-9 months (Nilsson et al., 2014; Saito et al., 2014). The same team developed another mouse line with the addition of the Arctic or G mutation (E694<u>G</u>), called APP^{NL-G-F}, located in the middle of the Aβ sequence (**Figure 1.3**). This modification makes Aβ more predisposed to oligomerisation, fibrillisation and therefore actively promotes the formation of plaques (Cheng et al., 2004; Saito et al., 2014). Amyloidosis is faster and more aggressive (starting at 2 months, and evident deposition by 4 months old) than what APP^{NL-F} mice show (Saito et al., 2014; Latif-Hernandez et al., 2017).
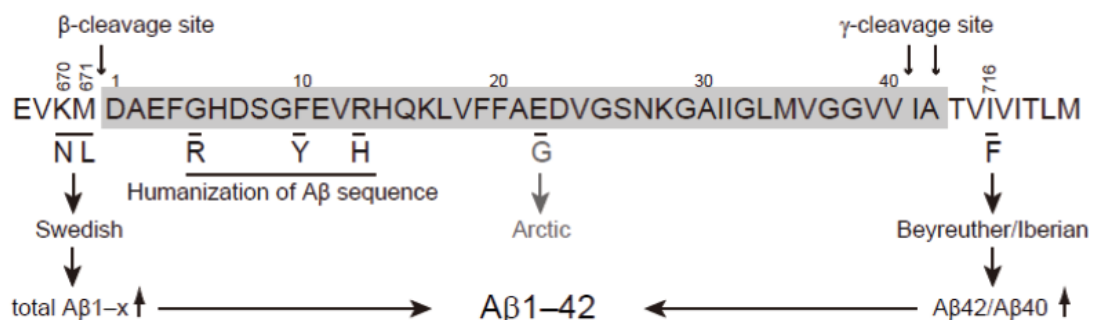
Figure 1.3 APPKI humanization and mutations design. The Swedish (NL) mutation increases β site cleavage of APP and in turn Aβ_{40} and Aβ_{42} rise; the Beyreuther/Iberian mutation rises Aβ_{42}/Aβ_{40} ratio by augmentation of γ-cleavage at the C-terminal position 42. Besides, the Arctic mutation located in the middle of the Aβ sequence gives the APP^{NL-G-F} model with strong amyloidosis as Aβ fibrils become predisposed to oligomerisation (Nilsson et al., 2014).

The remarkably early pathology of APP^{NL-G-F} triggers different behavioural changes such as anxiolytic-like behaviour by 3 months of age, which worsens by 6 months (Latif-Hernandez et al., 2017; Sakakibara et al., 2018); learning

(spatial, reversal and associative) and memory impairments (Latif-Hernandez et al., 2017; Sakakibara et al., 2018; Mehla et al., 2019) accompanied with locomotor/exploratory activity deficits by 6 months of age (Whyte et al., 2018); and finally, impaired motivation is absent (Hamaguchi et al., 2019), but compulsivity and impulsivity are reported at 9 month-old mice. It has been proposed that this cognitive decline is due to the rapid and massive early Aβ accumulation (Masuda et al., 2016). Even if Aβ plaques are reported to be present by 2 months of age, it is not until 4 months later that microgliosis and astrocytosis are robust in cortical areas (Saito et al., 2014; Masuda et al., 2016; Mehla et al., 2019). In addition, it has been proposed that the presynaptic terminals are the earliest and most vulnerable cellular compartments affected in AD; Hark et al. (2021) very recently showed that presynaptic proteins in the APP^{NL-G-F} are significantly changed very early during Aβ pathology and by 6 months of age, when Aβ plaques are evident, steady-state levels trend to come back to physiological levels before eventual decrease associated with neuronal degeneration.

On the other hand, the APP^{NL-F} amyloidopathy takes longer to explicitly develop; by either using 3D visualization of the entire hemispheres or by immunofluorescent staining, Aβ immunolabeled plaques are mostly located in the cerebral cortex at 9 months of age and then around 12 months in the hippocampus (Hama et al., 2015; Sos et al., 2020; Hark et al., 2021). A recently published proteomics study showed upregulation and downregulation of several proteins associated with Aβ clearance, inflammatory-immune response, transport, mitochondrial metabolism and glial cell proliferation just when plaques are starting to be deposited in the APP^{NL-F}, at 8 months of age (Aladeokin et al., 2019). Interestingly, another very new proteomics publication showed also changes in expression of proteins related to synaptic transmission and plasticity in the hippocampus and cortex at 3 months of age, which is around 6 months before the deposition of plaques in the APP^{NL-F} mice. This publication described early high levels of soluble Aβ$_{42}$ which in turn could induce effects in synaptic signalling and protein degradation (Schedin-Weiss et al., 2020). These early synaptic proteins changes are supported by Zhang et al. (2015) who found a significant reduction in mushroom spines at 3 months

of age also in hippocampus, however total spine density remained unaltered. As formation of plaques rises in this APP^{NL-F} line, the microglial reactivity, but not astrocytes, also starts in the lateral entorhinal cortex at 10-18 months of age. Neurodegeneration in the hippocampus and neocortex is proposed to appear at 9-13 months as there is a reduction in the expression of calcium/calmodulin-dependent protein kinase II (CamKII). Interestingly, entorhinal cortex cells have an hyperactive behaviour at an early age, 4-6 months old, when Aβ plaques or microgliosis are not quite present yet, which could potentially explain the neuronal loss due to excitotoxicity and the lack of CamKII seen at a slightly older age (Petrache et al., 2019). Cognitive decline and memory impairments are not detectable in young or young-adult APP^{NL-F} (<19 months old) (Sos et al., 2020).

1.2.2 Early Aβ pathology affects synaptic transmission

Neuronal network and cellular changes are estimated to start 20-30 years before AD onset. There is a preclinical phase, thought to be the transition of an early reversible stage which evolves to a chronic and irreversible autonomous cellular stage and is therefore this a window of time that is critical in the disease progression and could be targeted for developing of treatments or therapy (Blennow et al., 2012; De Strooper and Karran, 2016) (**Figure 1.1**). It has been extensively reported in humans that neuronal dysfunction and alterations in synaptic transmission occur before the pathological accumulation of Aβ (Landau et al., 2018; Toniolo et al., 2020); for instance, by using functional magnetic resonance imaging (fMRI) on cognitively-intact PSEN1 carriers and in MCI patients, an increased functional hippocampal activity was found (Quiroz et al., 2010). Such hyperactivity was positively correlated with mild atrophy in the anterior parts of the hippocampus (Hamalainen et al., 2007) and with poorer memory trajectories but not with executive functions (Braskie et al., 2013). All this evidence suggests that Aβ is associated with neuronal hyperexcitability in very early AD although it has been also hypothesised that Tau causes hypoactivation later in the disease due to a decrease in excitation and neuronal damage (Toniolo et al., 2020).

The hippocampus is one of the first regions to be affected in ageing and AD due to the neuronal network damage which triggers neuroplasticity impairments (Braak et al., 1999; Bird and Burgess, 2008) and it is essential for the formation of new memories and storage (Neves et al., 2008). It is a region in the brain with a clear layered cytoarchitecture where cell bodies lie in clear cell bands and dendrites make contacts with fibres from a known origin. These characteristics make the hippocampus unique; it is composed by three connecting pathways that allow neuronal processes to flow in from the entorhinal cortex (EC) through the pathways and out to either the subiculum or the fimbria. This well-known excitatory trisynaptic loop is exclusively unidirectional with a highly organised distribution of neuronal inputs which is composed by the medial and lateral perforant, the mossy fibres and the Schaffer collateral (SC) pathways (**Figure 1.4**). The circuit begins in the EC, from cortical layer II the dentate gyrus (DG); perforant path axons make excitatory synaptic contact with the dendrites of the granule cells; axons from the lateral and medial EC innervate the outer and middle third of the dendritic tree. Granule cells project, through the mossy fibres pathway, to the proximal apical dendrites of CA3 pyramidal cells, which, consequently, project to ipsilateral CA1 pyramidal cells through SC and to contralateral CA3 and CA1 pyramidal cells through commissural connections (Neves et al., 2008; Van Hoeymissen et al., 2020).

To study the synaptic basis of hippocampal learning and memory, the physiological phenomenon called *long-termp potentiation* (LTP) first identified by Bliss and Lomo in 1973, is broadly investigated in AD animal studies to model synaptic plasticity. Induction of LTP is commonly achieved experimentally by brief trains of high-frequency stimulation (HFS) which leads to a long-lasting abrupt increase in the strength of synaptic transmission (Nicoll, 2017). It is based on the cooperativity and input-specificity of the connections in the hippocampus which shows the relation between the synaptic response and the firing of postsynaptic neurons (Bliss and Collingridge, 1993). Deficits in basal synaptic transmission and/or in LTP have been shown in AD models not only when Aβ pathology has developed, but

also at an early stage, when Aβ levels rising are just detected (Mango et al., 2019).
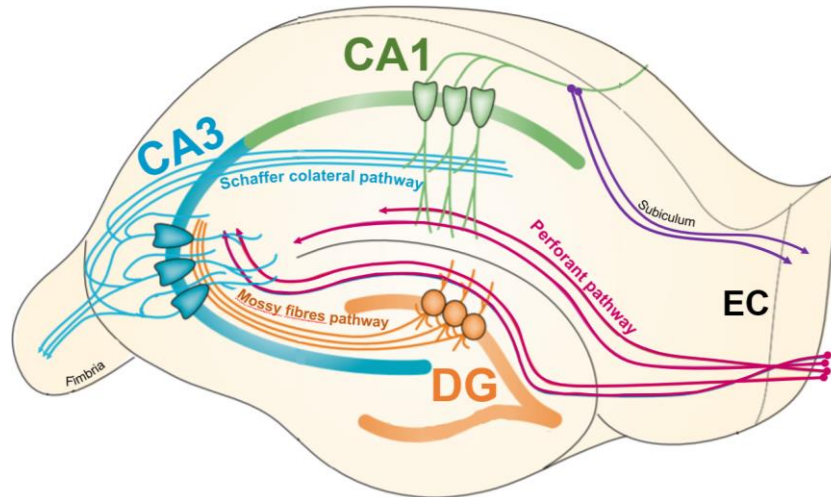
Figure 1.4 Basic schematic of the hippocampal network. The major input is carried by axons of the perforant path, which come from layer II of the entorhinal cortex (EC) to the dentate gyrus (DG). The axons contact the dendrites of granule cells and, in turn, they project their axons, mossy fibres, to the CA3 dendrites. CA3 pyramidal cells project to CA1 though Schaffer/commissural collateral connections (Neves et al., 2008).

Diverse studies in AD transgenic mouse models have reported pre-plaque alterations in hippocampal synaptic transmission, for instance, it has been suggested that Aβ induces changes in the excitation and inhibition equilibrium which consequently causes hyperactivity in cortical and hippocampal neurons (Busche and Konnerth, 2016). One of the first research showing impaired neural communication preceding plaques deposition was performed with APP mice carrying the Indiana mutation mice; there was a decrease in density of hippocampal presynaptic terminals and neurons which negatively impacted CA3-CA1 synaptic transmission (Hsia et al., 1999). Jacobsen et al. (2006) found a reduction in the number of dendritic spines, impaired synaptic plasticity and memory in the Tg2576 model when deposition of plaques was not yet expressed, but an increased fraction of Aβ$_{42}$/Aβ$_{40}$ ratio was detectable. In addition to this, another group found apoptotic features located in the hippocampal dendritic spines of the same mouse model which resulted in

downregulation of the surface expression of GluR1, enhanced long-term depression (LTD) and reduced spine size and density (D'Amelio et al., 2011). Similar to this report, in 2-month-old mice expressing the APP$_{Swe-Ind}$ mutation, when only soluble oligomers were found without Aβ plaques, CA1 LTP was considerably reduced due to decreased NMDA/AMPA receptors ratio (Tozzi et al., 2015). In another study, the 5-month-old J20 mice (Swedish and Indiana mutations) showed not only neural alterations, but also structural changes: there were reported low brain levels of Aβ$_{1-40}$ and Aβ$_{1-42}$ which triggered reduced numbers of pyramidal cells, synaptic densities and presynaptic sites, and even the volume of the whole hippocampus was found diminished in respect to non-transgenic mice (Beauquis et al., 2014).

Modulating neurotransmitter probability of release appears to be a physiological role of Aβ; it has been demonstrated that in wild type rats Aβ is synaptically released in an activity dependent manner which causes an increased glutamate release probability (Abramov et al., 2009). Cummings et al. (2015) found similar results when assessing synaptic activity in the hippocampus of young APP$_{Swe}$/PSEN1$_{M146V}$, or TASTPM mice: a decrease in the paired-pulse ratio reflecting an increase in glutamate release probability was seen when Aβ was just detectable but no plaques were deposited. To follow up this finding, Medawar et al. (2019) reported also enhanced LTP in the same mouse line at pre-plaque stage. Thanks to this evidence, it is considered that early accumulation of Aβ gives a specific window of time, when the neuronal network is only changing, but not entirely disrupted, and therefore it could be a good target to study and understand the processes underlying the progression of the disease.

Electrophysiological characterization of hippocampal synaptic functioning in the APP knock-in lines has only been reported by Latif-Hernandez et al. (2020). They reported no signs of synaptic impairments by 3-4 months of age in APP^{NL-G-F} despite the rising accumulation of Aβ$_{42}$ in the hippocampus and cortex. Basal synaptic transmission, LTP, mEPSCs and mIPSCs remained similar to the APP^{NL} control mice, however it is not until 6-8 months that LTP and STP are reduced alongside with increased frequency in mEPSCs and

mIPSCs which reflects abnormal presynaptic and postsynaptic mechanisms. Recently, the three APP knock-in models were compared and, partially supporting the findings from Latif-Hernandez et al., no major differences in evoked synaptic responses of young-adults APP^{NL-G-F} were found, not even at 6 months of age. This publication suggests that strength or number of synaptic inputs to hippocampal CA1 are unaffected when compared to the APP^{NL} line.

1.3 Microglia

Apart from Aβ plaques and neurofibrillary Tau tangles, neuroinflammation is another hallmark of AD (**Figure 1.1**). It has been suggested that the neurodegenerative progression of some diseases includes a determinant contribution of inflammatory mediators that are released after an immune response is activated. In the CNS the resident immune cells responsible for protecting and clearing the brain from external pathogens and cellular debris are the *microglial* cells (Garaschuk and Verkhratsky, 2019).

It was in 1919 when Pío del Rio Hortega defined one of the glia cells as *microglia*. He described that these cells had a unique origin and were the main supporters of the CNS network due to their interaction with other neuronal cells and their phagocytic activity (Prinz et al., 2019; Sierra et al., 2019). After 100 years from such discovery, it was during the first decade of the 2000s when the field drastically grew due to the fate mapping research findings. It was shown that the microglia ontological origin was, in contrast to other macrophages, from the embryonic yolk sac (Ginhoux et al., 2010; Sevenich, 2018; Stratoulias et al., 2019). Early microglia progenitor cells appear by E7.5 of murine embryogenesis and by E9 these cells are found in the developing brain. Such migration is through the blood circulation which happens before the establishment of haematopoiesis on the foetal liver or bone marrow and hence before the blood-brain-barrier (BBB) formation and before other glial cells arise (Ginhoux et al., 2010; Ginhoux et al., 2013).

After the Ginhoux team discovery (2010) and knowing that microglia cells constitute 5-12% of the total mouse brain cells population (Lawson et al., 1990), other studies refined the information about their precise cellular origin

and development. Microglia precursors are derived from a group of Runx1$^+$ CD45$^-$ c-kit$^+$ erythro-myeloid cells in the yolk sac from mesodermal/mesenchymal origin that, after migration to the CNS, depend on the transcription factor PU.1 and IRF-8 for their development (Schulz et al., 2012; Ginhoux et al., 2013; Kierdorf et al., 2013). Once in the CNS, they differentiate and proliferate to become the only tissue-resident macrophage that expresses a range of specific markers such as the glycoproteins F4/80 and CD68, the fractalkine receptor CX$_3$CR1, the integrin CD11b, the inhibitory immune receptor CD200R, the calcium binding protein, Iba-1, and the colony-stimulating factor-1 receptor, CSF1R (Schulz et al., 2012; Ginhoux et al., 2013; Askew and Gomez-Nicola, 2018).

When microglia cells are settled in the embryonic brain, they constitute a dynamic and highly activated network that shape and remodel the CNS (Hong and Stevens, 2016). While the brain develops, microglia cells also undergo gene transcriptional changes that give them distinct functions throughout life. The early brain microglia are enriched with genes associated with neurogenesis and cell cycling but later, just before birth, genes involved in neuronal development (*Csf1, Cxcr2*) take over and become highly expressed until adulthood (Matcovitch-Natan et al., 2016). It is during development and early postnatal period, when some synaptic networks need to mature and others need to be eliminated, that microglia cells acquire a motile behaviour to monitor such processes and they also display a compacted or amoeboid shape indicating activation (Lawson et al., 1990; Prinz et al., 2019). At this stage, microglia cells become responsible for scavenging, pruning immature synapses and engulfing synaptic materials when necessary. Such microglial activity is mediated by the fractalkine signalling pathway, CX$_3$CR1, and plays a critical role in the refinement of the neuronal connectivity and synaptic transmission of the developing brain (Paolicelli et al., 2011). The peak of this pruning process in mice takes place during the first week after birth and continues until P40. After this time microglia cells are considered to be involved in tissue maintenance, signalling and homeostasis of the CNS (Amit et al., 2016; Matcovitch-Natan et al., 2016).

Once the CNS is fully matured, microglia cells change their morphology to a ramified "resting" phenotype, and they colonise throughout the healthy brain. They display a small rod-shaped soma with fine branches that sense and physically monitor the environment. At this stage, there is no longer input from exogenous immune sources, such as the bone marrow, and are therefore competent for self-renewal (Kettenmann et al., 2013). The expression of microglial genes also changes in adulthood when most of the genes expressed are related to surveillance and homeostasis, hence they acquire functions associated with tissue maintenance and signalling (Matcovitch-Natan et al., 2016). Microglial cells become the local phagocytes of the brain parenchyma where they clear dead or dying cells and debris. Depending on neuronal signals in the microenvironment, it has been shown by *in vivo* two-photon imaging that they have the capacity to migrate to injury sites; once their "resting" branches sense bioelectric or biochemical changes due to potential perturbations in the CNS, they become activated (Davalos et al., 2005; Nimmerjahn et al., 2005). The appropriate activation of microglial cells needs an "on" stimulus (infection, plasma proteins, abnormal aggregates or intracellular products), this stimulus signal appears in the extracellular space, when usually it is not present at all, and such environmental disruption is sensed by a wide variety of microglial membrane receptors to chemokines, cytokines, neurotransmitters and/or neurohormones. The most abundant microglial receptors are the purinoreceptors which are activated mainly by adenosine triphosphate (ATP). ATP is widespread released when neurons are highly activated and massive uncontrolled release could be accompanied by cell death and destruction; this ATP production is considered a "danger" signal and triggers microglia activation (Kettenmann et al., 2011). The rest of the microglia receptors could be grouped in the following categories: promoters of surveillance and viability (fractalkine -CX_3CR1, transforming growth factor-β - TGFβ, colony-stimulating factor 1-CSFR-1); promoters of motility and phagocytosis (purinoreceptors -P2Y6R and P2Y12R-, adrenergic receptor -AdR-, N-methyl-D-aspartate receptor -NMDAR-, gamma-aminobutyric acid - GABAR-); and promoters of inflammatory responses (AdR, P2X7R, TLR2/4, RAGE) (Wohleb, 2016). Microglia activated cells extend their processes and produce cytokines (TNF-α, interleukin IL-1, IL-6, IL-12, etc.), chemokines

(CCL2, CCL3, CCL5, CXCL1, CXCL2, etc.) and other signals to amend the damage. On the other hand, there are also "off" stimuli (CD200/CD45 interaction or the fractalkine system) that keep microglia in a steady state; synchronisation of both signal types is required for a proper performance of the microglial cells (Heneka et al., 2015; De Strooper and Karran, 2016; Ransohoff, 2016a).

When microglia cells are induced to an activation state, apart from producing cytokines and chemokines, several changes also take place: there is a considerable rebuild of the cytoskeleton, and a membrane re-organisation lead by sets of genes and enzymes responsible of migration and phagocytosis. Such phagocytic process relies on the highly developed lysosomal microglial compartments where critical protease activity is triggered to degrade tissue debris or damaged cells (Wake et al., 2009). Activated microglial changes culminate with two phenotypic outcomes, historically referred to as M1 and M2. The M1 phenotype is triggered by a "classical innate" activation route from microbial agents (lipopolysaccharide, LPS) and/or, TNF-α or IFN-γ and generally promotes Th1 responses. Additionally, it is characterised by the production of proinflammatory factors like IL-1β, TNF-α, IL-23, IL-6, IL-18 and reactive oxygen species (ROS) as well as an enhanced expression of surface markers including CD16/32, CD86 and CD40. The M2 is the "alternative" activation type, influenced by the IL-4 and IL-3 cytokines that produces TGFβ1, IL-10, IL-4, IL13 and arginase 1; this phenotype triggers a phagocytic activity and release trophic factors to evoke an anti-inflammatory response (Nakagawa and Chiba, 2015; Zhou et al., 2017). Recent studies have suggested that the M1 and M2 classification is not accurate, as microglia cells can receive input from several stimuli which will trigger several mediators and consequently express multiple responses that are not simply polarised to only one phenotype or profile (Boche et al., 2013; Ransohoff, 2016b). Misinterpretation or overlapping of M1 or M2 signals could have functional consequences when targeting microglia in research, therefore it is critical to consider genome-wide expression profiles, protein markers and epigenetic studies to improve the insight of microglia reactions.

Taking all these observations together, microglia cells can be considered the most dynamic cell type in the brain, they constantly respond to neuronal signals and adapt to changes in the environment. Hence, their role in synaptic transmission and network maintenance is crucial for the CNS in health and disease.

1.3.1 Microglia-neuron interaction

Physiological functions of microglia in the healthy brain are essential and very dynamic. Due to this dynamism, the specific role of microglia and its molecular mechanisms involved in synaptic or neuronal activity have not been clearly defined. What it is clear, is that neurons and microglia are in a constant feedback or communication, such crosstalk involves a reciprocal release of soluble factors that maintain the brain homeostasis and the neuronal network (Szepesi et al., 2018; Marinelli et al., 2019).

Physical interactions between microglia and synaptic elements can modulate transmission and plasticity of neuronal circuits by several signalling pathways. Pre- or postsynaptic modulation by microglia depends on the functional and activity status of neurons. (Wake et al., 2009; Tremblay et al., 2010; Ji et al., 2013). When there is intense neuronal activity NMDAR activation due to glutamatergic transmission induce a recruitment or outgrowth of microglia processes or extensions (Dissing-Olesen et al., 2014; Eyo et al., 2014); also, it has been seen that induction of LTP in mouse hippocampus involves a clear increase of surrounding microglia contacts with dendritic spines (Pfeiffer et al., 2016). Such microglia-neuron interactions could be disturbed by blocking NMDARs or by inhibiting microglial CX3CR1 expression in mice (Rogers et al., 2011; Zhan et al., 2014). Both mechanisms disrupt LTP induction including a decrease in microglia contacts with multi-synaptic buttons and deficits in learning and memory behaviours are also seen. Furthermore, disruption of the complement signalling, C3-CR3, which is present in synaptically-enriched areas, affects microglial phagocytosis and there is sustained deficits in the neuronal network (Schafer et al., 2012). Taking these ideas together, it is suggested that microglia cells are capable of

modulating synaptic plasticity and that appropriate microglia signalling pathways in the healthy adult CNS are crucial for hippocampal circuitry.

In addition to synaptic plasticity, microglia have also been suggested to mediate changes in basal synaptic transmission (Ji et al. (2013)); after eliminating microglia *in vitro*, synaptic numbers and glutamate receptors expression was altered. Such changes triggered hyperexcitability in functional synapses and a clear increase in PSD95, synapsin and spine numbers in hippocampal neurons (Ji et al., 2013). It was concluded that microglia cells are necessary for the correct modulation of synaptic activity. Later that year, Parkhurst et al. partially supported the Ji et al. findings by using the same microglial numbers manipulation rationale. In mice genetically modified to drive microglia specific depletion, after 4 days of elimination via CX3CR1, there was not only a clear density deficiency of NMDAR and AMPAR proteins (GluN2B, GluA2 and VGlut1) which triggered a decrease in frequency of excitatory postsynaptic currents, but also there was a lack of elimination and formation of spines. Such uncontrolled modulation of glutamatergic excitatory activity and spines population were related impairments in learning and memory behavioural tasks (Parkhurst et al., 2013)

These reports highlight how microglia processes are key to contacting and approaching synaptic sites, and depending on the neuronal signal, microglia cells are able to feedback to the environment to maintain homeostasis. Although this microglia-neuron interaction is evident, there are still limitations in understanding the specific molecular mechanisms that control such communication (Marinelli et al., 2019).

1.3.2 Microglia in AD

The presence of clear abnormal gliosis in post-mortem examinations of AD brains was first described by Alois Alzheimer himself (Alzheimer 1907, translated in Stelzmann et al., 1995) , and decades later, further studies reported reactive astrocytes and microglia when amyloid deposits and neurofibrillary tangles were exhibited (Griffin et al., 1989; Itagaki et al., 1989; Lue et al., 1996; Sanchez-Mejias et al., 2016). During this decade,

development of positron emission tomography neuroimaging techniques have provided more evidence for confirming inflammatory activity in AD patients (Kreisl et al., 2020). *In vivo* detection of (R)-PK11195, a specific ligand that binds activated microglia or brain macrophages, revealed a significantly increased regional binding in the entorhinal, temporoparietal and cingulate cortex from AD patients (Cagnin et al., 2001). Also, measurements of TSPO (18kDa translocator protein) radiotracers, a marker for microglial activation, were found to be positively correlated with fibrillar amyloid depositions, especially at a prodromal stage of the disease and in EOAD patients (Hamelin et al., 2016; Tondo et al., 2020). A recent study employing a highly selective radiotracer for microglial CSF1R, [^{11}C]CPPC, confirms an elevated uptake in an AD mouse model and in post-mortem AD human tissue (Horti et al., 2019). Alongside the confirmation of reactive microglia presence in AD brains from humans and animal models, inflammation-related molecules like MHC-II, IL-1b, IL6, IL12, TNF-α and complement proteins are also increased (Rogers et al., 1996; Prokop et al., 2013). Based on these findings, the specific role of microglia in AD has brought the attention of neuroscientists as not only their presence but also their functional state needs clarification; until date, the mechanisms by which microglia act remains poorly understood.

Recent genetic studies support the vital role of chronic neuroinflammation in AD. Genome-wide association studies (GWAS) have identified genes that are strongly linked with the immune response and dysregulation of the immune system which represent a risk for the disease. Microglial genes such as *TREM2*, *CR1*, *CD33*, *CLU* and *MS4A* (Guerreiro et al., 2013; Lambert et al., 2013; Karch and Goate, 2015; Bellenguez et al., 2020) are clearly now identified in AD populations; this information is helping to understand the biology of the disease more effectively showing the importance of microglia in the progression of the pathology.

TREM2 (triggering receptor expressed on myeloid cells) is a transmembrane glycoprotein that acts as a receptor on the surface of microglial cells where it is highly expressed. It senses lipids produced from cellular damage, attenuates inflammatory reactions, promotes cell activation, phagocytosis, chemotaxis and survival (Efthymiou and Goate, 2017). *TREM2*

gene mutations are associated with dementia and they impair microglia activation; the most common variant in European-descent population is R47H (Arginine-47-Histidine), which is reported to increase AD risk by three-fold and this mutation is the most clearly associated with the disease. (Guerreiro et al., 2013; Jonsson et al., 2013; Yeh et al., 2017; Hansen et al., 2018). In three different amyloid mouse models (5xFAD, APPPS1, PS2APP), TREM2-deficient microglia show increased apoptosis and a lack of activation phenotypes, also they fail to assemble or proliferate around plaques which leads to a worsened deposition and to an elevated Aβ42:Aβ40 ratio, including more soluble and fibrillar Aβ oligomers in the brain (Wang et al., 2015; Wang et al., 2016; Jay et al., 2017; Meilandt et al., 2020). All these genetic finding strongly suggest that microglia play an important role in AD; however, the specific pathway by which TREM2 contributes to the disease is still under investigation.

After confirming by positron emission tomography and genetic evidence that microglia are definitely involved in the progression of the disease, it is currently suggested that microglia cells are both: a beneficial reaction at the beginning of the disease which eventually becomes also a contributor that triggers neuronal damage.

1.3.3 Microglial changes in response to Aβ pathology in AD mouse models

Several amyloid transgenic mouse lines have been used to elucidate both ideas of microglia's positive and/or negative role in the disease. The first study showing a quantitative interaction between Aβ plaque formation and microglia activity in an AD mouse model was Frautschy et al., (1998); by using the Tg2576 (APP$_{Swe}$) mice at 10-16 months-old of age, it was found that within and close to Aβ plaques there was an increase of microglial density and size in the hippocampus and some cortical regions. One year later, it was confirmed that the plaque-associated microglia seen in this same transgenic mouse line were not only activated (CD45 and Mac-1 positive) but also produced proinflammatory IL-1β and TNF-α in response to fibrillar Aβ (Benzing et al., 1999). Similar results were obtained with APP23 mice where

33

hypertrophic microglia were shown to be clustered around dense core Aβ plaques and in contact with dystrophic neurites (Stalder et al., 1999; Bornemann et al., 2001). Collectively, these initial studies in mice contributed to the idea that, following Aβ recognition by microglia, the production of proinflammatory mediators could also promote the neurodegeneration of neighbouring neuronal populations triggering a toxic inflammatory response (Akiyama et al., 2000).

For more than a decade, plenty of evidence was rapidly build up about the association of microglial inflammatory processes with Aβ pathology in different transgenic mouse models; overall it was reported that the innate immune system could be manipulated to clear Aβ in the context of anti- or pro-inflammatory inhibition (DiCarlo et al., 2001; Matsuoka et al., 2001; Wegiel, 2001; Wegiel et al., 2003; Janelsins et al., 2005; Herber et al., 2007; Town et al., 2008; Chakrabarty et al., 2015). Additionally, most of the reports agreed with the idea that once early soluble Aβ starts accumulating in the brain, microglia are quickly stimulated, and proliferation begins. When plaques are formed, microglia cells cluster around them accompanied with clear morphology and gene expression changes, which subsequently leads to neuronal alterations (Bolmont et al., 2008; Jimenez et al., 2008; Meyer-Luehmann et al., 2008; Baron et al., 2014; Matarin et al., 2015; Kamphuis et al., 2016; Condello et al., 2018). Such gene expression changes in microglia revealed a potential new phenotype called "disease-associated-microglia (DAM)". This type of microglia is described as highly phagocytic and show downregulation of homeostatic genes but upregulation of AD genes such as *Trem2* or *Apoe* (Bisht et al., 2016; Keren-Shaul et al., 2017). In response to Aβ pathology, microglia switch to become DAM in the need for a more exhaustive clearance activity and to avoid further damage, however, as the disease progresses, microglia cells fail to maintain their protective role. Knowing that plaque-associated microglia depend on the *TREM2* gene and that the *TREM2* R47H variant increases the risk of developing AD, it is then suggested that microglial functions are play a critical role in the progression of the disease.

Microglial synaptic pruning function has a peak of activity during the first postnatal weeks in the rodent brain and, for several years now, it has been suggested that this pruning performance is reactivated in response to AD pathology or ageing and that microglial normal surveillance status is lost (Hong et al., 2016b; Hansen et al., 2018). Stevens' group proposed that the complement system, which mediates synapse elimination during development (Stevens et al., 2007), is the responsible for "tagging" synapses that are engulfed by microglia in the early AD brain; C1Q accumulates on pre-plaque J20 brains and promotes synaptic loss by attracting phagocytic microglia; also in the absence of C3, synapse loss and neurons are rescued in hippocampus of APP/PS1 mice (Fonseca et al., 2004; Hong et al., 2016a; Shi et al., 2017). This idea is supported by Fuhrmann et al. (2010) who found that neuronal loss was also recovered by knocking out *Cx3cr1*, another important microglial signalling pathway for circuit refinement (Paolicelli et al., 2014), in 5xTg mice. In contrast, beyond the complement or the fractalkine system contribution, it was recently demonstrated that enhancing microglial phagocytic activity promotes synaptic loss in the absence of amyloid pathology (Paolicelli et al., 2017). This microglial phagocytic phenotype is suggested to be harmful for neurons and synapses in AD; however, it was recently proposed that this microglia behaviour could be indeed protective. Edwards (2019) proposes that microglia remove damaged synapses to prevent spread of damage along axons. Microglia efficacy at not only restricting expansion of amyloid pathology but also at removing damaged synapses in early AD could determine the eventual progression to the Tau dissociation and cognitive symptoms onset.

There are only a few studies examining amyloid-associated inflammation in the relatively new APP knock-ins. For example, in the APP[NL-F] mice, Hama et al. (2015) showed with 3D visualisation how activated microglia are found in the brain even before evident Aβ plaque development. In contrast, in the APP[NL-G-F] there is no alteration of microglial proteins, even when Aβ plaque deposition is already evident at 3 months of age (Sebastian Monasor et al., 2020); in addition to this idea, Castillo et al. (2017) reported amyloidosis-dependant transcriptomic profiles where an upregulation trend of neuroinflammation-related genes was present in the APP[NL-G-F]. Also, this

publication shows that compared to the 3xTg mouse profile, the altered glial gene expression seen in the APP[NL-G-F] cortex turned out to be more similar to what happens in AD patients, not only regarding neuroinflammation-associated genes (*C4a/C4b*, *Cd68, Itgam, Gfap, S100b, Tgfbr2*, to name some) but also for AD risk factor genes like *Trem2* and *Apoe* (Saito and Saido, 2018; Sobue et al., 2021). Moreover, another research found that phagocytic microglia in APP/PS1 mice was impaired by 3 months of age; however, the microglial activity seen in the APP[NL-G-F] line at the same age remained unaltered and functional (Sebastian Monasor et al., 2020). Therefore, it is suggested that the APP-knock-in models could be targeting or mimicking the pathological features and mechanisms observed in human AD patients in a better way than the widely used transgenic mice.

1.3.4 The two faces of microglia in AD: beneficial and harmful

Overall, it is hypothesised that at the beginning of AD there is high, acute activation of microglia when such cells are trying to cope with the demand of potentially clearing the brain of Aβ. With time, however, clearance mechanisms fail, microglia promote a chronic inflammatory active state and compact Aβ aggregates into dense core plaques that shields them off from neurons (Heneka et al., 2015; Spangenberg and Green, 2017; Bartels et al., 2020). Eventually, neuronal networks become stressed and damaged and as a consequence, microglia phagocytose synapses, secrete neurotoxic cytokines (IL-1β, IL-6, TNF-α, TGF-β) and chemokines that injure more neurons (Hansen et al., 2018; Edwards, 2019). Aβ keeps its pathogenic build-up accompanied by Tau pathology and cognitive deficits start.

The double-edged sword of microglial function in AD complicates therapeutic approaches that could target the immune system. Stimulation/manipulation of microglial activity might be helpful at an early stage, as it could prevent AD development; however, such microglial changes could become detrimental at a later stage when the disease has reached a highly inflamed and neurodegenerative status (Hansen et al., 2018).

1.4 Alteration of microglia numbers

Although the specific role that microglia play in AD remains uncertain, it is clear that there is an association with the onset and development of Aβ pathology. In order to assess if microglia are protective or detrimental, several research groups have selectively manipulated microglial numbers to find the pathway by which they contribute to neurodegeneration (Han et al., 2017).

Genetic manipulation methods were first described in 2005 by Heppner et al. by using the suicide gene herpes simplex virus thymidine kinase, HSVTK. This gene can be selectively activated and becomes toxic by the administration of the drug ganciclovir. Transgenic mice expressing HSVTK under the specific CD11b promoter were generated and about 90% microglial depletion was achieved (Heppner et al., 2005). This approach was evaluated with the APP/PS1 model where Aβ pathology remained unchanged in the absence of microglia (Grathwohl et al., 2009). As an alternative genetic method, the diphteria toxin receptor (DTR) was coupled with CX3CR1^{CreER} mice and 90% of microglia were depleted after systemic administration of DT. The lack of microglia for 4 days caused a significant decrease in spine formation and mice showed impaired behavioural performance (Parkhurst et al., 2013); in the APP$_{Swe}$/PSEN1 model this method of elimination resulted in slightly bigger Aβ plaques found in cortex (Zhao et al., 2017). This finding supports the hypothesis that the accumulation of microglia around plaques is considered to be a physical barrier or shield that limits expansion of Aβ plaques by wrapping the core and actively protecting surrounding neurons from Aβ toxicity (Condello et al., 2015). However, this idea contrasts with Grathwohl et al. who concluded that there was no link between microglia and the numbers, formation or maintenance of amyloid plaques.

Pharmacological manipulation strategies to specifically deplete microglia in the CNS have also been studied. Liposomal clodronate is a liposome-encapsulated drug that when injected into the hippocampus provides an anatomical specific short-term ablation of Iba-1$^+$ microglia. This microglial manipulation lead to alterations in spatial learning and sociability; such changes could be recovered when microglia was allowed to repopulate (Torres

et al., 2016). This approach avoided microglial expression of mutant genes that could trigger side effects in non-targeted signalling pathways; however, it required intracerebral administration of drugs which involves BBB damage and potential myelotoxicity. In light of these disadvantages, other depletion approach was developed by targeting the colony stimulating factor 1 (CSF1) and its receptor (CSF1R), a signalling pathway that is critical for microglia survival and development (Han et al., 2017).

1.4.1 Colony Stimulating Factor 1 Receptor (CSF1R)

CSF1R is a transmembrane tyrosine kinase protein present in all myeloid-derived cells which is exclusively expressed in the CNS by microglia. Its two natural ligands are: CSF1 and IL34 (interleukin 34). Following ligand-receptor binding, there is a cascade of signal transduction pathways that promote differentiation, migration and survival of microglial cells (Ginhoux et al., 2010; Green et al., 2020). Mice with a null mutation in the *Csf1r* gene show a normal embryonic brain development despite 99% lack of microglia; however it is during the post-natal period when the neuronal cytoarchitecture is disrupted and mice rarely survive until adulthood (Erblich et al., 2011; Nandi et al., 2012). Csfr1$^{-/-}$ mice have smaller brains, lowered density of neurons, atrophy in the olfactory bulb, enlarged ventricles and disturbed connection of hemispheres (Posfai et al., 2019). Genetic studies have associated *CSF1R* mutations with dementia, seizures, leukodystrophies and parkinsonism (Rademakers et al., 2011). In humans, CSF1R expression is upregulated in AD post-mortem brains (Akiyama et al., 1994; Olmos-Alonso et al., 2016; Sassi et al., 2018). Therefore, it is thought that disturbances in microglial physiology via the CSF1R pathway could lead to neurodegenerative conditions.

In 2014, Elmore and colleagues developed an approach where microglia were specifically depleted by using a CSF1R/c-kit inhibitor, pexidartinib or PLX3397 (**Figure 1.5a**). This compound penetrated the BBB and, after 21 days of consecutive administration, 99% of the cells were wiped out (**Figure 1.5c**). Moreover, another more penetrant and depletion-efficient compound was developed by the same team, PLX5622 (**Figure 1.5b, d**). After only 3

days, this novel compound depleted >80% of microglia when using a high dose in adult mice (Acharya et al., 2016), microglia remained eliminated for as long as the treatment was given to the mice and for up to 2 months no behavioural or cognitive impairments were reported. Both PLX3397 and PLX5622 was found to be highly precise, as other type of brain cells remained unaffected (i.e. neurons, astrocytes and oligodendrocytes), and easy to manipulate, as withdrawal of the inhibitor resulted in rapid microglial repopulation (Elmore et al., 2014; Elmore et al., 2015).
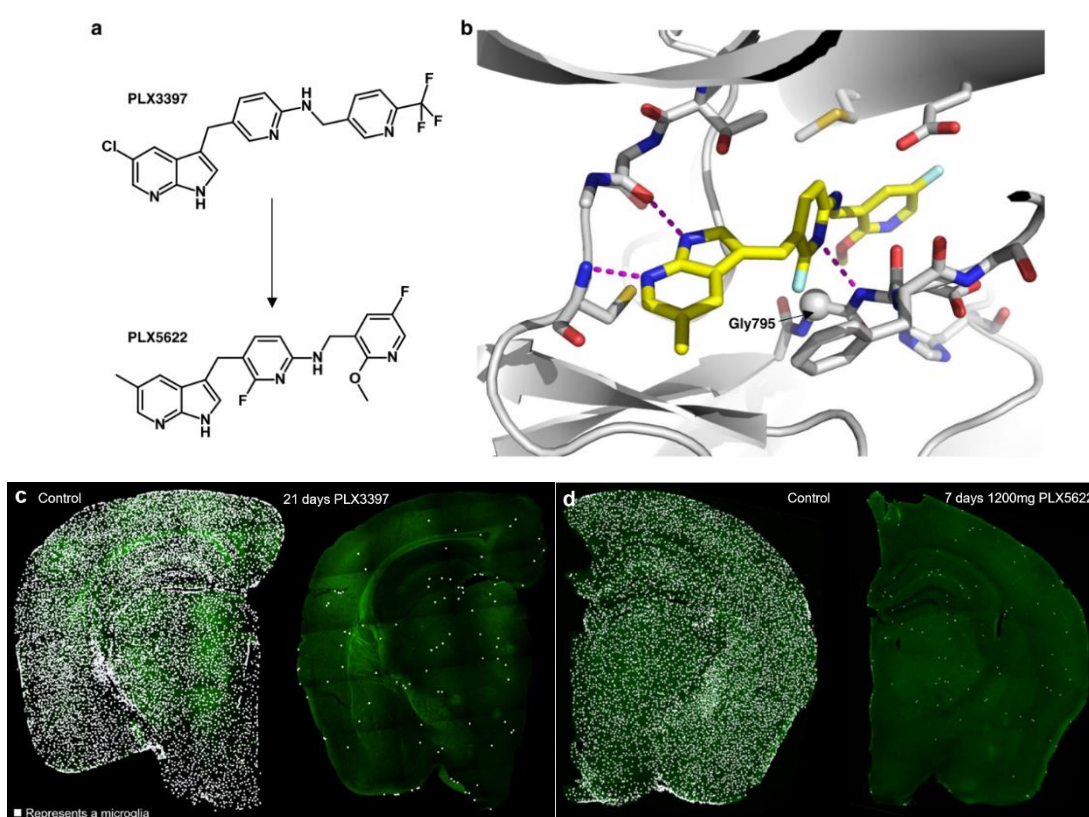
Figure 1.5 Chemical structures of selective CSF1R inhibitors PLX3397 and PLX5622 and depletion effectiveness. a. PLX5622 is similar to CSF1R/KIT/FLT3 inhibitor PLX3397. **b.** X-ray crystal structure of PLX5622, its higher selectivity is determined by the interaction of the compound with Gly795 (Spangenberg et al., 2019). **c.** Representative coronal sections of mice treated with control diet or with PLX3397, causing the elimination of microglia brain-wide (Elmore et al., 2014). **d.** Representative images of microglia elimination after 7 days of PLX5622 treatment (Dagher et al., 2015).

1.4.2 Microglia depletion and amyloid deposition in AD transgenic mice models.

Knowing that microglia are physiologically dependent on CSF1R and that they are genetically linked with AD, the same approach that Green's team developed for depleting microglia has been applied to several AD transgenic mice to assess their contribution to the disease. To date, most of the evidence suggests an unaltered Aβ pathology after depletion of microglia; however, recently, some authors have contradicted that idea. Such discrepancies could come from the fact that: a) different transgenic mice have been used, which consequently gives a different onset and progression of plaque deposition, and b) the depletion duration and time of treatment implemented in each model. First, in the 3xTg mice Aβ plaques and Aβ40 or Aβ42 concentration were found to be unaffected after reducing microglia numbers (~30% less) for 6 or 13 weeks (Dagher et al., 2015). Similar findings were seen in APP/PS1 mice where Aβ plaques did not change without the presence of microglia, but pro-/anti-inflammatory and phagocytosis relevant genes were downregulated in the hippocampus and cortex (Unger et al., 2018). Then, following this report, two experiments using the 5xFAD model reinforced this same concept; depletion of 75-95% of microglia cells for about one month did not change Aβ plaque numbers or Aβ levels in cortex, hippocampus, thalamus and subiculum (Spangenberg et al., 2016; Zhong et al., 2019), also spine density numbers were increased, which suggests a prevention of synaptic degeneration and a recovery of synaptic transmission in response to an absence of microglia (Spangenberg et al., 2016). This spine density rescue was also seen by Olmos-Alonso et al., (2016) in APP/PS1 mice, using another CSF1R inhibitor, GW2580, for 3 months. An improved performance in memory/behavioural tasks and a prevention of synaptic degeneration were seen; however, Aβ plaques remained stable. All this evidence clearly showed that microglia were not mediating or protecting directly the brain from amyloid pathology; however, their input and signalling inflammatory pathways could be contributing to neurodegeneration.

In contrast, for the last two years, some publications have suggested that microglia activity is a causal pathway leading to neurodegeneration by

modulation of Aβ burden. Sosna et al. (2018) published results where extracellular, intraneuronal and fibrillar amyloid levels were dramatically reduced in 5xFAD mice cortex and hippocampus after an early chronic depletion of microglia with PLX3397. Additionally, they pointed out that CSF1R signalling or microglia are necessary for neuritic plaque formation and that these effects can only be seen if manipulation of microglia numbers is made before the initiation of amyloid pathology. This hypothesis coincides with the fact that all previous results (i.e Dagher et al., 2015, Spangenberg et al., 2016, Unger et al., 2018, Zhong et al., 2019) induced microglial elimination for a short period of time or/and at an advanced AD stage, when amyloid plaque deposition was already quite robust. The Sosna et al. publication claims that there is a specific window of time when microglia ablation could interfere with the Aβ seeding process and this could represent a time window for preventative approaches. Taking this suggestion into consideration, Green's group explored the contribution of microglia to plaque formation in the initial stages of the disease by using PLX5622. This time, depletion was for >6 months in 5xFAD mice and they found there was a reduction of dense-core plaques in cortical regions but no changes in levels of soluble or insoluble Aβ. It was then suggested that the plaque onset relies on the presence and activity of microglia and that neuronally-derived Aβ is internalized within microglia which induces the secretion of factors that facilitated fibrilisation (Spangenberg et al., 2019). Recent publications also in 5xFAD mice showed that dense-core plaques were reduced and were more diffuse when microglia were depleted; additionally, there was an enhanced neuritic dystrophy and a downregulation of microglial homeostatic genes expression (Casali et al., 2020). If microglial numbers were reduced since a pre-plaque formation stage, then not only were Aβ levels and APP processing decreased but also synapse-associated protein levels improved in the cortex and hippocampus (Son et al., 2020).

Until now, all the published reports describing microglial depletion effects in AD have only been investigated in transgenic mouse models, and the role of microglia in plaque deposition still remains unclear. Partial or total absence of microglia by inhibiting the CSF1R either does not cause an effect or it alleviates the amyloid burden (but only in the 5xFAD mouse). However, a

recent paper described that the elimination of microglia could actually worsen the amyloid pathology and it is also the first report that avoids transgenic models and uses an APP knock-in. In 4-month-old APP^{NL-G-F} mice, PLX5622 effectively eliminated microglia after 2 months of treatment; in consequence Aβ plaques significantly increased in number, size and area covered in cortex. It is thus suggested that plaque compaction and clearance is a microglia-dependent process (Clayton et al., 2020).

1.5 Summary and current study

Alzheimer's disease is a chronic, progressive neurodegenerative condition and the most common type of dementia; numbers of people affected by this disease keep dramatically increasing every year and today it has become a critical challenge for society that implicates significant economic and public health aspects. Since its discovery, scientific research has focused on studying some key components in AD pathogenesis, such as Aβ deposition as an early initial factor and Tau tangles pathology as a leading hallmark for neurodegeneration and cognitive decline. However, it is clear that AD is a multifactorial disorder that still has several pieces missing to understand its complete story, for example why or what triggers Aβ to become toxic in a healthy brain, how Aβ pathology leads to Tau pathology, how the brain reacts or/and contributes to the progression of the disease, how other brain cells participate in the disease onset or progression, etc. GWAS revealed valuable information about a variety of AD risk gene variants associated with the immune system, especially related to the brain resident microglia. Particularly, TREM2 has gained recent attention, as it is one of the strongest risk genes highly expressed in microglia/myeloid cells in the brain but its specific role in regulating microglia functions is not clear.

The present study concentrated on microglia cells and the early deposition of Aβ plaques, specifically if their presence is crucial for the progression of the pathology and their implication in hippocampal synaptic transmission. This project aimed to investigate the effects of total or partial depletion of microglia in APP knock-in mice on hippocampal CA1 pyramidal cells using field

excitatory postsynaptic potentials and whole-cell patch clamp recordings. Currently, with the exception of our paper that is now published (Benitez et al., 2021), the APP knock-in mice line has not been yet extensively characterised with electrophysiology techniques, especially at early stages of amyloidopathy; additionally, all the reports published where microglia is pharmacologically depleted have been performed in transgenic AD mice only. I hypothesised that microglial activity might be contributing the development/dynamics of Aβ plaques, either in a positive or negative way. I administered CSF1R inhibitors to mice to ablate microglia for 1 or 3 months during early stages of pathology of APP^{NL-G-F} and APP^{NL-F}. I found that total absence of microglia cells did not affect basal synaptic transmission or LTP in both mouse lines; however when partially absent, microglia modified synaptic transmission without triggering an increase or decrease in number or size of Aβ plaques. I performed fluorescence immunohistochemistry to validate microglia depletion and presence of Aβ plaques in the hippocampus. These findings represent an important contribution to AD research that could be helpful to identify important biological pathways that link the immune system functions and dementia.

Chapter 2

MATERIALS AND METHODS

All mouse experiments were conducted according to UK Home Office regulations under the Animals (Scientific Procedures) Act 1986 and UCL local ethical guidelines.

2.1 Mouse model

APP knock-in mice used in this thesis were originally obtained from the Saito and Saido group, RIKEN Japan and then bred in the UCL Biological Services Unit as homozygous colonies. The mice had a C57Bl/6j background and a humanised form of the APP gene with 2 (APP^{NL-F}) or 3 (APP^{NL-G-F}) familial AD mutations knocked-in. Age matched C57BL/6j mice were used as wild type (WT) controls. All mice used in this study were male and they were weaned at 21 days of age. At this point, mice were group-housed (3-5 animals) in an enriched environment with a photoperiod of 12 h:12 h light/dark cycle, controlled humidity and temperature and *ad libitum* access to food (18% Protein Rodent Diet, Teklad Envigo, Madison, WI) and water. Environmental enrichment consisted in placing a cardboard shelter and tube, nesting/bedding material and wooden chew sticks.

2.2 Compound

2-fluoro-3-[(7-aza-5-methyl-3-indolyl)methyl]-6-[(5-fluoro-2-methoxy-3-pyridyl)methyl] aminopyridine (PLX5622) was developed and synthesised by Kim Green's lab, University of California, Irvine (Spangenberg et al., 2019) The compound was formulated in AIN-76A standard chow (Product data

D10001) by Research Diets Inc. (New Brunswick, NJ) at different doses: 0, 300 or 1200 mg/kg in food.

Standard diet (18% Protein Rodent Diet, Teklad Envigo, Madison, WI) was provided to APP[NL-G-F] animals until 1.5 months and APP[NL-F] animals until 7 months of age, then the diet was replaced with AIN-76A diet at 0 (Control), 300 (Low) or 1200mg/kg (High) of PLX5622 in chow for microglia elimination. APP[NL-G-F] mice were treated with the PLX5622 diet for 7 weeks and APP[NL-F] animals for 3 months (n=10/group). Both treatments targeted an early Aβ plaque deposition stage (Saito et al., 2014). An extra control animal group whose diet was never changed was considered.

2.3 Electrophysiology

<u>Acute brain slice preparation</u>

After treatments, mice were killed by decapitation. The brain was quickly removed (<1 min) and submerged in ice-cold dissection artificial cerebrospinal fluid (ACSF) containing 125 mM NaCl, 2.4 mM KCl, 26 mM $NaHCO_3$, 1.4 mM NaH_2PO_4 and 19.4 mM D-glucose (300-310 mOsm/l, pH ~7.4). A high concentration of 3 mM $MgCl_2$ and a low concentration of 0.5 mM $CaCl_2$ was used to reduce excitotoxicity by blocking NMDARs and consequent synaptic transmission. The cerebellum and olfactory bulbs were removed, and the rest of the brain was sectioned through the interhemispheric fissure to separate the two hemispheres. One hemisphere was randomly chosen for preparation of acute brain slices and the other was drop-fixed in 4% paraformaldehyde (PFA Thermo Fisher Scientific) for hippocampal immunohistochemical analysis. To obtain acute slices, the dorsal part of the cortex was removed by a cut of a 110° angle to the sagittal plane and the whole hemisphere was glued to the slicing stage (Henkel Loctite Adhesive, Ltd). The tissue was submerged in cold ACSF and 400μm transverse acute hippocampal slices were obtained with a ceramic blade using a vibratome (Integra-slice 7550MM, Campden Instruments Ltd.). On average, 4-5 hippocampal slices with attached entorhinal cortex were obtained. The slices were placed into incubation in ACSF at room temperature for 5 minutes, then they were sequentially

transferred into 3 heated chambers at 37°C containing ACSF with increasing $CaCl_2$ and decreasing $MgCl_2$ concentration (0.5 mM/1 mM, 1 mM/1 mM and 2 mM/1 mM), for approximately 5 minutes each. Changing the concentration of ions gradually, prevents the sudden release of neurotransmitter. Once in the last chamber, slices were allowed to recover from the dissection trauma for 45 min and to cool to room temperature (22-25°C). The slices were then transferred to the recording chamber as required with running ACSF bubbled with 95% O_2/5% CO_2 (Carbogen, BOC Medical).

Extracellular field recordings

Only slices with a clear *Cornu ammonis* 1 (CA1) cell body layer and *stratum radiatum* visible were selected and once submerged in the chamber (Eclipse Inc., Sheffield, England) they were allowed to acclimatise for at least 45min. Carbogenated recording ACSF ($1Mg^{2+}$, 2 Ca^{2+} mM concentration) was pumped into the chamber through a peristaltic pump at about 1.5 ml/min flow which was prewarmed by a heater to reach 30±1°C in the recording chamber. Slices were placed in the desired orientation and held by a platinum holder or "harp".

Field responses were evoked using borosilicate glass capillaries (Harvard Apparatus, Kent UK) (inner diameter of 0.86mm and an outer of 1.5mm; 1-2MΩ resistance), which were pulled with a PP-83 puller (Narishige, Japan) and filled with recording ACSF. The recording electrode was positioned in *stratum radiatum* of CA1 and the stimulating electrode was placed amongst the Schaffer collaterals (SC) in the hippocampus using a Nikon dissecting microscope and micromanipulators.

Responses were evoked (100 µs, 50 ms interval, 0.1 Hz; Grass SD9 stimulator (RI, USA)) and the potentials amplified using an Axoclamp-2B amplifier (Axon Instruments, USA) with the signal filtered at 3 kHz (Brownlee Precision 440, USA). Finally, the field excitatory postsynaptic potentials (fEPSP) signals were digitised (10 kHz, ITC-16 Digitizer, Instrutech NY, USA), saved into a Dell computer and Windows Whole Cell Program (WinWCP v4.5; Dempster, J., University of Strathclyde) software was used for data acquisition

and analysis. Sweeps were averaged in blocks of six, giving an averaged field potential for 1 minute of recording time.

Once the electrodes were positioned in the slice and a fEPSP was obtained, three protocols were applied:

1. Input-output relationship (I-O): adjustment of the stimulation intensity to examine the synaptic efficacy of the fEPSP. Two pulses were delivered at different voltages in 10 V incremental steps between 10-50 V at 0.1 Hz and the stimulus intensity was set to the voltage that evoked a response of 30-50% of the maximum amplitude or 30-50% of the amplitude at which a population spike was detected. The fEPSP slope provides a measure of the efficacy of the synaptic CA3-CA1 connection (**Figure 2.1**). Six sweeps were recorded and averaged for each stimulus intensity.

2. Paired-pulse profile: Paired stimuli were delivered at different inter-pulse intervals of 25, 50, 100, 200 and 400 ms and the ratio (PPR) of the second fEPSP over the first was measured to analyse probability of release under basal conditions.

3. LTP induction: a baseline (paired stimuli at 50 ms intervals delivered at 0.1 Hz) was recorded for 10 minutes and fEPSPs were closely monitored to ensure stable synaptic transmission. If the slope was fluctuating more than 10%, the stimulus intensity was reset, and a new baseline was recorded. 10 min of stable baseline was considered prior induction of LTP by a tetanus protocol. This protocol consisted of 3 trains (1.5 s interval) of 20 pulses at 100 Hz at test-pulse stimulus intensity. Following tetanus, pairs of fEPSP responses were recorded for a further 60 minutes at 0.1 Hz to determine the presence and magnitude of LTP. Signals recorded for 10 min prior induction of LTP were considered as the baseline and all following records were considered as the percentage of the mean of that baseline.

Whole-cell patch clamp recordings

Following incubation time, one slice was placed into a recording chamber perfused with carbogenated ACSF (1 Mg^{2+}, 2 Ca^{2+} mM concentration) at room temperature (22-25°C). Glass borosilicate capillaries were pulled (PP-830 Narishige, Japan) to obtain micropipettes with a tip resistance of 4-6 MΩ. The stimulating micropipette was filled with ACSF and carefully placed in the SC of CA1 using a micromanipulator. Patch-target pyramidal cells were identified by their location and distinctive soma. The recording micropipette was filled with a CsCl-based internal solution prepared with: 140 mM CsCl, 2 mM $CaCl_2$, 5 mM HEPES, 10 mM EGTA and 2 mM Mg-ATP (pH 7.2-7.4) ~292-295 mOsm/l). Cs^+ was used to block K^+ channels, which reduces the background noise as fewer channels are opening and closing and also to improve the uniformity of the space-clamp when a patch is obtained due to higher input resistance; Cl^- improves the detection of inhibitory events at -70 mV. Target CA1 cells were identified by their location and appearance.
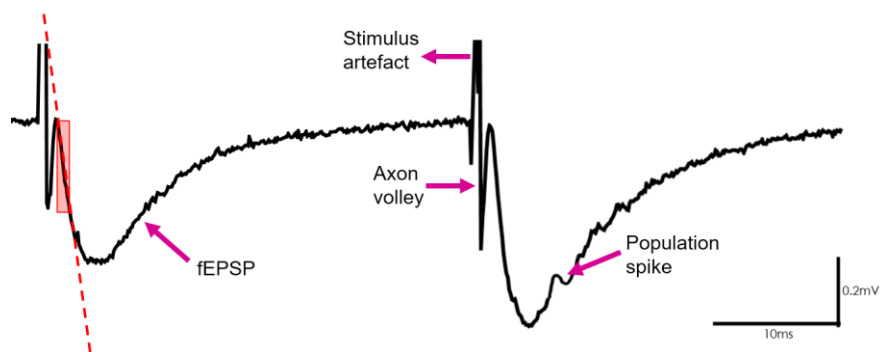
Figure 2.1 Representative averages fEPSP traces. The stimulus artefact, fibre volley, slope and population spike are indicated. The 50% of the slope measured is shown by the red square and corresponds directly to the activation of depolarising synaptic currents in CA1 pyramidal neurons in response to glutamate release from SC terminals.

Whole-cell patch clamp from CA1 pyramidal neurons was obtained with an Axon amplifier (Multiclamp 700B Axon instruments/Molecular Devices Corp.) and the signals were filtered through a low pass filter (Bessel filter, Frequency devices 900, Scensys) at 10 kHz followed by 2 kHz. Recordings were digitized (Digidata 1322A; Axon Instruments/Molecular Devices, Corp.)

with a sampling rate of 10 kHz. Cells were voltage clamped at -70 mV, x10 gain was used, access resistance (<30-50 MΩ) and holding current (<250 pA) were monitored by applying a 5mV square test pulse. Synaptic currents were acquired using WinEDR (v3.2.6, Dempster, J., Strathclyde Electrophysiology Software. University of Strathclyde) and analysed with Windows Whole Cell Program (WinWCP v4.6.1; University of Strathclyde) software. WinWCP was also used for the acquisition and analysis of evoked signals.

Spontaneous and miniature excitatory postsynaptic currents

Spontaneous excitatory postsynaptic currents (sEPSCs) were isolated by washing 6 µM SR 95531 (gabazine, Hello Bio, UK), a $GABA_A$ receptor antagonist, into the recording chamber. Recordings of miniature excitatory postsynaptic currents (mEPSCs) were isolated by washing 1 µM tetrodotoxin (TTX, Latoxan), a voltage-gated Na^+ channel blocker, into the chamber in the presence of SR 95531. Drugs were prepared in distilled water and aliquots stored at -20°C as a 1000-fold concentrated stock. Working concentrations were diluted in ACSF and washed into the chamber and slice for 5 min before recording. The recording was kept as long as the patch was in optimal conditions.

Evoked excitatory postsynaptic currents

Evoked currents (eEPSCs) were recorded in the presence of 6µM SR 95531 via stimulation (Digitimer Ltd. Model DS2 Constant voltage isolated stimulator) of the SC pathway. CA1 pyramidal cells were patched using the whole-cell configuration previously described. Stimulation (pulse duration 100µs) was applied by a stimulation glass micropipette filled with ACSF at a constant voltage (<20 V) and seal quality was monitored through the recording time. Paired currents were evoked every 10 s with 25 or 50 ms inter-stimulus interval. Each pair of stimuli was one sweep. Thirty sweeps were recorded for both inter-stimulus intervals. Paired-pulse ratios were calculated as the amplitude of eEPSC2/eEPSC1.

The criteria for spontaneous and miniature EPSC detection were that events must have an amplitude larger than -3 pA for longer than 2 ms, with a baseline tracking time of 10 ms, a dead time following an event of 10 ms; the rise from the start to the end must not last more than 4 ms. All events that had a faster decay time than rise were excluded. Instantaneous frequency of the events was calculated as a reciprocal of the mean of the intervals between the events. For analyses of amplitude and decay, events that arose from the decay of the previous EPSC were discarded. To obtain an average amplitude and decay time constant value per recording, the number of averaged digitised points was set at 5. Events where the decay was disrupted were excluded before obtaining the decay time from the time constant (τ) of the exponential curve fitted to the averaged signal.

For evoked currents, 30 sweeps were recorded for each inter-stimulus interval. Sweeps were averaged to obtain one trace for each interval and the amplitude (taken as the mean of five digitized points) of each evoked response was measured. eEPSC2/eEPSC1 was used to determine the ratio for each inter-pulse interval.

Statistical analyses

Appropriate statistical analyses were carried out to determine the significance between drug treatments and genotypes; GraphPad Prism 7 software was used. The sample sizes (n) refer to the number of animals used per condition. Means ± standard error of the mean (SEM) were used for analyses of fEPSPs and evoked EPSCs. Student`s t-test and two-way analysis of variance (ANOVA) followed by Sidak`s posthoc test was used to analyse the data. Statistical analysis of the last 10 minutes of LTP was performed by one-way ANOVA comparing all treatments per genotype. Differences were considered statistically significant if $p<0.05$.

When more than one recording was collected from the same animal, the results were averaged to give an n=1. Outliers which were mean ± 2 × standard deviation were discarded from the data set before carrying out statistical analyses. When measuring the amplitudes, the median was used as

the variation of events do not show a normal Gaussian distribution. As the medians would be expected to be normally distributed across animals within treatments, the means of the median amplitudes were considered for the statistical analysis. Unpaired t-tests were used to assess the difference in synaptic activity between genotypes only. Two-way ANOVA was used to determine the significance of increasing the dose of PLX5622 between genotypes on synaptic activity. Sidak's post hoc test was used to define the source of significance when a significant interaction between genotype and treatment was identified.

2.4 Histology

To evaluate the effects of depleting microglia by PLX5622 in the brain, microglia staining by immunohistochemistry was performed in the hemisphere that was not used for acute slices. Following 4% PFA fixation for 24 h, the brain was cryoprotected and stored in 30% sucrose (0.03% NaN_3 in PBS) at 4˚C until sectioning.

The brain hemisphere was sectioned transversally in 30 µm sections with a frozen sledge microtome (SM 2000-R, Leica) and stored in PBS (0.03% NaN_3) until the immunohistochemistry protocol was performed. In order to study the interaction of microglia with Aβ plaque deposition throughout the whole hippocampus, this region of the brain was sliced entirely and collected into a 24-well plate containing PBS (0.03% NaN_3). First, 24 sections were placed sequentially in the wells and the next 24 slices were added until the hippocampal region was no longer visible. Approximately four sections per well, representing slices through all areas of the hippocampus, were obtained.

A combination of primary antibodies was used to identify the activation of microglia by Iba-1/CD68 and also, to visualise Aβ plaques, luminescent conjugated oligothiophene dye, LCO, was used (**Table 1**).

All free-floating sections were washed in PBS and then permeabilised with 0.03% Triton X-100 PBS three times before application of blocking solution (3% goat serum 0.03% Triton PBS, 1hour, room temperature).

Primary antibodies (**Table 1**) were diluted in blocking solution and sections were incubated overnight at 4°C. Next day, sections were washed in PBS (0.03% Triton X-100) three times and incubated in the appropriate secondary antibody dilutions (3% Goat serum 0.03% Triton PBS) for 2 hours in the dark. After two PBS washes, sections were incubated for 30 minutes in diluted LCO Amytracker™ at room temperature and washed once more in PBS. Lastly, DAPI (4',6-diamidino-2-phenylindole 1:10,000 in PBS) was applied to all sections for 5 min. A final PBS wash was performed, and all tissue was mounted on SuperFrost Plus slides (Fisher) with Fluoromount G medium (Southern Biotech).

Primary antibody	Antigen/protein	Dilution	Secondary antibody	Dilution
Rabbit anti Iba-1 (Wako Pure Chemical Industries, 019-19741).	Ionised calcium binding adaptor 1): cytosolic marker by resting and activated microglia (Ito et al., 1998).	1:500	Goat-anti-rabbit, Alexa fluor 647nm (Invitrogen).	1:1000
Rat anti-CD68 (BioRad, MCA 1957).	Cluster of differentiation 68: mouse macrophage marker expressed on the intracellular lysosomes of activated microglia (da Silva and Gordon, 1999a).	1:500	Donkey ant-rat IgG, Alexa fluor 594nm (Invitrogen).	1:1000

Amyloid dye	Protein Detection	Dilution		
Luminescent conjugated oligothiophene, LCO (Amytracker™520)	Amyloidogenic proteins or peptides, it binds to cross-β-sheet structures (Rasmussen et al., 2017).	1:1000		

Table 1 Antibodies used in the present experiment. Description of the antigens, dilutions and catalogue references are indicated. Secondary antibodies are colour coded according to their emission signal.

Imaging and quantification

All slices were imaged by taking multiple photomicrographs across the hippocampus at 20X, which at the end were stitched together to obtain a single image per hippocampal region by using an epifluorescent EVOS® FL Auto Cell Imaging System microscope (Life Technologies). The images were produced using constant settings in light, exposure and gain. For quantification of microglia, Adobe Photoshop CC 2018 was used, and Aβ plaque detection was performed with Image-Pro (Version 7.0.0.591 for Windows Media Cybernetics, Inc. Rockville, USA).

Microglia cells were manually counted in the hippocampal region of a given section, considering CA1, CA3 and dentate gyrus (DG). Only cells with a clear DAPI cell body and ramified structure were counted as Iba-1$^+$, and cells with at least 30% of their body stained were considered as CD68$^+$ (**Figure 4.2**). Quantification was made blind to the genotype and treatment. Counts of three slices per animal were averaged to obtain the final count (n=6 animals).

For quantification of labelled Aβ plaques, the hippocampus was outlined and areas with overlapped or damaged tissue were excluded from the region of interest. Every image was calibrated, and a threshold of colour intensity was set individually to differentiate stained background from the real signal. Two parameters were considered for analysis: the percentage of plaque coverage and number of plaques that were detected in the whole hippocampus.

Statistical analyses

Appropriate statistical analyses were carried out to determine the significance between drug treatments and genotypes. Means ± standard error of the mean (SEM) were used throughout. Statistical analysis of the data was performed using GraphPadPrism 7 software. Student`s t-test and two-way ANOVA followed by Sidak`s posthoc test was used to analyse the data. Differences were considered statistically significant if $p < 0.05$.

Chapter 3

RESULTS:

SYNAPTIC TRANSMISSION CHANGES IN EARLY Aβ PLAQUE DEPOSITION OF APP[NL-G-F] AND APP[NL-F]

3.1 Introduction

In AD, both Aβ and Tau are suggested to have physiological roles in the synapse. APP and its fragments, including Aβ, could affect both excitatory and inhibitory synaptic transmission in health and disease (Hefter et al., 2020). Intense investigations in transgenic mouse models have shown alterations in varied synaptic properties at early stages of Aβ pathology before substantial synaptic loss, neuronal degeneration or plaque deposition (Marchetti and Marie, 2011). The earliest effects of Aβ rising levels under disease model conditions is suggested to be reflected in an increase of glutamate release probability, which occurs when Aβ concentration is barely detectable (Abramov et al., 2009; Cummings et al., 2015). By the time this project started, the APP knock-in mouse models were still relatively novel and electrophysiological characterisation showing excitatory synaptic transmission and plasticity was not available. Previous data from Edwards' laboratory analysed early synaptic changes in APP[NL-F] mice at 9 months of age: they identified an increased glutamatergic release probability from SC to pyramidal CA1 cells before Aβ plaques were evident in the hippocampus (Joel et al., 2018).Therefore, based on this evidence, I aimed to investigate if similar synaptic changes could be found in the APP[NL-G-F] model at an early stage of Aβ plaque development, 3.5 months-old. I also analysed excitatory synaptic transmission in APP[NL-F] mice at 10 months of age, just when the first Aβ

plaques start being visible, and both APP knock-in models were compared versus age-matched WT mice.

Within this chapter, I will show both extracellular field recordings and whole-cell patch clamp experiments, performed using 400 µm thick acute slices cut transversely to the long axis of the hippocampus. Careful attention to the process of slicing and incubation was considered to produce as many healthy neurons and dendrites as possible. Slices from mice under the described conditions were kept healthy for up to 8 hours. The excitatory trisynaptic hippocampal circuit is well preserved in the transverse view; this orientation optimizes the angle of the apical dendrites within the tissue slice for CA1 pyramidal neurons. Because the 3D structure of the intact hippocampus *in vivo* is curved, it is desired to expose the dendrites to course towards the surface in the plane of the slice along their length rather than to deeper into the slice. This preparation increases the likelihood of making proximal apical recordings providing stability and clarity of the cell layers needed for electrophysiological recordings (**Figure 3.1**).
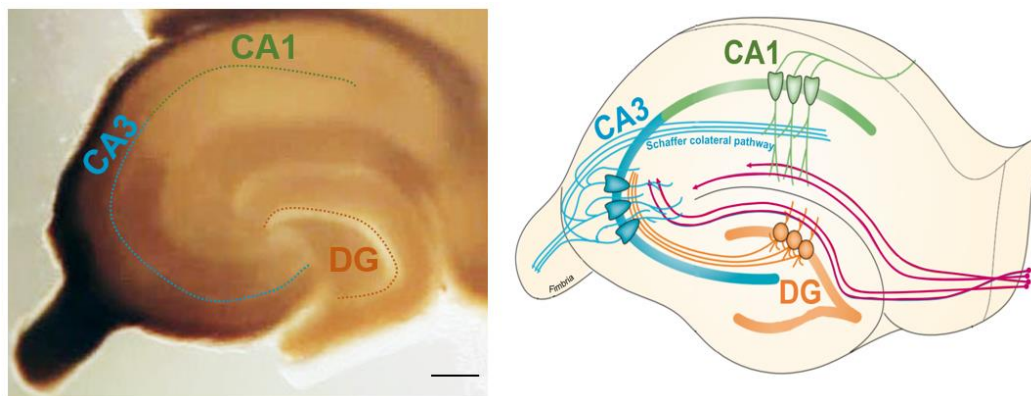
Figure 3.1. Image of an acute transverse hippocampal slice used in electrophysiology experiments. 400µm slice showing different cell body layers, obtained using a Stereo zoom Nikon microscope at 10x. Scale: 200µm (Neves et al., 2008).

The major form of hippocampal fast excitatory synaptic transmission depends on the release of glutamate from the presynaptic terminals which then binds kainate, AMPA and NMDA receptors from the postsynaptic terminal. Pyramidal neurons from the hippocampus and entorhinal cortex are the first affected in AD (Braak and Braak, 1991) and in consequence, these

synaptic alterations lead to the well-known memory deficits that represent the core symptoms of the disease. As synaptic plasticity is widely held to be the physiological basis of learning and memory, the effects of APP and Aβ on LTP have been widely studied (Hefter et al., 2020). LTP is a plasticity process that is typically mediated by NMDAR and the subsequent intracellular calcium cascades. Initially, after presynaptic stimulation, AMPARs are incorporated into the postsynaptic membrane; adding more receptors make subsequent inductions easier to elicit a response, the network becomes stronger and also long-lasting. As hippocampal CA3 cells project to ipsilateral CA1 pyramidal cells through SC (Neves et al., 2008), for this project, the hippocampal SC-CA1 path was chosen as the target of interest to analyse if synaptic transmission was impaired at the beginning of the APP knock-in mice pathology. First, electrophysiological characterization of young APP^{NL-G-F} mice is described, extracellular field recordings and evoked postsynaptic currents using whole-cell patch clamping. For the second part of this chapter, APP^{NL-F} evoked, spontaneous and miniature excitatory currents are also reported.

3.2 Electrophysiological characterization of SC-CA1 synapses of 3.5-month-old APP^{NL-G-F} mice

For the field configuration, synaptic responses from a population of neurons were recorded as a variation in the extracellular potential, and to assess the efficacy of synaptic transmission the fEPSP slope was analysed. Stimulation of CA3 fibres was performed to evoke dendritic responses from CA1 pyramidal neurons. The recording methodology consisted of first analysing the basal properties of the SC-CA1 synapses, by using I-O and PPR protocols, and then LTP was induced to study synaptic plasticity

3.2.1 Basal and short-term synaptic transmission of APP^{NL-G-F}

A good synaptic response was considered when there was a measurable fEPSP slope following a fibre volley signal, which was an indication of the presynaptic action potential arriving at the recording site (**Figure 2.1**). The fEPSPs considered in the following results showed a smooth decaying phase

at a stimulus intensity between 10 to 30 V. Then the I-O and PPR protocols were used; the I-O reflects overall synaptic efficacy evoked after stimulation of CA3 fibres; such fibres evoke an action potential, and their synaptic release/activity is indicated by the CA1 postsynaptic response from the dendrites recorded. If the stimulus is stronger, more fibres are recruited, and the amplitude (slope) of the response is bigger. The PPR protocol reflects a measure of short-term plasticity that occurs when two stimuli are applied in close succession. Varying the time between the two pulses provides information about the interval times at which the responses interact. The PPR is the ratio of the amplitude of the second response to that of the first and it depends on the probability of vesicular release at the synapse. The PPR is inversely related to the glutamate release probability and it is used as a measure of the release probability (Manabe et al., 1993).

The fibre volley could not be analysed as it was indiscernible from the stimulus artefact. The I-O relationship from both genotypes showed increased fEPSP size when the stimuli were intensified, and the APP^{NL-G-F} particularly showed a significant increase in the I-O relationship when stimulation was more than 30 V. There was a main significant effect of input voltage identified ($p<0.0001$) and also an interaction between input stimulus and genotype was revealed ($p<0.0001$) (**Figure 3.2A**). The PPRs from APP^{NL-G-F} mice did not differ significantly from WT mice and as expected, the inter-stimulus interval had a significant effect on the responses evoked ($p<0.0001$); PPR higher than 1 was seen from 25 ms to 200 ms intervals which represent paired-pulse facilitation (PPF) mechanism (enhancement of the second response when two stimuli are delivered in a short period of time), but responses at 400 ms decreased slightly (not significant between genotypes). No interaction was detected between the genotype and the inter-stimulus interval **(Figure 3.2B)**

A Input-Output

B Paired-pulse profile
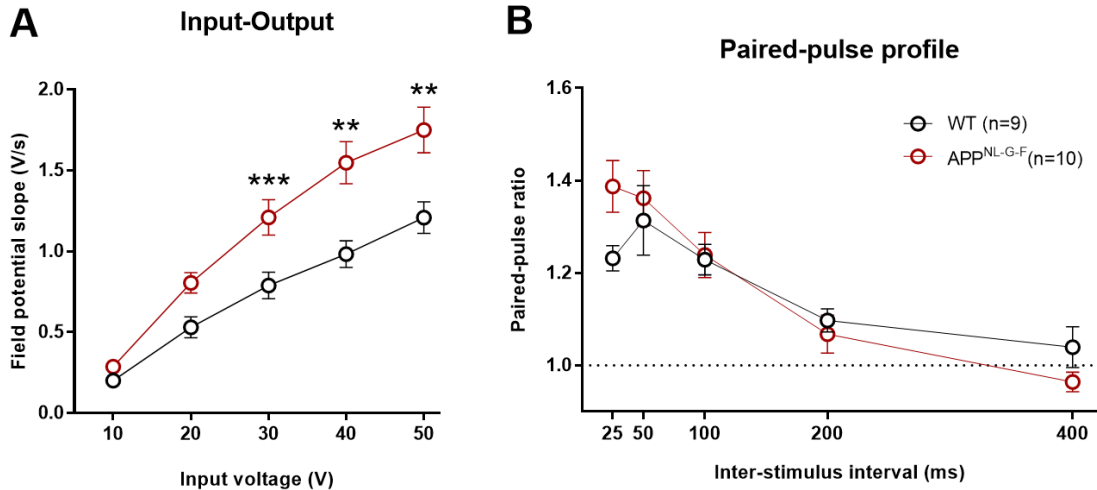
Figure 3.2 Basal synaptic transmission recorded at the SC-CA1 synapse of 3.5-month-old mice. (A) I-O relationship plot shows the mean of fEPSP slopes at different stimuli intensities for both genotypes used. Two-way ANOVA, Sidak's post hoc comparison indicated a significant effect in the APP^{NL-G-F} at >30 V (**p<0.01; ***p<0.001). **(B)** The Paired-pulse ratio in WT and APP^{NL-G-F} obtained from a population of CA1 neurons in response to stimulation of SC fibres. No difference was detected between genotypes at 25-400 ms inter-stimulus intervals (two-way ANOVA). Error bars indicate SEM.

3.2.2 Long-term synaptic plasticity of APP^{NL-G-F}

High-frequency stimulation (HFS) of excitatory synapses on to hippocampal pyramidal cells of the CA1 region can lead to strengthening evoked fEPSP. It is thought that this neuronal activation resembles the physiological activity in the brain when information is being acquired and stored (Abrahamsson et al., 2016). Tetanisation is a standard LTP induction paradigm that uses HFS which potentiates the postsynaptic response amplitudes for an extended period of time (Bliss and Lomo, 1973). To investigate whether the expression of the triple mutation in the APP gene affects the long-term synaptic plasticity, fEPSPs were recorded in slices prepared from APP^{NL-G-F} and responses were monitored for 60 minutes post-HFS. Synaptic plasticity assessment was split into post-tetanic potentiation (PTP, 1st-minute post-tetanus), short-term potentiation (STP, 8-12 minutes post-tetanus) and LTP (51-60 minutes post-tetanus).

LTP was successfully induced in both WT controls and APP^{NL-G-F} mice. The APP^{NL-G-F} initial levels after induction were almost identical to the WT

group (**Figure 3.3B**). No significant differences were found when analysing PTP or STP (**Figure 3.3D**), and eventually by minute 20 both genotypes reached similar fEPSP slope values which remained during the rest of the recording time. As expected LTP induction after HFS resulted in a larger magnitude (WT: 143.4±7.3% vs APP^{NL-G-F}: 147.1±7.3%) of the response indicating that SC-CA1 communication is not affected by amyloid pathology in the young APP^{NL-G-F} (**Figure 3.3D**).

LTP recordings were monitored every 10 seconds using paired stimuli with a 50 ms interval. This protocol allows calculation of PPR throughout field recording experiments to analyse presynaptic mechanisms. WT and APP^{NL-G-F} PPRs values obtained did not differ between baseline and LTP; as expected, PPR values in PTP are decreased indicating that there was a higher neurotransmitter release (**Figure 3.3C, E**). The absence of difference between genotypes means that APP^{NL-G-F} mice were able to maintain strong stimulation at the SC-CA1 synapses and plasticity mechanisms are not impaired.

3.2.3 Evoked Excitatory activity in APP^{NL-G-F}
EPSC recordings at 3.5 months of age were obtained in collaboration with MSc student Carlijn Peerboom.

Apart from assessing basal synaptic transmission and plasticity in 3.5-month-old APP^{NL-G-F} mice, a high-resolution electrophysiological characterisation was performed by evoking activity to a particular axonal SC pathway and recording the responses of a recipient CA1 neuron. Excitatory postsynaptic currents (EPSCs) were measured using whole cell voltage clamp on CA1 neurons while applying paired voltage stimuli in SC in the presence of the GABA$_A$ receptor antagonist gabazine throughout the recording.
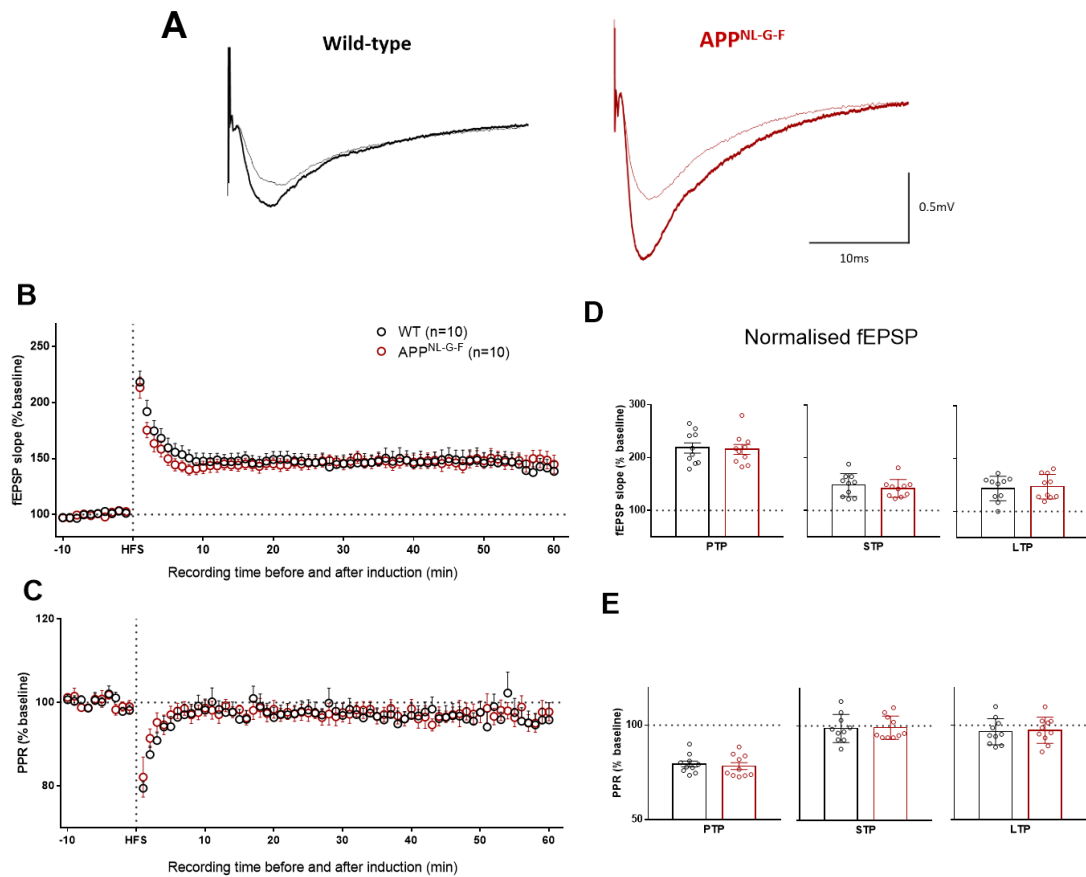
Figure 3.3 No difference in LTP recorded at the SC-CA1 synapse of APP^NL-G-F mice. (A) Sample fEPSP traces from individual experiments in acute hippocampal slices. They represent the trace just before LTP induction (thin line) and an hour after LTP induction (thick line). Black traces are examples from the WT group, and red traces are APP^NL-G-F. **(B)** The left panel shows a comparison of the fEPSP slope before (baseline) and after high-frequency stimulation (HFS) in WT and APP^NL-G-F mice over time. All data presented were normalised to the 10 min baseline. **(C)** Time course of the paired-pulse ratio (PPR) calculated relative to baseline (50 ms inter-stimulus interval). Data presented as mean ± SEM. **(D, E)** Qualitative analysis of the fEPSP slope and PPR shown in scatter plots relative to baseline. PTP represents the 1st minute after induction, STP 8-12 min and LTP 51-60 min. T-tests showed no significant differences between the genotypes.

The responses of CA1 pyramidal neurons to SC stimulation were recorded and the PPR was calculated using two different inter-pulse intervals. As expected, WT synapses show paired-pulse facilitation with both inter-stimulus intervals (**Figure 3.4B**). APP^NL-G-F PPRs were almost identical to the WT values and no statistical difference was identified.
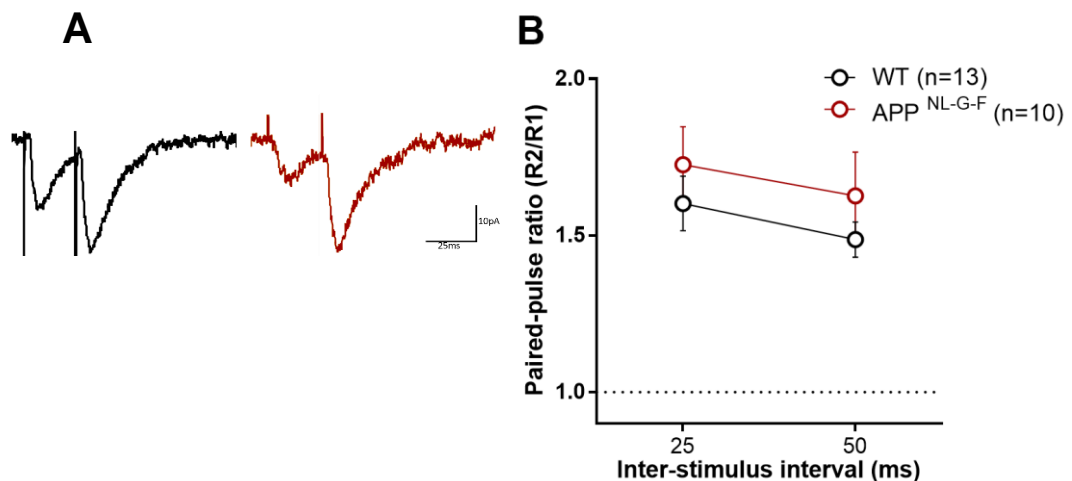
Figure 3.4 No difference in the paired pulse ratio recorded at the SC-CA1 synapse of APP^{NL-G-F} mice. (A) Representative traces of CA1 evoked postsynaptic excitatory currents after paired stimuli at an inter-pulse interval of 25 ms. **(B)** PPRs obtained from CA1 pyramidal cells in response to stimulation of the SC pathway. No difference was detected between genotypes at 25 ms and 50 ms of inter-stimulus intervals. Error bars indicate SEM.

3.3 Electrophysiological characterization of SC-CA1 synapses of 10-month-old APP^{NL-F} mice

The APP^{NL-F} Aβ_{42} levels start rising at 2 months of age but it is until around 6 months of age when the first couple of Aβ plaques can be identified in cortical areas (Saito et al., 2014). Eventually, by 9 months, very early deposition of plaques in hippocampus is noticeable together with unaltered long-term synaptic plasticity, however what is changing at this age is the glutamate release probability from SC-CA1 synapses (Benitez et al., 2021). Based on the unpublished Edwards' lab evidence and to follow up on Joel et al (2018), I investigated in 10-month-old APP^{NL-F} mice more specific synaptic properties by evaluating EPSCs from CA1 pyramidal cells with and without exogenous stimulation using whole-cell patch clamp configuration. By recording spontaneous activity certain information can be inferred that relates to the presynaptic network such as, the frequency of action potential driven neurotransmitter release, number of release sites and neurotransmitter release probability of individual synapses. Additionally, postsynaptic factors like changes in postsynaptic receptor density, the conductance of channels and receptor kinetics can be explored. By using the high-resolution patch

clamp technique, frequency, amplitude, and decay time of spontaneous synaptic events were measured.

For this set of experiments, about half of the animals from WT and APP[NL-F] groups were fed with standard grain-based diet, and for the other half the mice diet was changed to a refined food used as PLX5622-vehicle. There was no main effect of food type when both groups or mice were compared in synaptic transmission (p>0.1), and therefore both diet groups were combined. It should be noted that there was a trend towards an interaction between the type of food and genotypes (p>0.05), but this was not statistically significant (two-way ANOVA).

3.3.1 Spontaneous excitatory postsynaptic currents in APP[NL-F]
sEPSCs and mEPSCs recordings at 10 months of age were obtained in collaboration with MSci student Natalie Wong

Spontaneous postsynaptic currents can reflect both a single quantum or action-potential-induced multi-quantal synaptic responses. It is considered that a solitary quantum response is evoked by neurotransmitter release from a single vesicle representing discharge at a single synapse, this activity is known as miniature EPSCs (mEPSCs); these miniature responses can be detected during total blockade of action potentials by tetrodotoxin (TTX). On the other hand, spontaneous action potentials within a presynaptic neuron can trigger neurotransmitter release from either one or multiple presynaptic sites, then it is called spontaneous EPSCs (sEPSCs) (Malkin et al., 2014).

Under voltage-clamp at -70 mV, sEPSCs were isolated by inhibiting GABA$_A$ receptors. The membrane resistance of the patched CA1 pyramidal cells was obtained from examination of a test pulse (+5mV, 40ms) applied just after achieving the whole-cell configuration. The frequency of sEPSCs and mEPSCs within the CA1 of the hippocampus were not found to differ significantly between genotypes, indicating that the number of release sites, release probability and action potentials generation are not affected by the presence of the double mutation in the humanised APP sequence at this age. A significant main effect of TTX was detected (p<0.0001), indicating the

contribution of spontaneous AP-driven release in the absence of TTX (**Figure 3.5A**). TTX treatment was seen to result in a significant reduction in the median amplitude of EPSCs recorded from both WT and APP^{NL-F} mice ($p<0.001$). The decay time of EPSCs was not seen to differ between genotypes or with TTX application (**Figure 3.5C, D**), indicating that neither the presence of the mutations nor TTX affects AMPA receptors kinetics.
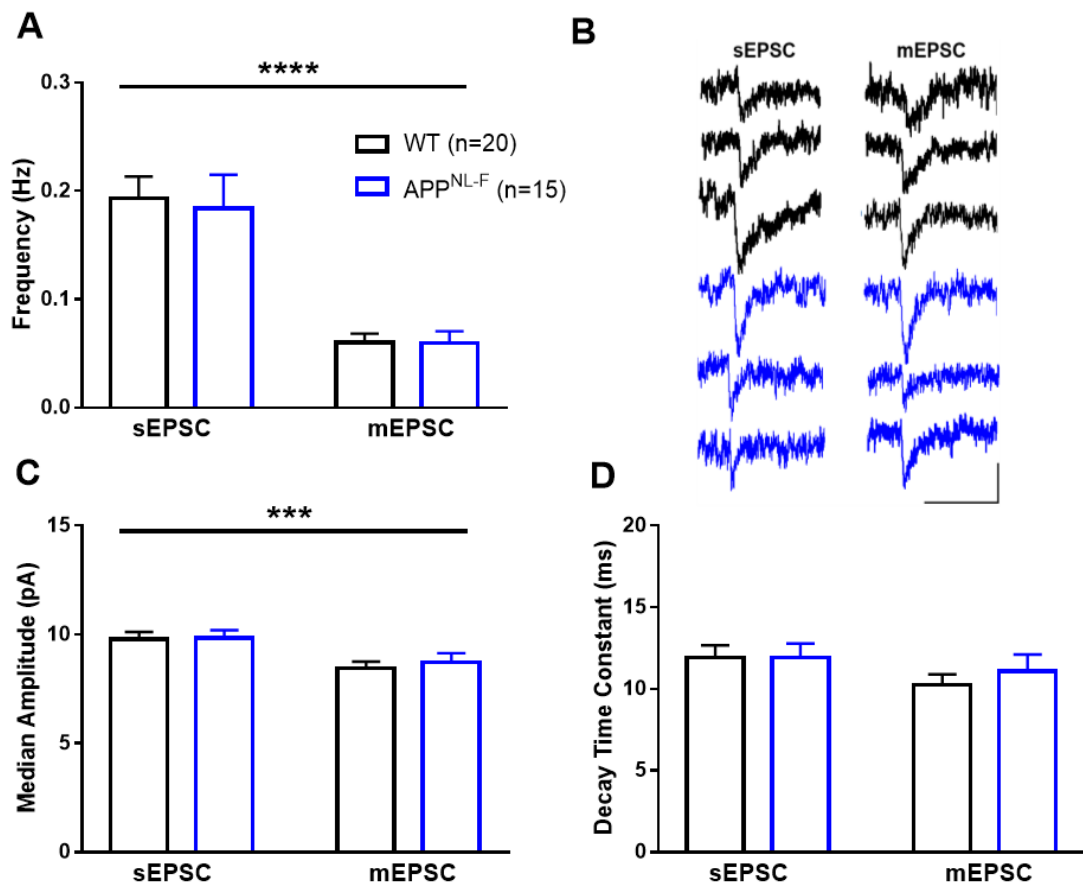
Figure 3.5 No difference between genotypes in spontaneous excitatory currents recorded with (mEPSC) or without (sEPSC) TTX from CA1 pyramidal neurons at 10 months of age. (A) Frequency of excitatory currents, a significant effect of TTX was detected using two-way ANOVA (****$p<0.0001$). **(B)** Representative current traces recorded in the presence and absence of TTX, scale: 10 pA, 50 ms. **(C)** Mean of the median amplitude. A significant effect of TTX was detected using a two-way ANOVA (***$p<0.001$) **(D)** No significant changes detected in the decay time of excitatory currents. Error bars indicate SEM.

3.3.2 Evoked Excitatory activity in APP^{NL-F}

In order to investigate the possibility of glutamate release probability impairments from SC-CA1 synapses due to early Aβ plaque deposition in APP^{NL-F} mice, I recorded responses from CA1 pyramidal cells in response to paired pulse stimulation of the SC using the same method described for the APP^{NL-G-F} experiments. 10-month-old mice in the present study, irrespective of genotype, were observed to display typical PPF at both inter-stimulus intervals tested (**Figure 3.6**). Interestingly, APP^{NL-F} mice displayed a decreased PPR which resulted in a significant overall effect of genotype ($p<0.0001$) and an interaction ($p<0.05$), but no significant effect of inter-stimulus interval by two-way ANOVA. At 25 ms inter-stimulus interval, APP^{NL-F} had a significantly lower paired-pulse ratio than the WT mice ($p<0.0001$).
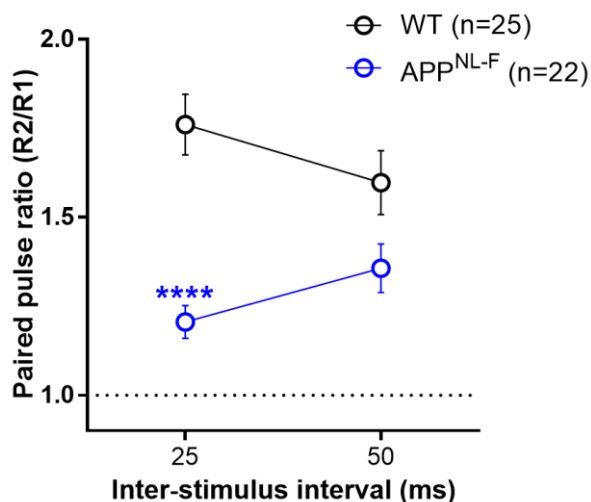
Figure 3.6 APP^{NL-F} mice showed decreased paired-pulse ratios recorded at the SC-CA1 synapse at 10 months of age. PPRs obtained from CA1 pyramidal cells in response to stimulation of CA3 axons. At 25 ms of inter-stimuls interval a significant reduced PPR was found by two-way ANOVA (****$p<0.0001$). Error bars indicate SEM.

SUMMARY

The results presented in this chapter revealed an overall absence of synaptic impairments at early stages of amyloid pathology in both APP knock-in models. Basal synaptic transmission, short-term plasticity, LTP and evoked excitatory postsynaptic activity showed no discernible differences to WT control mice at 3.5 months of age. Additionally, I analysed APP^{NL-F} model at 10 months of age. There were no differences between WT and knock-in mice in terms of the frequency, amplitude and decay time of spontaneous and miniature excitatory currents recorded. However, an increase in glutamate release propability (reflected as a decreased paired-pulse ratio) was revealed in these mice. These data indicate that Aβ-mediated synaptotoxic effects partially failed to cause any significant functional deficits in the hippocampal CA1 region of APP knock in mice when first plaques are found in the brain, and it was clear that neurotransmitter probability of release is differently affected in the APP^{NL-F} and the APP^{NL-G-F} mice.

Chapter 4

RESULTS:
MICROGLIA REMOVAL EFFECTS IN EARLY PLAQUE DEPOSITION OF APP KNOCK-IN MICE – A HISTOLOGICAL STUDY

4.1 Introduction

Neuroinflammatory markers have been widely reported in both human subjects and transgenic mouse models for AD. Accumulated and activated microglia are crucial features of AD pathology that are hypothesised to be part of an abnormal immune response that may drive neuronal death and cellular dysfunctions in the disease (Griffin, 2006). This idea is supported by GWAS that have identified polymorphisms in inflammation-associated genes as risk factors for the development of AD (Guerreiro et al., 2013; Lambert et al., 2013). It is considered that some protein markers associated with cell activation, such as cluster of differentiation 68 (CD68), or with resting characteristics, such as ionized calcium-binding adaptor molecule-1 (Iba-1), are consistently elevated in the AD brain (Hopperton et al., 2018). Highly up-regulated microglia can be especially found in the proximity of amyloid plaques in AD brains (Condello et al., 2018), which particularly indicates an activated response to Aβ pathology and a clear interaction between those two hallmarks of the disease.

Iba-1 is a cytoplasmic protein expressed in monocyte lineage cells in the brain and it is mainly expressed in microglia; it is considered a general marker for microglia that does not distinguish between different subsets or phenotypes (Ito et al., 1998). **CD68** is common in macrophage lineage cells and it is localised in microglia within the brain parenchyma, and perivascular

macrophages. It labels the lysosome and then it is a marker for activated phagocytic microglia; gene expression and histochemistry reports using CD68 have found high levels of positive cells in the hippocampus of AD samples (da Silva and Gordon, 1999b; Hopperton et al., 2018). According to Saito et al. (2014) microgliosis is present in both APP knock-in lines when Aβ plaque deposition is robust at 18 months of age, and they concluded that the Arctic mutation triggered a stronger pro-inflammatory response than just the Swedish and the Iberian/Beyreuther mutations. Masuda et al. (2016) confirmed such information and found that the APP^{NL-G-F} mice had a dense distribution of Iba-1 positive cells in the hippocampus around Aβ plaques at 12 months, but such levels started increasing from 6 months of age.

It has been demonstrated that microglia are fully dependent on CSF1R signalling for their survival (Ginhoux et al., 2013; Green et al., 2020). Manipulation of microglia numbers has been shown by administering CSF1R inhibitors that cross the BBB which leads to ~80% of cell elimination within 7 days of treatment (Elmore et al., 2014). Such effect is drug-dependent, and microglia can remain eliminated for weeks or months, but repopulate when the drug is withdrawn. It has been stated that microglia are the only cell type to express CSF1R in the brain parenchyma which makes such treatments highly specific and efficient, however a very recent publication showed that peripheral monocytes/macrophages could also be affected by CSF1R treatments and their functions could be compromised due to inhibition (Lei et al., 2021).

In this study, first I explored the efficacy of the drug PLX5622 to deplete microglia numbers in the APP knock-in mice and alongside this set of experiments, synaptic transmission was also evaluated after PLX5622 administration, described in Chapter 5. Until now, most of the reports showing microglia depletion models in AD have used transgenic mice, which as explained before, present overexpression of APP fragments that misconceive the development and progression of the disease. Here, I used the APP knock in mice to avoid such overexpression and I eliminated microglia at an early stage of Aβ plaque deposition. To eliminate microglia and assess their role, PLX5622 was administered to WT and APP knock-in mice; finally, by using

immunohistochemistry, I analysed numbers of proliferative and phagocytic microglia with or without the presence of Aβ plaques.

Performing pathological Aβ plaques and cell count analysis allows these novel APP knock-in mice to be placed in context with existing literature using these models or other transgenic mice. Most of the reports published until now have focused on heavy plaque load stages where microgliosis is evident, then the upcoming results will contribute to the histological characterisation and validation of these mice for future AD research.

4.2 Microglial survival and activation in the hippocampus of APP^NL-G-F mouse model, 3.5 months old.

To elucidate the net contribution of microglia to synaptic function before profound deposition of plaques, PLX5622 compound, mixed with standard control food, was provided to 1.5-month-old mice for 7 weeks (**Figure 4.1A**). As APP^NL-G-F line develops Aβ plaques in the hippocampus at around 3 months of age (Saito et al., 2014), I aimed to target the stage when plaques were not yet deposited in the brain, and also I considered physiological synaptic pruning by microglia, which is generally proposed to be complete by postnatal week 4 (Paolicelli et al., 2011). Two doses of PLX5622 were used to assess partial (Low: 300 mg/kg) or total (High:1200 mg/kg) depletion of microglia. After starting the PLX5622 treatments, mouse weights were monitored weekly until recording day to verify food intake and optimal growth. All the treated mice gained weight consistently which was a reflection of food being consumed and no adverse effects were found (**Figure 4.1B**).
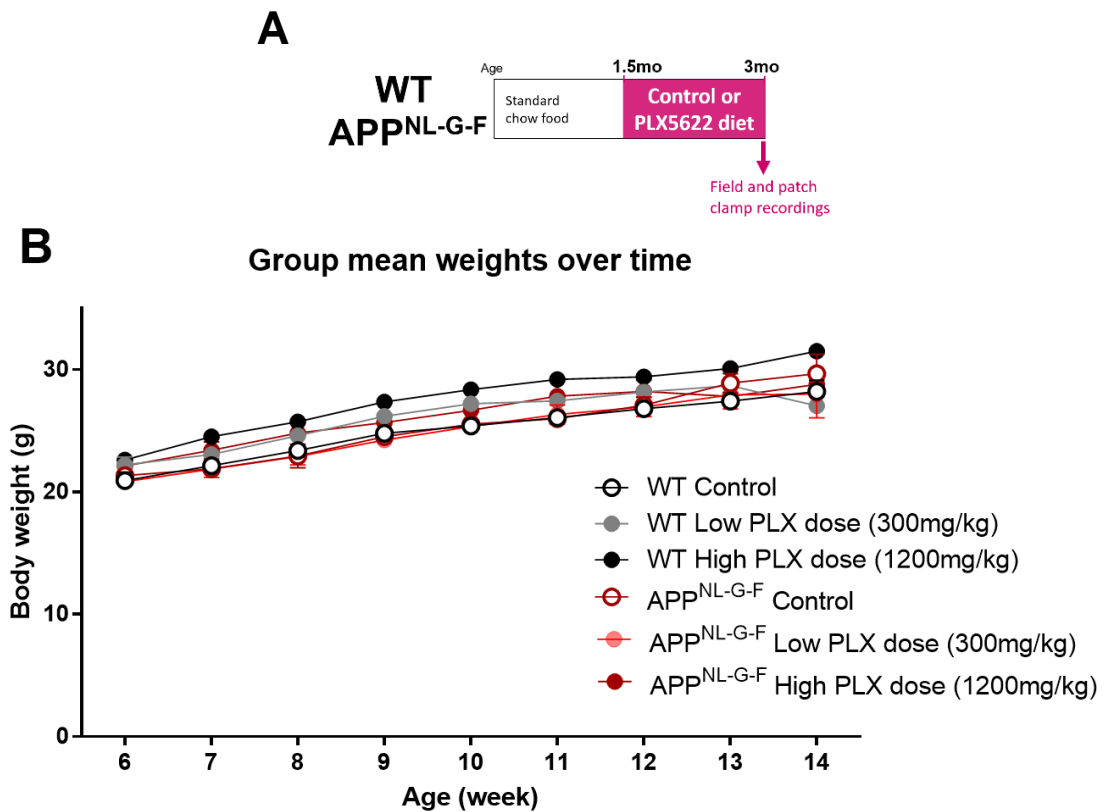
Figure 4.1 Timeline of experiments and average weights of mice treated with or without PLX5622 across the whole experiment. (A) 1.5-month-old WT or APP^NL-G-F mice were treated with control food or PLX5622 for 7 weeks to eliminate microglia. **(B)** Average weights of mice placed on different diets at 1.5 months of age until approximately 3.5 months (n=8). Error bars indicate SEM.

In order to characterise microglial survival and activation at an early amyloid pathology stage, I applied fluorescent immunohistochemistry to brain sections of APP^NL-G-F and WT mice at 3.5 months of age and quantified the total and CD68 positive microglia (CD68+) in the hippocampus. Hippocampal sections were produced by tile-stitching captures with an x20 objective lens using epifluorescent microscopy. Iba-1 positive cells (Iba-1+) were manually quantified only when they presented a clear cell body colocalised with the nuclear counterstain DAPI. Activated microglia was considered when about >30% of the cell body was co-stained with CD68 (**Figure 4.2**).
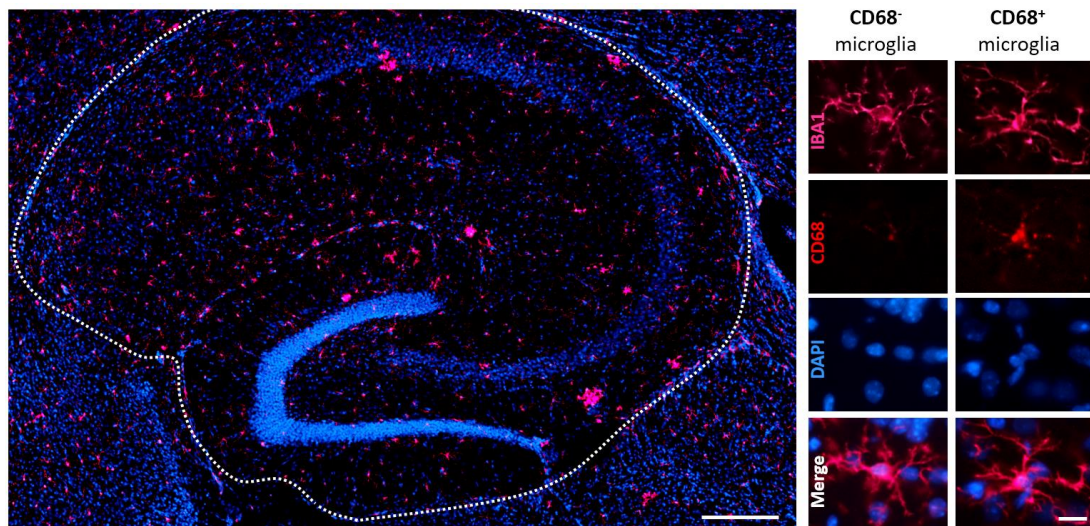
Figure 4.2 Microglial activation in the hippocampus of the APP^{NL-G-F} mouse model. Left panel is a representative image to show the transverse hippocampus of a 3.5-month APP^{NL-G-F} mouse. Dotted white line shows the area of interest employed for microglia and Aβ plaques quantification. Scale bar 200μm. Right panel shows representative Iba-1 non-activated microglia (CD68⁻) and activated microglia (CD68⁺) with colocalised nuclear DAPI signal. Scale bar 20μm.

4.2.1 CSF1R inhibition effects in Aβ plaque deposition of young APP^{NL-G-F}.

Following 7 weeks of PLX5622 or control treatment, APP^{NL-G-F} mice hippocampal sections were treated with luminescent conjugated oligothiophenes (LCO) and antibodies for Iba-1 with CD68 to visualise Aβ plaques and microglia, respectively. LCOs are a unique class of amyloid dyes that yield fluorescence emission spectra when bound to the protein aggregates (Rasmussen et al., 2017). PLX5622 treatments were successful in both genotypes, WT and APP^{NL-G-F}, and microglia cells were clearly reduced (**Figure 4.3**). Low dose of PLX5622 of the drug reduced microglia numbers by about 50% and the higher dose showed almost no microglial signal, about ~90% less cells. Microglia were clustered around Aβ plaques in the APP^{NL-G-F} mice, showing an activation state.

Control | Low PLX dose | High PLX dose

WT · App^NL-G-F · WT · App^NL-G-F · WT · App^NL-G-F

Iba-1 · CD68 · Aβ · Merge

Irrespective of genotype, PLX5622 decreased densities of Iba-1$^+$cells and two-way ANOVA revealed a main effect of drug dose (p<0.0001) (**Figure 4.4A**), but no effects between genotypes nor an interaction. I further quantified the CD68$^+$ cells in the same region. Similarly, CD68$^+$ microglia numbers were significantly reduced after PLX5622 treatments in both genotypes (p<0.0001). Sidak corrected simple comparison within drug indicated that all doses were different from each other except for the low dose versus control group (**Figure 4.4B**). Finally, in order to assess the activation ratio, CD68$^+$ microglia were calculated relative to the Iba-1$^+$ cell counts. Although the overall number of CD68$^+$ decreased, the proportion of the remaining microglia that were CD68$^+$ increased with PLX5622 treatment (p<0.0001) (**Figure 4.4C**). There were no significant main effects of genotype, nor were there drug with treatments interactions.
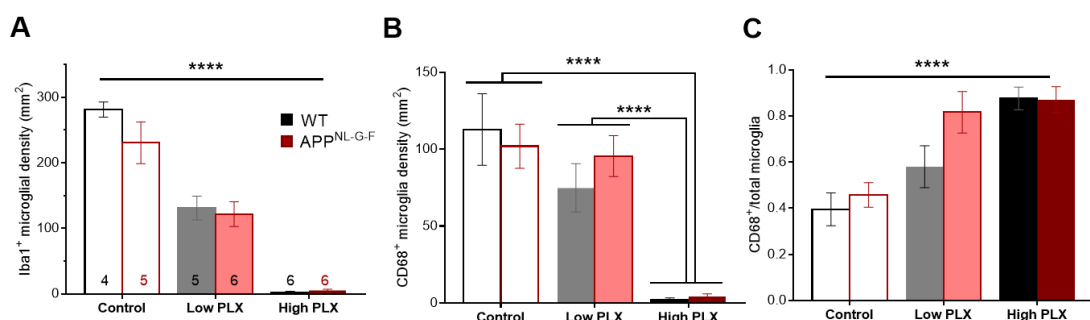
Figure 4.4 PLX5622 depletion of microglia in WT and APP^{NL-G-F} 3.5-month-old mice. (A) Densities determined as cells that were Iba-1$^+$ microglia. **(B)** Total densities of Iba-1$^+$ microglia that were also CD68$^+$ in the hippocampus of mice treated with or without PLX5622. **(C)** Densities of CD68$^+$ microglia in the total microglia population showed an overall significant effect of PLX5622 drug treatments in both genotypes. Data shown as mean ± SEM. Two-way ANOVA followed by Sidak corrected simple comparisons, ****p<0.0001.

To further investigate if PLX5622 treatments altered Aβ plaque development in APP^{NL-G-F} mice, plaque deposition was also assessed by quantification of LCO signal (**Figure 4.5A**). The percentage of plaque coverage of the hippocampus was not significantly different between the doses (**Figure 4.5B**) nor was the density of plaques within the hippocampal region per section (**Figure 4.5C** insert). There was an overall significant effect of plaque size (p<0.0001; two-way ANOVA), reflecting that there are more small than large plaques. While there is no main effect of drug, there was a significant interaction between size and dose (p<0.01). Post hoc analysis comparisons showed significant effects of both low dose (p<0.001) and high dose (p<0.0001) PLX5622 for plaques up to 200μm^2 but not for larger plaques (**Figure 4.5C**).
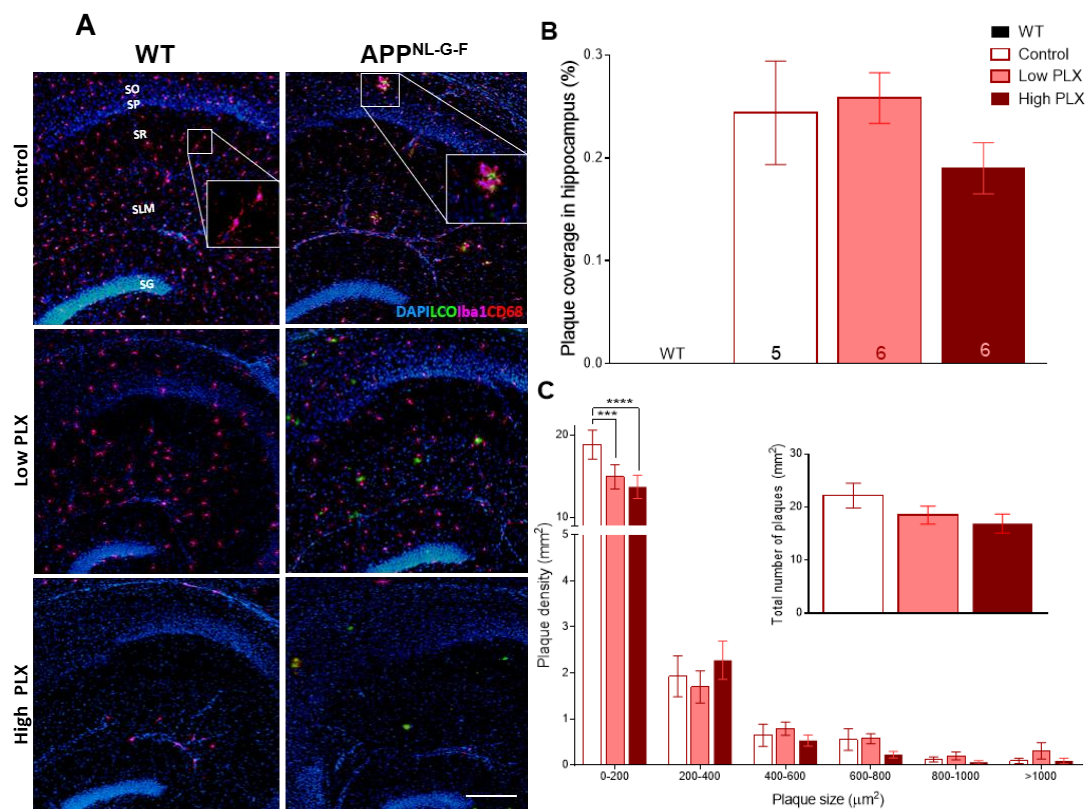
Figure 4.5 Aβ plaque deposition in 3.5-month-old APP^{NL-G-F} mice treated with PLX5622 for 7 weeks. (A) Representative fluorescent micrographs of WT and APP^{NL-G-F} CA1 region of hippocampus following labelling of Aβ with LCOs and fluorescent immunohistochemical staining for Iba-1 and CD68. *Stratum oriens* (SO), *stratum pyramidale* (SP), *stratum radiatum* (SR), *stratum lacunosum moleculare* (SLM) and *stratum granulosum* (SG) are indicated in the WT Control condition. Scale bar 200 μm. **(B)** Plaque coverage % in the whole hippocampus showed no effects of treatments with PLX5622.

Sample sizes are indicated in each bar. **(C)** Size-frequency distribution in APP^{NL-G-F} mice at 3.5 months of age. Post hoc test for within plaque size bin comparisons showed a significant reduction of small plaques when partial or total ablation of microglia was induced, ***p<0.001, ****p<0.0001. Insert: Overall density of Aβ plaques in the hippocampus of young APP^{NL-G-F}. Error bars indicate SEM.

4.3 Microglial survival and activation in the hippocampus of APP^{NL-F} mice, 10 months old.

To further investigate the status of microglia in the APP knock in mice, I studied Iba-1 and CD68 expression in the APP^{NL-F} mouse model versus WT. It has been stated that microglia accumulate with age starting at around 6 months of age, concurrent with plaque formation (Saito et al., 2014). The same method previously described was followed: this time, mice were treated chronically for 3 months with the low or high dose of PLX5622 to deplete microglia, double the time than in the APP^{NL-G-F} experiment, from 7 to 10 months of age (**Figure 4.6A**). After starting the PLX5622 treatments, mice weights were monitored weekly until recording day to verify food intake. All mice treated showed a steady weight and no adverse effects or abrupt loss of weight were found (**Figure 4.6B**). 10-month-old APP^{NL-F} mice brains were immune-stained for Iba1 and CD68 and stained with LCOs to analyse the microglial contribution to the progression of the pathology.
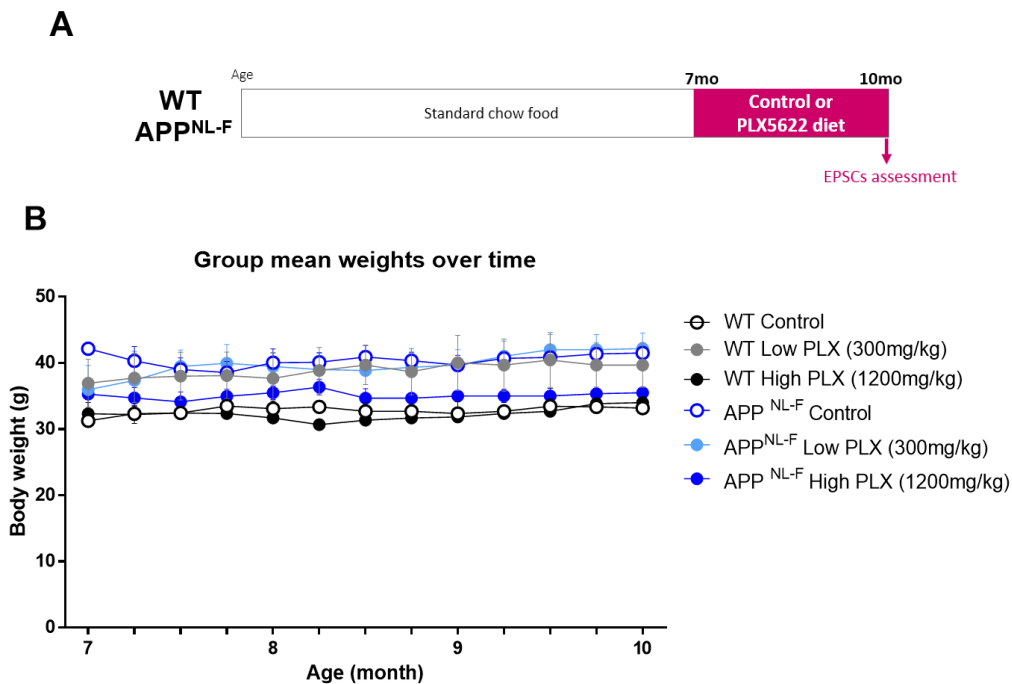
Figure 4.6 Timeline of experiments and average weights of mice treated with or without PLX5622 across the whole experiment. (A) 7-month-old WT or APP[NL-F] mice were treated with control food or PLX5622 for 3 months to eliminate microglia. **(B)** Average weights of mice placed on different diets at 7 months of age until 10 months (n=3). Error bars indicate SEM.

4.3.1 CSF1R inhibition effects in Aβ plaque deposition of APP[NL-F].

It was evident that PLX5622 treatment was successful in both genotypes, as microglia cells were clearly partially or almost totally eliminated (**Figure 4.7**). Also, plaque deposition was considerably lower than the one observed in the APP[NL-G-F] mice.

Quantification of total Iba-1^{+} microglia was performed after inhibition of the CSF1R by using PLX5622 and, irrespective of genotype, cells number were clearly reduced. Two-way ANOVA revealed a main effect of drug ($p < 0.0001$) but no effects of genotype or an interaction. Sidak corrected simple comparisons within drug revealed significance between all doses (**Figure 4.8A**). PLX5622 also decreased densities of microglia that were CD68^{+}. A significant main effect of drug dose was revealed by two-way ANOVA ($p < 0.0.0001$), but again no effects of genotype nor an interaction were found. Sidak corrected simple comparisons within drug indicated differences between all the groups analysed (**Figure 4.8B**). Similar to what it was seen in the APP[NL-G-F] groups, although the number of Iba-1^{+} and CD68^{+} microglia

significantly decreased, the proportion of the remaining microglia were still activated and the numbers increased with drug treatments ($p<0.001$) (**Figure 4.8C**). There were no significant main effects of genotype and there was not an interaction between PLX5622 dose with the genotypes.

To assess if the chronic absence of microglia was altering Aβ plaque deposition in the APP^{NL-F} model, density of plaques and size were also analysed by quantification of the LCO signal (**Figure 4.9A**). Similar to the APP^{NL-G-F} result, the percentage of plaque coverage of the hippocampus was not significantly different after 3 months of PLX5622 treatments (**Figure 4.9B**), nor was the total density of plaques within the hippocampal region per section (**Figure 4.9C insert**). Contrasting with the APP^{NL-G-F} model, the tendency for a reduction in small plaques was less evident and did not reach a statistically significant value by two-way ANOVA (**Figure 4.9C**); none of the comparisons showed interactions between drug doses and the variables evaluated. Overall, at 10 months of age, the APP^{NL-F} displayed a very early development of Aβ plaques, this level of deposition was unaffected by partial or total depletion of microglia.

Control   Low PLX dose   High PLX dose

WT   APP^NL-F   WT   APP^NL-F   WT   APP^NL-F

Iba-1

CD68

Aβ

Dapi/Merge
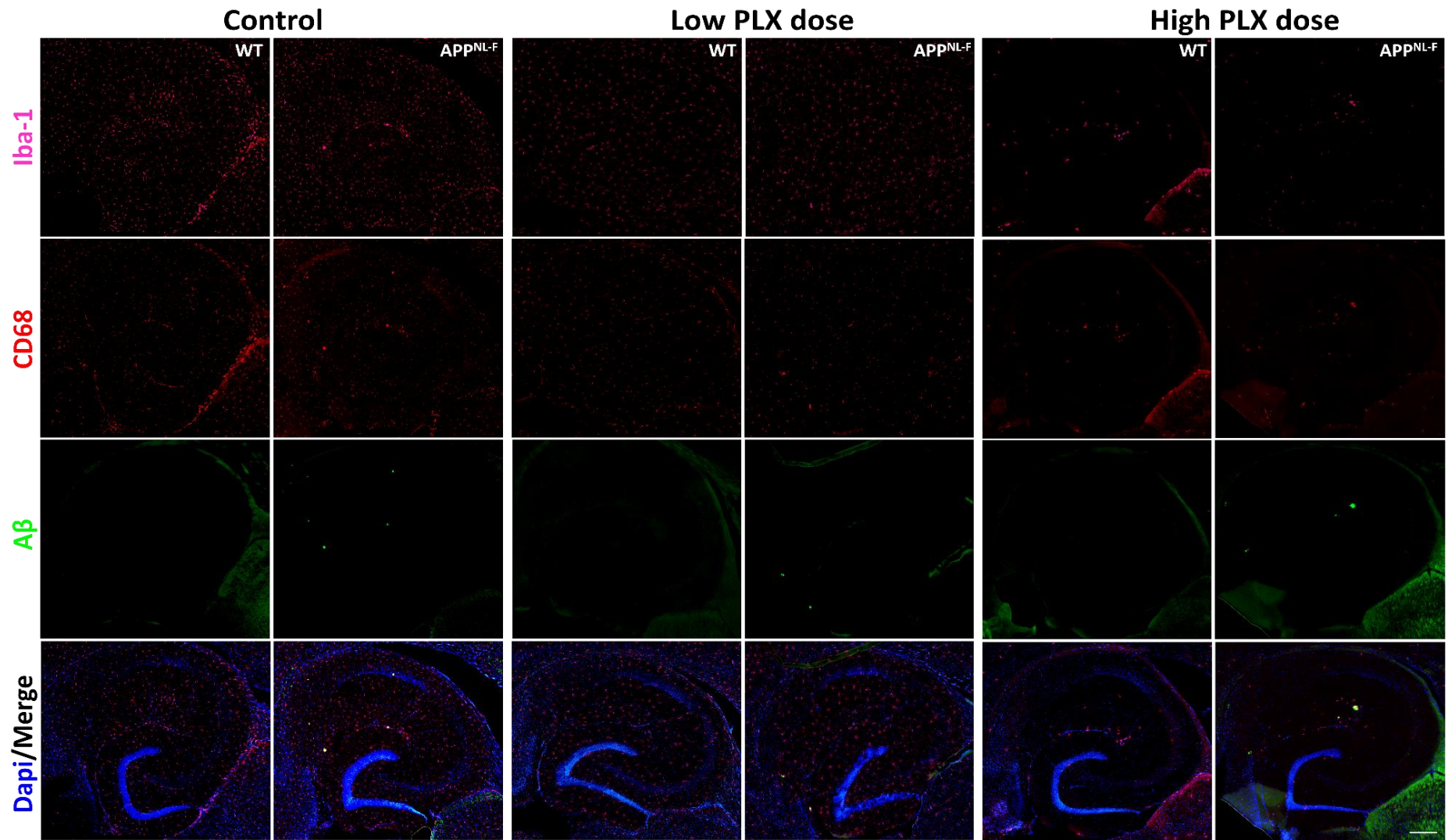
Figure 4.7 Representative images showing expression of Iba-1, CD68 and Aβ plaques after elimination of microglia with PLX5622, 10 month-old WT and APP^{NL-F}. Mice were placed on either control or inhibitor diet (low dose: 300 mg/kg; high dose: 1200 mg/kg) for 3 months, causing partial or almost total elimination of microglia in the hippocampus. Iba-1 immunofluorescent signal shows survival of microglia, CD68 shows microglial clustered around Aβ plaques, merged staining in the bottom row with DAPI in blue. 20x images, scale bar in the merge APP^{NL-F} high PLX dose image: 200μm.
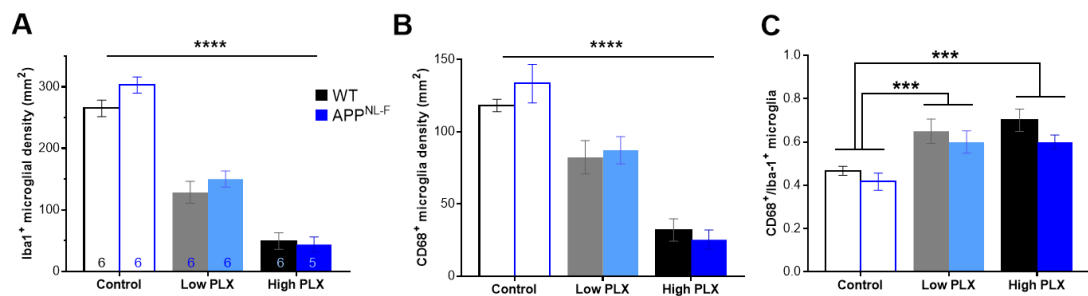
Figure 4.8 PLX5622 depletion of microglia in WT and APP^{NL-F} 10-month-old mice. (A) Densities determined as cells that were Iba-1$^+$ microglia, PLX5622 treatments significantly reduced the numbers of cells. **(B)** Total densities of Iba-1$^+$ microglia that were also CD68$^+$ in the hippocampus of mice treated with or without PLX5622. **(C)** Densities of CD68$^+$ microglia in the total microglia population showed an overall significant effect of drug; remaining microglia were activated and the numbers increased with both PLX5622 treatments. Data shown as mean ± SEM. Two-way ANOVA followed by Sidak corrected simple comparisons, ***p<0.001, ****p<0.0001.
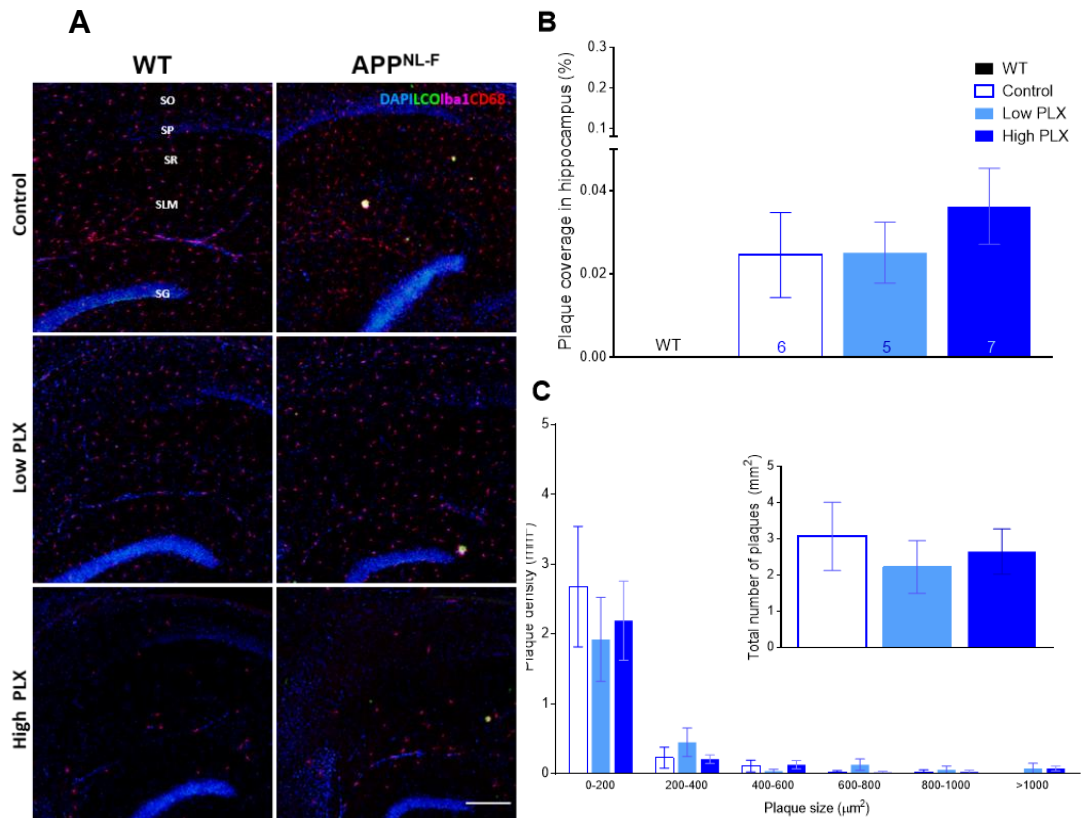
Figure 4.9 Aβ plaque deposition in 10-month-old APP^{NL-F} mice treated with PLX5622 for 3 months. (A) Representative fluorescent micrographs of WT and APP^{NL-F} CA1 region of hippocampus following labelling of Aβ with LCOs and fluorescent immunohistochemical staining for Iba-1 and CD68. *Stratum oriens* (SO), *stratum pyramidale* (SP), *stratum radiatum* (SR), *stratum lacunosum moleculare* (SLM) and *stratum granulosum* (SG) are indicated in the WT Control condition. Scale bar 200 μm. **(B)** Plaque coverage % in the whole hippocampus showed no effects of treatments with PLX5622. Sample sizes are indicated in each bar. **(C)** Size frequency distribution and total density of plaques were not affected by partial or total ablation of microglia numbers. Error bars indicate SEM.

SUMMARY

It was confirmed that microglia are critically dependent upon CSF1R signalling for their survival and that the CSF1R inhibitor, PLX5622, serve as an effective tool to achieve partial or total microglial depletion. Both APP knock-in models showed microglial prescence along with pathology development using immunohistochemistry; microglia cells were clearly displayed around Aβ plaques. First, LCO staining revealed a small quantity of Aβ plaques present in the hippocampus of both APP knock-in models, which confirmed the early stage of pathology in these mice. Second, quantification of Iba-1$^+$ and CD68$^+$, microglial presence and activation respectively, was not different compared to WT mice regardless the amount of Aβ plaques. Third, PLX5622 treatments successfully depleted microglial numbers; the low dose eliminated around 50% of the cells, while the high dose reached almost 90% elimination. This partial or almost-total depletion of microglia did not alter Aβ plaque coverage or density, but only a trend was revealed when a reduction of small plaques only was seen in the APP^{NL-F} and a significant difference was found in the APP^{NL-G-F} group. These results provide us with important information on how microglia respond to Aβ pathology associated with AD, and how microglia may contribute to the progression of the disease.

Chapter 5

RESULTS:

IDENTIFYING THE ROLES OF MICROGLIA IN SYNAPTIC TRANSMISSION AT EARLY AMYLOIDOPATHY IN APP KNOCK-IN MICE

5.1 Introduction

Amyloid plaques and neurofibrillary Tau tangles are classical hallmarks present in the progressive and neurodegenerative AD. Additionally, histological studies demonstrate that neuroinflammation is also an important feature in the human diseased brain (McGeer and McGeer, 1998; Cagnin et al., 2001) as well as being commonly found in APP transgenic models. Under healthy conditions, microglial cells are responsible for synaptic pruning and removal of damaged tissue or debris. During AD it has been established that microglia cluster around extracellular amyloid plaques, potentially attempting to clear the brain from such toxic and abnormal deposits, therefore they become activated and positive for inflammatory markers such as MHC-II, TNF-α, IL-1β and IL-16 (Akiyama et al., 2000). Eventually, the sustained microglial activity results in a chronic neuroinflammatory state that triggers not only production of pro-inflammatory cytokines but they could also contribute to the progression of the disease. As previously mentioned, AD mice display spine and neuronal loss associated with activated microglia and plaque deposition (Hong et al., 2016a). Over the last decade, GWAS has revealed several risk-associated genes for sporadic AD; most of these genes are expressed by microglia or relate to their reactivity, such as *TREM2*, *CR1*, *CD33*, *CLU* and *MS4A* (Guerreiro and Hardy, 2013). Thanks to this evidence, it has been

proposed that changes in microglia-associated genes are strongly linked with an increased risk of developing AD.

It is still unclear the specific role that microglia play in the development of amyloid plaques and AD progression. While microglia are thought to phagocytose Aβ, some studies have shown that they do not modulate plaque numbers/sizes in the brain but that they could be contributing to synaptic damage and neuronal loss (Grathwohl et al., 2009; Spangenberg et al., 2019). Selective depletion has been used to investigate microglial functions in AD synaptic network; in this study, I explored how microglia in health and disease are dependent on CSF1R signalling and set out the effects of microglia elimination in hippocampal synaptic transmission. As seen in Chapter 4, PLX5622 successfully decreased numbers of microglial cells and now in this chapter, electrophysiological recordings (fEPSP and whole-cell patch clamp) were performed in PLX5622-treated WT and APP knock-in mice. Knowing how the hippocampal synaptic network adapts to the absence of microglia during pathology, could be helpful to identify important biological pathways that link AD and neuroinflammation.

5.2 Microglia elimination effects in synaptic transmission of 3.5-month-old APP[NL-G-F] mice

All the treatments and electrophysiology experiments were interleaved between genotypes and drug doses, here the results are divided according to genotypes for presentation. As analysed in Chapter 3 under control conditions, there were mainly no statistically significant differences between WT vs APP[NL-G-F] regarding synaptic transmission. Synaptic plasticity, basal and evoked transmission values did not show alterations when Aβ plaques started being deposited in the brain at 3.5 months of age. Based on these results, microglia elimination effects were analysed per genotype and at the end of this chapter both mouse lines and PLX5622 doses are compared all together.

5.2.1 Basal synaptic transmission of PLX5622 treated WT mice.

After administration of PLX5622 for 7 weeks, fEPSPs were recorded as previously described. The I-O relationship of WT mice after depletion of microglia with PLX5622 did not show significant differences when compared with the control group. A main effect of voltage was detected by two-way ANOVA test ($p<0.0001$) (**Figure 5.1A**). Similar results were found in PPR analysis, as we observed before at SC-CA1 synapses, the PPR decreased with increasing inter-stimulus interval and by 200 ms both responses were independent of each other, reaching almost equal slopes. No interaction between the inter-stimulus interval and drug doses was observed, but an overall effect of inter-stimulus interval was detected ($p<0.0001$) (**Figure 5.1B**).
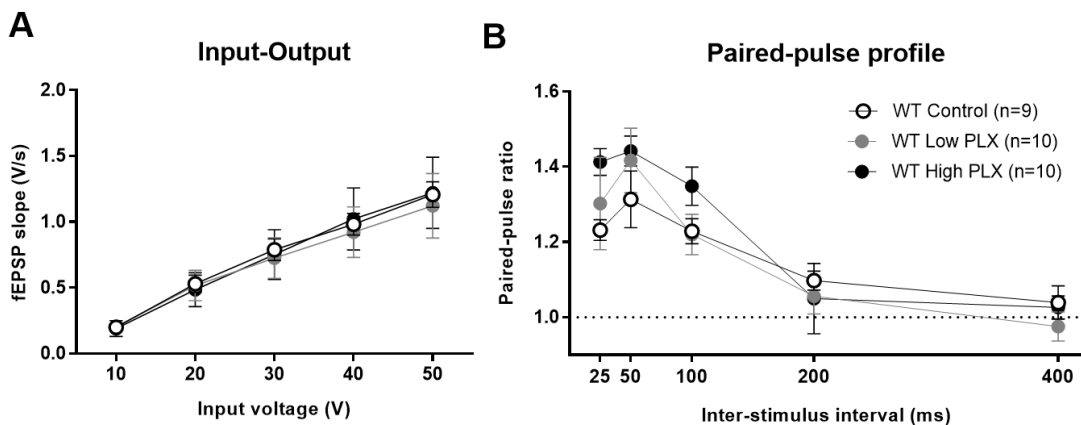
Figure 5.1 Basal synaptic transmission recorded at the SC-CA1 synapse of PLX5622 treated 3.5-month-old mice. (A) Input-Output relationship plot shows increased fEPSP amplitude in response to increasing stimulus intensity applied to SC axons for both PLX5622 doses. **(B)** PPR obtained from a population of CA1 neurons in response to stimulation of SC axons. No difference was detected between PLX5622 doses. Error bars indicate SEM.

5.2.2 Long-term synaptic plasticity of PLX5622 treated WT mice.

Long-term synaptic plasticity was evaluated after partial or total microglia depletion by PLX5622. fEPSP slopes in WT groups with the administration of the drug had a clear induction of LTP, as the magnitude of the responses increased as expected, and differences between PLX5622 doses were not detected. EPSPs increased immediately after tetanisation and then the potentiation decreased over the next few minutes, stabilising at a larger slope

(~150%) than baseline for the remainder of the recording. (**Figure 5.2A**). The PPRs recorded during LTP in WT mice were not found to differ significantly between PLX5622 doses (**Figure 5.2B**). Among the drug conditions tested, there was not any considerable changes in PTP, STP and LTP obtained in fEPSP slopes or PPR (**Figure 5.2C,D**).
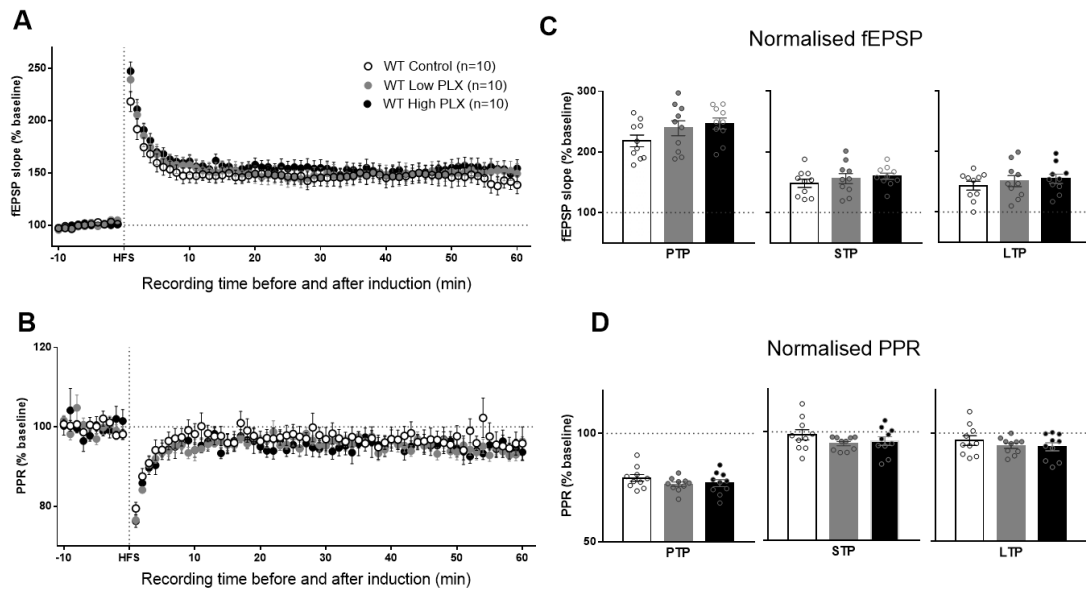
Figure 5.2 PTP, STP and LTP recorded at the SC-CA1 synapse in the partial or total absence of microglia at 3.5 months of age. (A) Field recordings from WT with Low or High PLX5622 doses. **(B)** PPR obtained (50ms inter-stimuls interval) with or without depletion of microglia. (C)(D) PTP, STP and LTP for fEPSPs and PPRs obtained in WT mice treated with PLX5622. One-way ANOVA showed no significant differences between treatments. Error bars indicate SEM.

5.2.3 Basal synaptic transmission of PLX5622 treated APP^{NL-G-F} mice.

The same experimental protocols and drug doses were applied to the APP^{NL-G-F} mouse line to evaluate the role of microglia in synaptic plasticity but now including early Aβ plaque deposition. The initial increase in slope seen in the APP^{NL-G-F} control group at >30 V was recovered when the mice were treated with PLX5622 (Control vs low dose, $p<0.01$; control vs high dose, $p<0.0001$). Also, an interaction between PLX5622 doses and voltage input was revealed by a two-way ANOVA, followed by a Sidak's post hoc test (interaction

p=0.0005) (**Figure 5.3A**). However, after setting the appropriate voltage for the PPR protocol, no effects were shown in the ratios, similar to wild types, the paired responses displayed facilitation (**Figure 5.3B**).
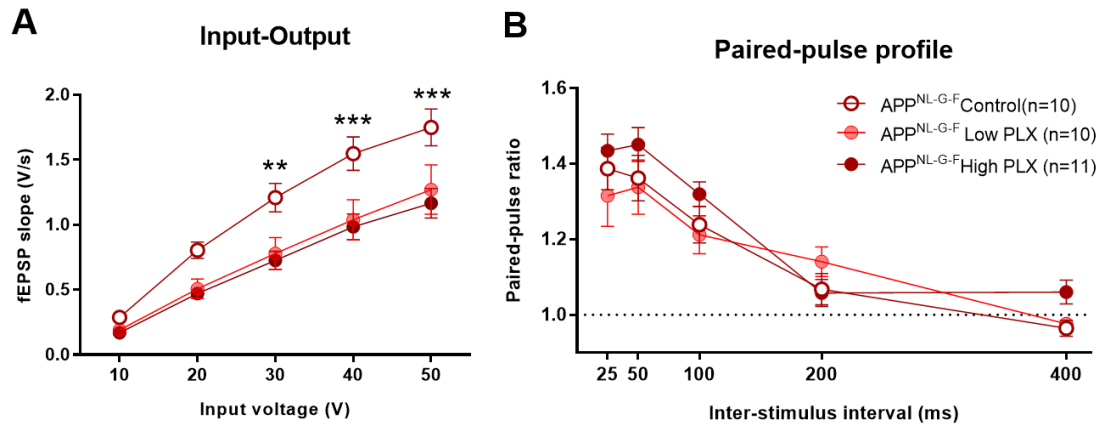
Figure 5.3 Input-Output curves and PPRs of APP^{NL-G-F} mice with PLX5622 treatments. (A) Both PLX5622 doses significantly decreased the fEPSP slopes values and an interaction between drugs and input voltage was found by two-way ANOVA and Sidak`s post hoc test (**p<0.01, ***p<0.0001). **(B)** PPRs did not change after partial or complete ablation of microglial numbers at inter-stimulus intervals of 25-400ms. Error bars indicate SEM.

5.2.4 Long-term synaptic plasticity in APP^{NL-G-F} mice treated with PLX5622.

LTP was consistently observed in APP^{NL-G-F} mice after PLX5622 treatments and PPR values were not affected by the drug doses (**Figure 5.4A, B**). Analysis of variance revealed that the high PLX5622 dose caused a significant increase of PTP compared to the lower or control dose groups (p<0.05) (**Figure 5.4C**). However, such change in the magnitude of the fEPSP eventually got smaller and stabilised over time, then STP and LTP of the showed no significant differences after depletion of microglia. Regarding the change in PPRs following induction of LTP, there were no significant effects of both drug doses in any of the periods analysed (**Figure 5.4D**).
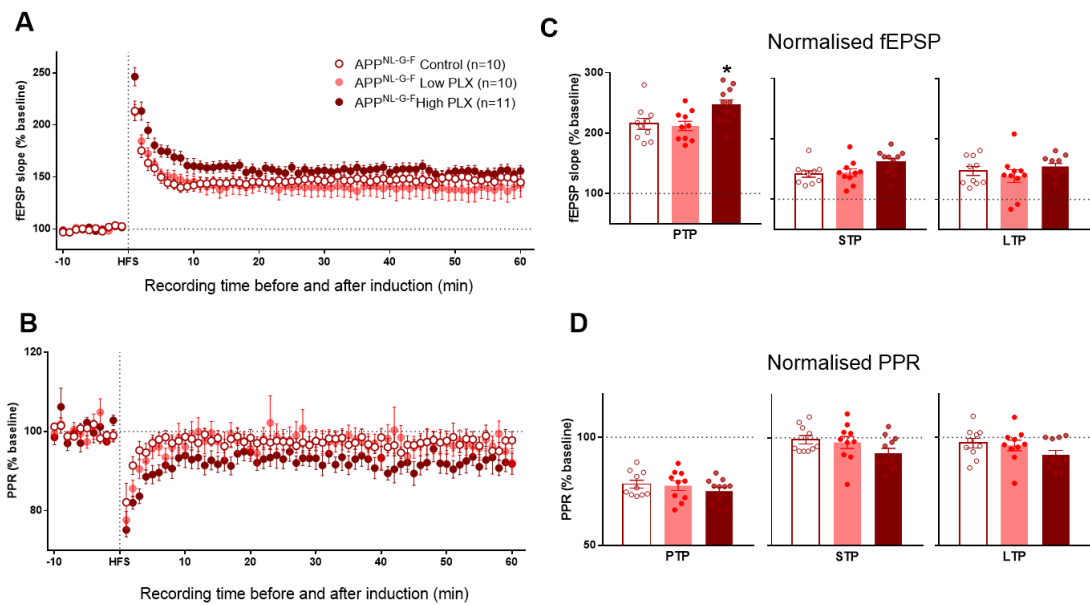
Figure 5.4 LTP recorded from the SC-CA1 synapse of APP^{NL-G-F} mice at 3.5 months of age in the presence of PLX5622. (A) Field recordings from APP^{NL-G-F} after 7 weeks of PLX5622 treatments. **(B)** PPRs obtained at 50ms of inter-stimulus interval. **(C)** PTP, STP and LTP obtained after high frequency stimulation (HFS); PTP of high PLX significantly higher than the rest of the groups (*$p<0.05$, one-way ANOVA). **(D)** PTP, STP and LTP obtained from PPRs values from groups treated with or without PLX5622.

5.2.5 PLX5622 effects in extracellular field recordings of WT and APP^{NL-G-F} at 3.5-months.

When PLX5622 treatments and both genotypes are compared all together, the only significant difference detected is in the I-O relationship (**Figure 5.5A**). There a is clear increase of the APP^{NL-G-F} control group slope values at >30 V ($p<0.05$, two-way ANOVA test), not seen in the WTs, which is then rescued by the PLX5622 doses. There were no differences detected in long term synaptic plasticity when genotypes and drug doses were compared (**Figure 5.5C, D**).

For the comparison of the overall PTP, STP and LTP data, no significant differences were detected between genotypes or between PLX5622 partial and total depletion treatments (**Figure 5.6**).
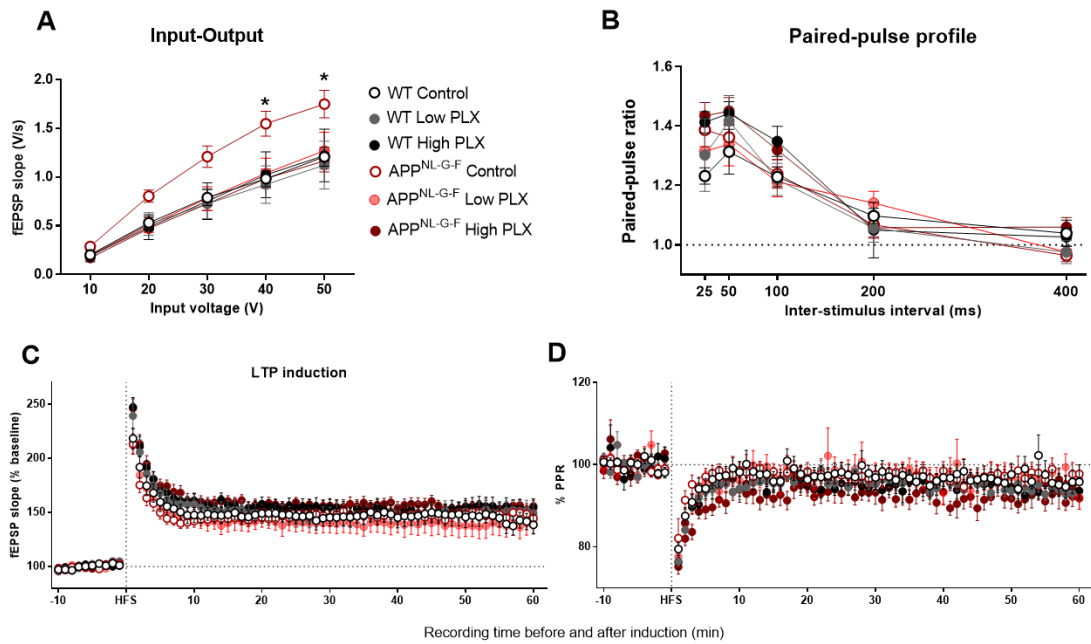
Figure 5.5 Basal synaptic transmission and synaptic plasticity analysis of WT and APP[NL-G-F] with microglia depletion induced by PLX5622. (A) Input-output relationship showed an overall increase in fEPSP amplitude in response to increasing stimulus intensity, APP[NL-G-F] control group showed bigger amplitudes compared to the PLX5622 treatments and WT groups (*$p<0.05$). **(B)** PPR obtained from CA1 neurons in response to stimulation of SC from CA3 at different time intervals, no differences between groups were detected. **(C, D)** No statistical differences in LTP or its PPR recorded after HFS, LTP remained constant for one hour in all the groups. Error bars indicate SEM.
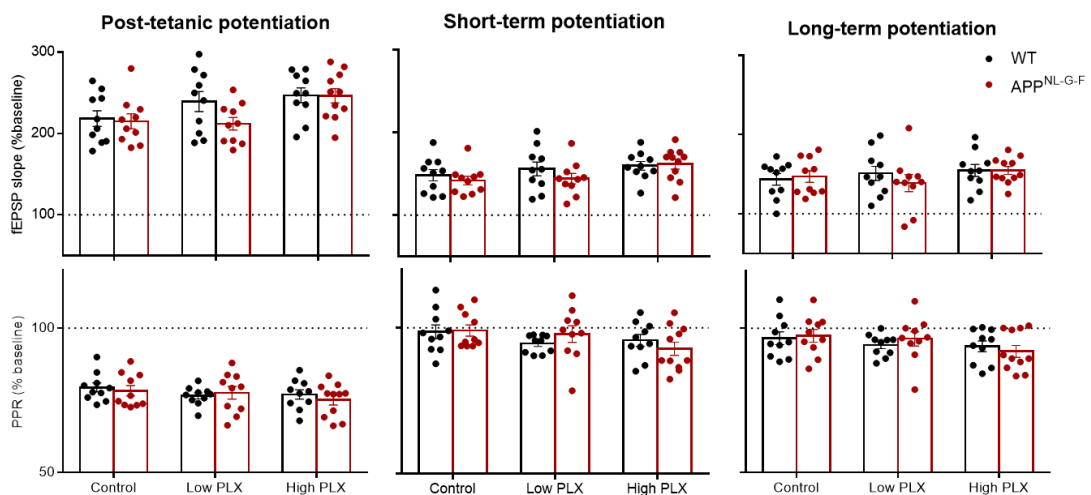
Figure 5.6 PTP, STP and LTP recorded at the SC-CA1 synapses of 3.5 months of age of WT and APP[NL-G-F] with PLX5622 treatments. The top row shows the fEPSP obtained with both genotypes; no significant differences were detected by two-way ANOVA when comparing treatments. The bottom row shows the PPR obtained (50 ms inter-stimulus interval), there were no significant main effects, or interaction between, genotype and treatments.

5.2.6 Evoked excitatory activity of PLX5622 treated WT and APP^{NL-G-F} mice

The effect of chronic PLX5622 treatment on glutamatergic release probability was also assessed on WT and APP^{NL-G-F} groups by using a whole-cell patch clamp configuration. In WT animals, a decrease in PPR was observed at the 25ms only when microglia were partially depleted, indicative of an increased probability of glutamate release ($p<0.05$) (**Figure 5.7A**); interestingly, in APP^{NL-G-F} mice, the PPR at that same inter-stimulus interval under the same partial microglia depletion condition indicated the same significant effect ($p<0.05$) (**Figure 5.7B**). Two-way ANOVA followed by a Sidak's corrected simple comparison of drug dose revealed an overall significant effect when animals were treated with low dose PLX5622 irrespective of genotype and compared with hontrol and high dose PLX5622 groups. No differences in PPR were observed at 50 ms inter-stimulus interval by either drug dose.
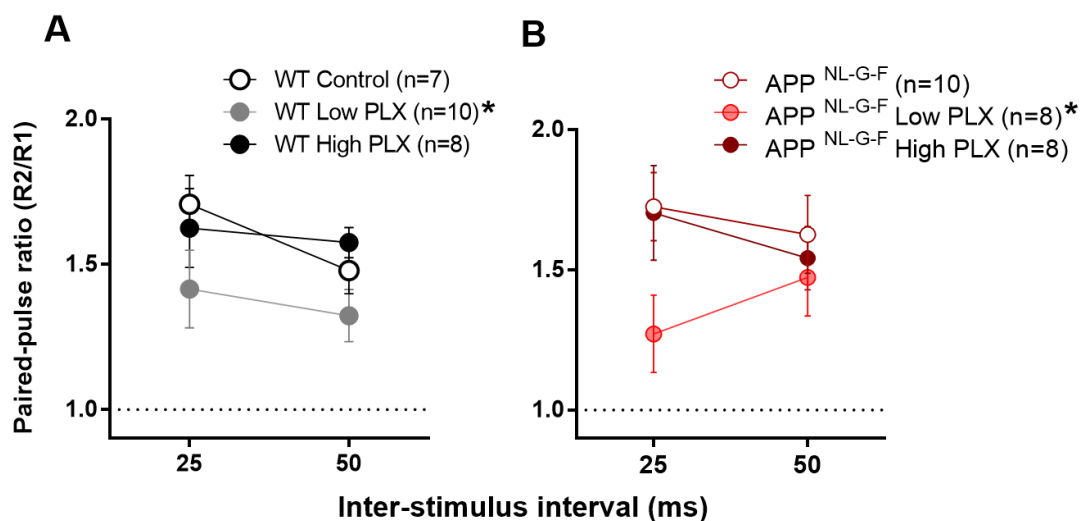
Figure 5.7 Paired-pulse ratios from PLX5622-treated mice. (A) WT and **(B)** APP^{NL-G-F} mice displayed a significant reduction at 25 ms inter-stimulus interval (*$p<0.05$) when low PLX was applied for 7 weeks (two-way ANOVA, sequential Sidak comparisons). Error bars indicate SEM.

5.3 Microglia elimination effects in synaptic transmission of 10-month-old APP^{NL-F} mice

I next asked whether depleting microglia for a longer period of time and before Aβ plaques formation in APP^{NL-F} could have any effects on spontaneous

excitatory and evoked synaptic transmission in the CA1 hippocampal region. This mouse model develops amyloid pathology at a slower pace than the APP^{NL-G-F}, and therefore the first Aβ plaques are not explicitly displayed until around 9 months of age (Saito et al., 2014). For these reasons, the APP^{NL-F} mouse could be considered a relatively more similar subject to consider modelling human AD. By introducing PLX5622 to the experimental method I wanted to target the course of plaque initial development and assess if the absence of microglia could alter not only synaptic transmission but also the number, size and onset of Aβ plaques (Chapter 5). As mentioned previously for this experiment, PLX5622 was applied chronically for 3 months, from 7 to 10 months of age. Previous data from Edwards' laboratory reported unaltered synaptic plasticity when analysing fEPSPs in APP^{NL-F} at 9 months of age compared to WT mice, therefore the results displayed in this section focused on synaptic transmission by whole-cell patch clamping only (Benitez et al., 2021).

5.3.1 Excitatory postsynaptic currents of PLX5622 treated WT and APP^{NL-F} mice

The effect of chronic PLX5622 treatment from 7 months of age on the frequency of sEPSCs in APP^{NL-F} and WT mice was assessed using two-way ANOVA. Partial or total depletion of microglia significantly reduced the frequency of sEPSCs in both groups of mice ($p<0.001$) (**Figure 5.8A**), there was not an effect of genotype or interaction between the parameters assessed.

Comparison of the median amplitude and decay of sEPSCs were not affected by PLX5622 treatments and the values were very similar in the APP^{NL-F} group compared to the WT; two-way ANOVA showed no significant effect of treatment, genotype, or interaction (**Figure 5.8B, C**).
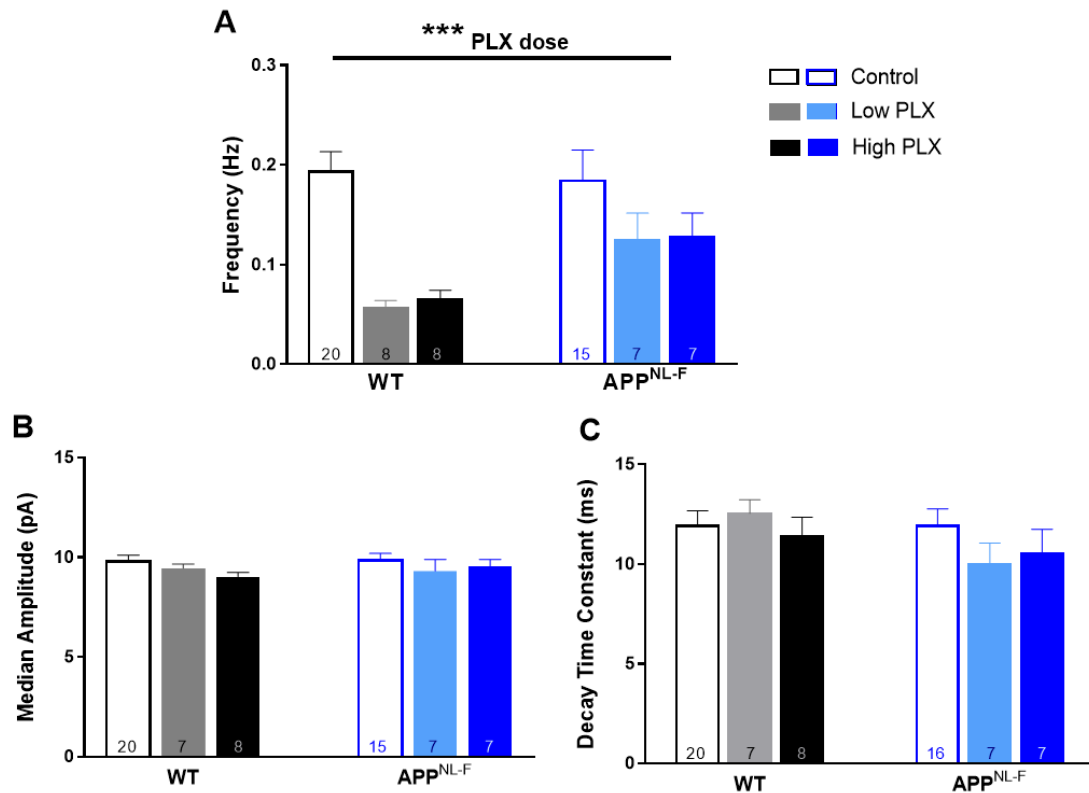
Figure 5.8 Effects of chronic PLX5622 treatment in sEPSCs from 7 months of age had in CA1 pyramidal neurons from APP[NL-F] and WT mice at 10 months of age. (A) Frequency of sEPSCs in APP[NL-F] and WT mice treated chronically with different doses of PLX5622. Two-way ANOVA revealed a significant reduction irrespective of genotype (***$p<0.001$). **(B)** Median amplitude of sEPSCs in APP[NL-F] and WT mice treated chronically with different doses of PLX5622 were unaffected. **(C)** Decay time constant (τ) of sEPSCs in mice treated chronically with different doses of PLX5622. (***$p<0.001$). Error bars indicate SEM. Sample sizes (animals) are indicated within the bars of each panel.

Chronic PLX5622 treatment from 7 months of age reduced mEPSCs frequency in both genotypes, two-way ANOVA test a significant effect of treatment ($p<0.01$), but there was not an interaction between PLX treatments and genotypes (**Figure 5.9A**). The amplitude and decay of mEPSCs was unaltered between genotypes and PLX5622 doses (**Figure 5.9B**) indicated by two-way ANOVA showing no significant effect of treatment, genotype, or interaction between genotype and treatment (**Figure 5.9C**).
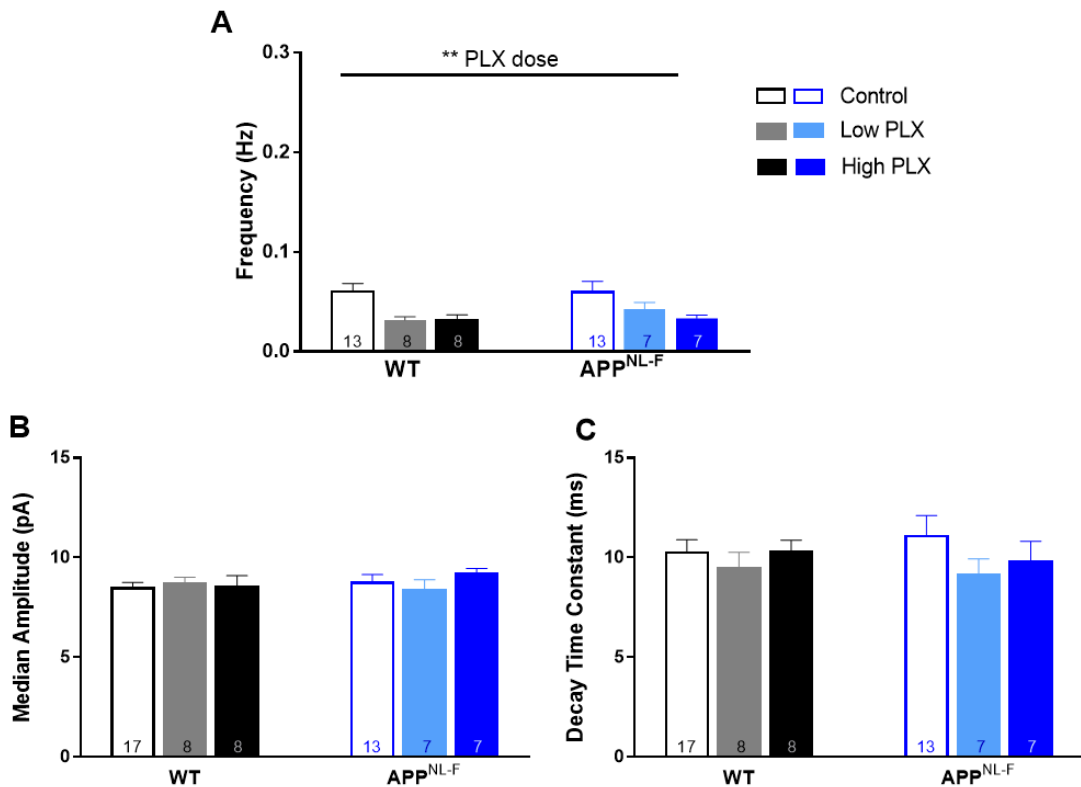
Figure 5.9 Chronic PLX5622 treatment from 7 months of age reduced the frequency of mEPSCs in CA1 pyramidal neurons from APP^{NL-F} and WT mice at 10 months of age. (A) Frequency of mEPSCs in APP^{NL-F} and WT mice treated chronically with different doses of PLX5622. Two-way ANOVA revealed a significant effect of treatment (**p<0.001), but no effects in genotype or interaction between genotype and treatment were revealed. **(B)** Median amplitudes of mEPSCs mice treated chronically with different doses of PLX5622 were not significantly different. **(C)** Decay time constant (τ) of mEPSCs in APP^{NL-F} and WT mice treated for three months with different doses of PLX5622 no significant changes were found. Error bars indicate SEM.

5.3.2 Evoked excitatory activity of PLX5622 treated WT and APP^{NL-F} mice

As discussed in Chapter 3, section 3.3.2, APP^{NL-F} mice showed a reduced PPR at 25ms of inter-stimulus interval, indication of an increase in glutamatergic release probability which reached a statistically significant value when compared with age-matched WT control group. Here, when mice were treated with a low or a high dose of PLX5622, some additional alterations were revealed. In WT groups, a decrease in PPR was observed at both inter-stimulus intervals when microglia were partially or totally depleted, this main effect of PLX5622 was revealed to be statistically significant by two-way

91

ANOVA (p<0.0001) and an interaction between the variables tested was found to be significant (p<0.05) (**Figure 5.10A**). Similarly, in APP^{NL-F} mice, low and high dose of PLX5622 significantly altered the PPRs of 10-month-old mice; a main effect of drug treatment was revealed by two-way ANOVA (p<0.05), but no interaction was shown (**Figure 5.10B**). Finally, an overall significant effect was specially found when mice were treated with the low PLX5622 dose, irrespective of genotype, PPRs at 25 ms were considerably lower when compared with the control groups.
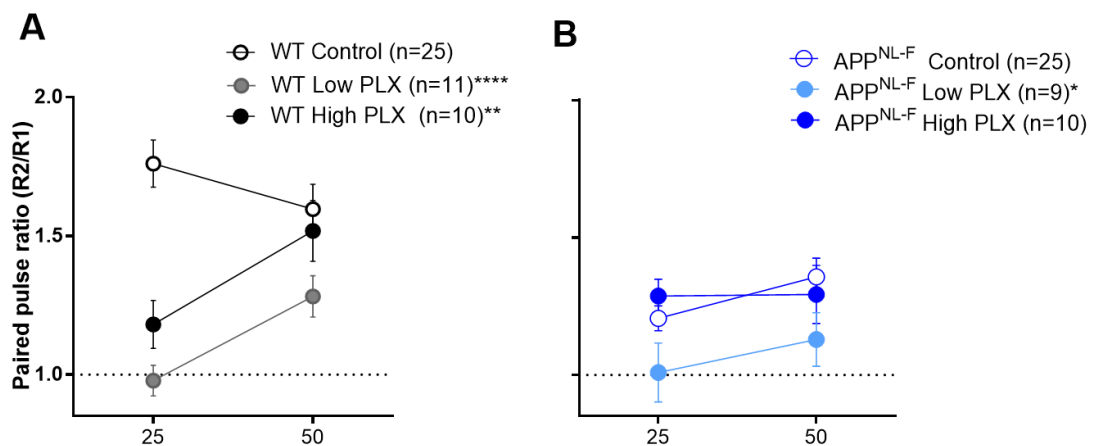
Figure 5.10 Partial chronic depletion of microglia by Low PLX5622 dose decreased the paired-pulse ratio recorded at the SC-CA1 synapse. (A) (B) PPRs obtained from CA1 pyramidal cells in response to stimulation of the SC pathway from mice treated with PLX5622 for three months. Low dose of PLX5622 revealed an overall significant effect in WT and APP^{NL-F} mice; ****p<0.0001, **p<0.01, *p<0.05; two-way ANOVA. Error bars indicate SEM.

SUMMARY

Overall, the results presented in this chapter show that short-term microglial elimination (1.5 months) is not detrimental in WT and APP^{NL-G-F} animals; hippocampal basal synaptic transmission and synaptic plasticity remained unaltered when 50% or 90% of microglial cells were depleted. If anything, microglia absence reduced neuronal large response in APP^{NL-G-F} mice when a considerable number of axons were recruited (>30 V). On the other hand, chronic PLX5622 treatments (3 months) reduced the frequency of spontaneous and miniature EPSCs in both WT and APP^{NL-F} groups; the APP^{NL-F} mice tended to be less affected. Finally, partial microglia depletion seemed to exacerbate the APP^{NL-F} phenotype by decreasing the PPR and, in healthy WT mice, there was also a decrease in PPR, which revealed that the increase in glutamatergic probability of release was replicated by both PLX5622 treatments.

Chapter 6

DISCUSSION

Alzheimer's disease is the most common type of dementia that has become a significant challenge for our society. Its long progression, late diagnosis and lack of effective treatments are currently threatening about 600,000 ageing people in the UK (Wittenberg et al., 2019). In the last decade, GWAS studies have highlighted the importance of immune-related gene variants as AD risk factors, such as *TREM2*, *CR1*, *CD33*, *CLU* and *MS4A* (Guerreiro et al., 2013; Lambert et al., 2013; Karch and Goate, 2015; Bellenguez et al., 2020). These genes are closely associated with microglial functions and several studies have evidenced the involvement of microglia in the pathology of AD. However, the precise roles that microglia play in the progression and development of the disease remain unclear.

Microglia depletion, using CSF1R inhibitors or other approaches, has been employed to examine amyloid plaque deposition, Tau pathology and spread, synaptic functions and cognition in diverse neurodegeneration models (Grathwohl et al., 2009; Gomez-Nicola and Perry, 2015; Olmos-Alonso et al., 2016; Zhao et al., 2017; Mancuso et al., 2019). PLX5622 is a highly selective CSF1R blocker that has previously shown to reduce microglia numbers in healthy, injured and disease mouse models (Elmore et al., 2014; Dagher et al., 2015; Spangenberg et al., 2019; Casali et al., 2020; Clayton et al., 2020; Son et al., 2020). In this thesis, I aimed to define the role of microglial cells in mediating Aβ plaque development in Alzheimer's disease through the PLX5622 inhibitor at two doses which were sufficient to eliminate partial or total microglia numbers. For this project, I used APP knock-in mouse models in which the Aβ sequence within APP was humanised and two or three mutations were added, known as APP^{NL-F} and APP^{NL-G-F}.

Both APP knock-in mouse models of AD were developed to overcome limitations inherent to first-generation transgenic AD models (Saito et al., 2014; Sasaguri et al., 2017). However, despite avoiding the problems of transgene technology, such as overexpression of APP, the knock-in mice remain good models of early stages of plaque deposition but do not go on to translate amyloidosis into the later stage pathologies of Tau tangles and neurodegeneration. Since synaptic dysfunction is considered to start in the early stages of AD pathogenesis (Chen et al., 2019), I first set out to characterise the APP^{NL-G-F} and APP^{NL-F} synaptic phenotype with rising Aβ and plaque deposition by performing electrophysiological techniques.

6.1 Electrophysiological phenotypes of young APP knock-in mice during early amyloid pathology.

The hippocampus was chosen for this initial characterisation as it is one of the regions that are affected early by Aβ pathology in humans (Thal et al., 2002). Particularly, the CA1 region of the hippocampus is the most investigated brain area for the processes of synaptic plasticity and memory formation (Takeuchi et al., 2014). Field extracellular postsynaptic potentials (fEPSPs) were recorded in the CA1 *stratum radiatum* to examine if basal synaptic transmission, short-term plasticity and LTP evoked from CA3-SC in acute slices of 3.5-month-old APP^{NL-G-F} mice show any differences from WT control mice. The input-output (I-O) relationship of evoked fEPSPs from hippocampal slices of APP^{NL-G-F} mice was observed to be steeper than from WT mice (**Figure 3.2A**). It has been described that enhanced synaptic excitability could be triggered by the oligomerisation state of Aβ (Busche et al., 2008; Dietrich et al., 2018). In this case, the "G" or Arctic mutation makes Aβ more prone to aggregate and oligomerise in the APP^{NL-G-F} mice (Cheng et al., 2004; Saito et al., 2014). At 3.5 months of age, soluble and insoluble Aβ$_{42}$ levels are considerably higher in the hippocampus of APP^{NL-G-F} than WT mice (Latif-Hernandez et al., 2020), and therefore they could underlie the larger fEPSPs solpe change when higher inputs are applied as more axons are recruited. As reviewed by Dietrich et al. (2018), several research groups that have analysed the I-O relationships from the CA1 subfield in young AD mouse models prior

to plaque development, have reported little change or a decrease in synaptic strength or synaptic function, which is opposite to what I found with the APP^{NL-G-F} model. Such reports correspond to transgenic mice only; until date, just Latif-Hernandez publication (2020) has reported analyses of synaptic transmission in the APP^{NL-G-F} model. Interestingly, they found unchanged basal synaptic transmission when comparing *versus* the APP^{NL} control mice. It should be pointed out that using the APP^{NL} mice as control group is a considerable difference compared to the results that I am presenting in this thesis. Potentially, the APP^{NL} model could be expressing effects of a very mild amyloid pathology due to the Swedish mutation (Saito et al., 2014), and when compared *versus* the APP^{NL-G-F} such changes/effects become indiscernible. Using a WT group as control could provide more accurate information about electrophysiological phenotypes under physiological healthy conditions. On the other hand, the increase in the fEPSP slope of the I-O relationship seen in my experiment could be due to an increase in the maximal number of axons recruited, the number of postsynaptic receptors or a difference in the excitability of each axon at higher stimulus intensities. Finally, according to the statistical analysis, the increased slope amplitude seen at >30 V in basal synaptic transmission did not remain when short- and long-term plasticity were analysed due to the fact that all the recordings were performed using the half maximal stimulus intensity obtained from the I-O curve, which was at 15-25V. Regarding the PPRs, which is a measure of presynaptically mediated short-term plasticity, varying the inter-stimulus intervals led to indistinguishable profiles between the WT and APP^{NL-G-F} mice. From 50 ms, as expected, PPF declined as inter-pulse duration increased; it is then suggested that presynaptic release probability or calcium dynamics are not altered in this knock-in model at 3.5 months of age (**Figure 3.2B**).

Data from transgenic mice suggest that Aβ has a role in the induction and consolidation of LTP; several research groups have reported either an absence of LTP or even induction of LTD rather than LTP (Ricciarelli and Fedele, 2018). Previous results from Edwards' lab reported a biphasic effect on magnitude of LTP in transgenic models (Medawar et al., 2019), where an increase in LTP was present as Aβ levels first started to increase, before the

deposition in plaques and a subsequent decline in LTP when plaques were already deposited. In addition, Aβ oligomers can target the postsynaptic sites of excitatory synapses which trigger structural and functional changes in the synapse (Haass and Selkoe, 2007; Koffie et al., 2009; Pickett et al., 2016). High-order oligomers (Obata et al., 2020; Hark et al., 2021) and Aβ plaques (Saito et al., 2014; Latif-Hernandez et al., 2019; Monasor et al., 2019; Clayton et al., 2020; Rice et al., 2020; Saifullah et al., 2020; Benitez et al., 2021) are detectable in the APP^{NL-G-F} brains at the age of 3.5 months. Based on the evidence, I hypothesised that synaptic plasticity would be affected by the amyloid pathology presented in this model. To test this hypothesis, dendritic fEPSPs were recorded at the SC-CA1 synapses and the magnitude of LTP. Similar fEPSP values between WT and APP^{NL-G-F} mice were found (**Figure 3.3**). These results indicate that Aβ-mediated synaptic-toxic effects failed to trigger any significant functional deficits in the hippocampal CA1 area at 3.5 months of age. The pathology in this model appears fast and strong, plaques are robust and they keep depositing almost linearly with time (Saito et al., 2014; Benitez et al., 2021). The change of PPR after the induction of LTP remained intact between compared to baseline, therefore, the presynaptic mechanisms were not affected by the amyloid pathology. Potentially, the absence of deficits in synaptic transmission could be due to the levels of Aβ oligomers that lack synaptotoxic effects at this young age in the APP^{NL-G-F} model. Insoluble amyloid plaques are thought to be able to sequester soluble oligomers, restricting their capacity to dissociate and become damaging for the synaptic network (Yang et al., 2017). This would be particularly true for the Arctic mutation which pushes the equilibrium towards deposition (Walsh and Selkoe, 2007) .

Pairs of stimuli were applied to SC to evoke EPSCs; as expected from CA3-CA1 synapses, PPF (the second EPSC amplitude greater than the first, indicative of a low probability of glutamate release) was observed in slices from WT and APP^{NL-G-F} at 3.5 months of age (**Figure 3.4**). The decrease in PPR at the 50 ms inter-stimulus interval was expected due to the increase in the time for residual calcium to be buffered (Zucker and Regehr, 2002). Again, the hypothesis for this experiment was to find if there were alterations in

glutamatergic release probability due to the Aβ levels and plaques observed at 3.5 months of the APP^{NL-G-F} mice, which has been seen in other transgenic models at a similar early pathology stage (Cummings et al., 2015; He et al., 2019; Medawar et al., 2019). In the results presented, the glutamate release probability was unchanged between the WT and APP^{NL-G-F} mice. This result was accompanied by unaltered dendritic spine density of pyramidal CA1 neurons (Edwards' lab, unpublished). The lack of difference in probability of glutamate release could be again, due to the Arctic mutation. The accelerated fibrillisation of Aβ$_{40}$ and Aβ$_{42}$ to form plaques means that there could be some removal of Aβ from the neuropil which results in an alleviation of the phenotype. Presumably, there is always some soluble Aβ in the immediate vicinity of the plaque that, with time, would evolve into a heavier plaque load strong enough to affect synapses. In press results from Edwards' lab team have demonstrated that, by 9 months of age, when Aβ plaques have considerably increased in size and number, there is a decrease in the PPR; by 20 months of age evoked EPSCs display paired-pulse depression (PPD) rather than facilitation and large accumulation of amyloid (Benitez et al., 2021) (**Figure 6.1**). It is then confirmed that APP^{NL-G-F} glutamatergic transmission is impaired at later ages, when the pathology is pronounced and when synapses would be in the vicinity of Aβ plaques.

Electrophysiological characterisation of the APP^{NL-F} mice started being investigated by Edwards' laboratory team before this PhD project started. Some preliminary results showed that this model had unaltered synaptic plasticity and an increased glutamate release probability at 9 months of age when compared to WT mice (Benitez et al., 2021). In contrast to the APP^{NL-G-F} model, amyloid pathology in the APP^{NL-F} mice evolves at a slower pace and by 9 months, according to Saito et al. (2014), just a few Aβ plaques are present in cortical areas but none in hippocampus together with a steady high production of soluble and insoluble Aβ$_{42}$ in cortex. Based on this evidence, I was interested in further examining the electrophysiological phenotypes of the APP^{NL-F} model at an age when the first Aβ plaques are deposited in the hippocampus, which it was found to be at 10 months.
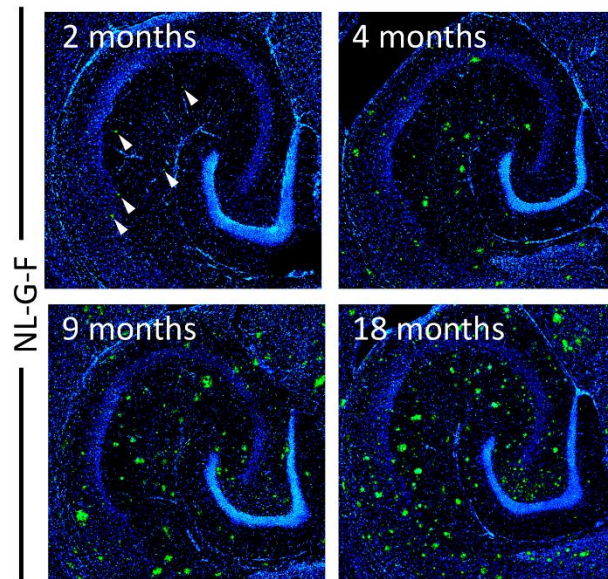
Figure 6.1 Plaque development in APP^{NL-G-F} mice. Representative hippocampal images of amyloid plaques detected using LCO (green) at the ages indicated. White arrows indicate small amyloid plaques (Benitez et al., 2021).

Studies in transgenic mice have shown loss of spontaneous EPSCs before Aβ plaque deposition (Jacobsen et al., 2006; D'Amelio et al., 2011; Cummings et al., 2015; Tozzi et al., 2015; Medawar et al., 2019), however, in the APP^{NL-G-F}, this occurs at 9 months of age, when the plaque load is very heavy (**Figure 6.1**; Benitez et al., 2021). In the case of APP^{NL-F} model, I found that action potential-dependent spontaneous events were not affected at 10 months of age (**Figure 3.5**); frequency, amplitude and decay time of sEPSCs were similar to the age-matched WT control group. Additionally, when miniature EPSCs were isolated, no significant differences between genotypes in terms of frequency, amplitude and decay time were identified. This result coincides with a recent pre-publication which shows that, at around 10 months of age, APP^{NL-F} gene and protein expression levels involved in synaptic function, such as transmitter-gated ion channel signalling or synapse membrane components, remain unchanged when compared to WT (Pauls et al., 2021). In this APP^{NL-F} model it is not until the age of 20 months that the frequency of sEPSCs is significantly reduced (Benitez et al., 2021), by this time plaques are clearly present in the brain and soluble Aβ could be affecting synapses (**Figure 6.2**). Based on previous reports and the results presented

in this thesis, it can be considered that the loss of spontaneous synaptic activity, identified before plaque deposition in transgenic mice, could be the result of an artefact of overexpression while in the APP^{NL-F} model, such effect comes later likely due to the very high Aβ levels as the pathology develops. This late effect on sEPSCs suggests that either a much higher concentration of Aβ is necessary or that there is a gradual compensation in excitability of the presynaptic axons to counteract for the higher release probability seen in the PPRs.
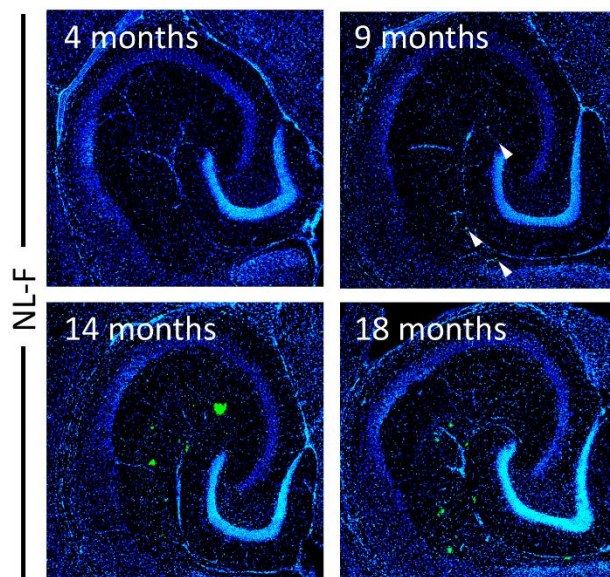
Figure 6.2 Plaque development in APP^{NL-F} mice. Representative hippocampal images of amyloid plaques detected using LCO (green) at the ages indicated (Benitez et al., 2021).

Examination of PPRs at 10 months of age in the APP^{NL-F} showed an increased probability of glutamate release compared with WTs (**Figure 3.6**). As previously mentioned, increased release probability is common in transgenic mice, before plaque deposition, presumably in response to rising Aβ levels (Cummings et al., 2015; Medawar et al., 2019) and, in the case of the APP^{NL-F} model, it seems that this effect is similar. Aβ-driven increase in probability of glutamate release could be the result of an altered regulation of synaptic vesicle life cycle and/or SNARE proteins expression (Russell et al., 2012; Yang et al., 2015; Park et al., 2017). SNARE proteins are present on synaptic vesicles and the target membrane, they form a tight complex to

mediate docking and fusion at the presynaptic active zone (Marsh and Alifragis, 2018). It was recently reported that some of the synaptic vesicle cycle proteins and glutamatergic presynaptic compartments are impaired in the APP^{NL-F} mice at early stages of the pathology (Hark et al., 2021). At 6 months, before significantly increased Aβ_{42} levels are detectable, proteins such as SNAP25, VAMP2, CALM and SNCA are elevated in the APP^{NL-F} hippocampus. This altered proteostasis seems to keep changing over time and by 12 months, when amyloid plaques have formed, presynaptic proteins are either reduced or trending back to control levels. Additionally, analysis of synaptic vesicle density was found to be increased in the CA1 area of the hippocampus of 6-month-old mice (Hark et al., 2021), which is consistent with increased release probability seen in these mice (Benitez et al., 2021). Also, it has been demonstrated that Aβ-induced presynaptic calcium influx enhances the release probability of neurotransmitter-containing synaptic vesicles, which triggers an abnormal high level of glutamate release in the extracellular space from neuronal cultures (Parodi et al., 2010; Brito-Moreira et al., 2011). Based on this information, we can suggest that SNARE proteins levels are potentially impaired by the age of 10 months, which triggers not only changes in the numbers of synaptic vesicles but also an increased glutamate release probability. It is at this age when Aβ levels start elevating in a significant manner and when plaques are being deposited in the APP^{NL-F} model. Finally, it is worth mentioning, that Hark et al., (2021) used as control group, the APP^{NL} model which harbours just the Swedish mutation; this mutation by itself elevates the total amount of Aβ_{40} and Aβ_{42} when compared to APP^{WT} mice (Saito et al., 2014). Potentially the changes seen in the SNARE proteins and synaptic vesicles of the APP^{NL-F} model could show an exacerbated change if compared to WT mice instead of APP^{NL}. An improved control for these models would be one where the Aβ sequence has been humanised without mutations.

In summary, increased release probability is an effect seen in some transgenic lines and APP knock-in models. The loss of this effect in APP^{NL-G-F} mice at 3.5 months of age could be due to a strong equilibrium shift towards Aβ deposition caused by the Arctic mutation. Indeed APP^{NL-G-F} mice have lower soluble Aβ levels than APP^{NL-F} mice at similar pathology stages, despite

heavier loads (Saito et al., 2014). Soluble Aβ is the more likely mediator of synaptic modulation which could lead to changes in the presynaptic calcium influx or in the SNARE complex proteins. These presynaptic changes trigger the increased glutamatergic release probability observed in the 10-month-old APP^{NL-F} model. There is potentially more soluble Aβ in the neuropil far from plaques as the equilibrium is not pushed towards deposition in the APP^{NL-F} mice; hence, the synapses affected might be far away from plaques and therefore, despite very few plaques the synapses recorded are affected. Whereas in the APP^{NL-G-F} only the synapses that are very close to the plaques would be affected and for that, a very heavy plaque load would be necessary. The APP knock-in mice avoid many problems associated with transgenic models, notably overexpression and inappropriate expression driven by non-endogenous promoters. The pattern of rising Aβ shown in these models mimics early stages of the disease without the artefacts of transgenic mice and provides a good design for the addition of further risk factors that may lead to improvements in the available models and understanding of the disease.

6.2 Microglial phenotypes at early amyloidopathy of APP knock-in mice

Microglial phenotypes have been long-established as part of Alzheimer's disease pathology. In the last decade, GWAS have highlighted the importance of microglia in AD by identifying gene variants related to the immune system that strongly associate with risk of being diagnosed for AD (Lambert et al., 2013; Karch et al., 2014). Many of the genes that have been shown to have variants that increase AD risk such as *TREM2*, *CR1*, *CD33*, *CLU* and *MS4A*, to name some, are expressed specifically or preferentially in microglia relative to other cell types (Naj et al., 2011; Guerreiro et al., 2013); this genetic trend implicates microglial dysfunction as a contributing factor to AD pathogenesis. Therefore, understanding the roles that microglia play in the healthy and AD brain is essential to determine how the immune system is affected and involved in the disease.

The progression of the amyloid pathology is accompanied by gliosis and a loss of the homeostatic functions in microglia (Keren-Shaul et al., 2017); microglial cells generate pro-inflammatory cytokines and chemokines in response to danger signals. Specifically, in the APP^{NL-G-F} it has been reported, that microglial activation starts at about 5 months of age (Sacher et al., 2019), which is also when phagocytic microglia become impaired (Sebastian Monasor et al., 2020; Pauls et al., 2021). Moreover, APP^{NL-G-F} cortical tissue exhibits altered expression of genes associated with immune/microglia modulation functions approximately at 6 months of age (Castillo et al., 2017). Consistent with these findings, despite the mild accumulation of Aβ plaques in the hippocampus, I observed unchanged microglia density at the age of 3.5 months (**Figure 4.4**). It is potentially a very early stage in the pathology to see glial effects in the brain. My results are in agreement with a recent poster publication from Imperial College London, where Iba-1$^+$ cell density and CD68$^+$ activated microglial density remained unchanged until 7 months of age (Tang, 2021). Moreover, I obtained a similar unchanged finding for the APP^{NL-F} model at a time when the first Aβ plaques were deposited in the hippocampus: microglial presence and activation numbers were not different from the WT group at 10 months of age (**Figure 4.8**). This could be explained by the fact that microglial gene expression of *Aif1* (the gene encoding for Iba-1) and *Trem2* remain unchanged in the hippocampus at this amyloid pathology stage (Benitez et al., 2021). Additionally, Pauls et al. pre-print (2021) strongly support these results by showing that AD related-microglial transcriptional analyses are not altered at 10 months of age due to the low accumulation level of Aβ plaques in the brain, but such profile changes with time in response to Aβ accumulation.

6.3 Unaltered Aβ plaque deposition following microglia depletion in APP knock-in mice

It has been previously shown that microglia elimination can be achieved in the healthy adult mouse brain by targeting the CSF1R with small-molecule inhibitors (Elmore et al., 2014; Dagher et al., 2015; Najafi et al., 2018). For AD pathology, selective microglia depletion using CSF1R inhibitors seems to be

an efficient approach to examine the effects of microglia depletion on amyloid plaque deposition, Tau pathology and spread progression, synaptic integrity and cognitive behaviour in mouse models (Spangenberg et al., 2016; Bennett et al., 2018; Spangenberg et al., 2019; Clayton et al., 2021). In this study, I sought to define the roles of microglia in mediating amyloid plaque deposition through the administration of PLX5622 at doses sufficient to almost fully eliminate microglia or to partially eliminate them to assess modulating functions at the earliest stages of plaque deposition.

Firstly, this project set out to determine if microglia in the brains of young APP^{NL-G-F} mice were dependent on CSF1R signalling for their survival. Consistent with previous reports, it was shown that 7 weeks of continuous treatment with either a low dose or a high dose of PLX5622 lead to a ~50% and ~90% reduction in microglia numbers, respectively, throughout the hippocampus in adult APP^{NL-G-F}. All the mice treated with PLX5622 gained weight similarly to controls and did not show any overt abnormal behaviour upon home cage observation. Knowing that the PLX5622 was successfully working, I then increased the feeding time for the APP^{NL-F} mice to a 3-month treatment duration due to the fact the Aβ pathology progresses at a slower pace in this model. I aimed to target the earliest plaque deposition stages in both APP knock-in models, and therefore different ages were used for PLX5622 treatments.

The elimination of microglia for 7 weeks from APP^{NL-G-F} or 3 months from APP^{NL-F} mice permitted the role that these cells play in early Aβ plaque development to be investigated. It has been repeatedly suggested that microglial cells react to the presence of Aβ plaques by clearing them from the brain via phagocytosis of Aβ fibrils (Pan et al., 2011; Ries and Sastre, 2016). Reactive microglia surround plaques, bind and internalise Aβ aggregates (Paresce et al., 1997). It has further been proposed that this cell arrangement acts as a barrier around plaques that aims to limit plaques expansion and toxicity to other cells (Paresce et al., 1997; Condello et al., 2015). However, once plaques are deposited in the brain, even with substantial microglia proliferation and clustering, they continue spreading (e.g. (Medawar et al., 2019). Diverse reports have demonstrated controversial findings when

assessing the effects of depleting microglia in mouse models for AD. For example, inducing microglia ablation in APP/PS1 overexpressing mice resulted in unaltered amyloid pathology in cortical tissue (Grathwohl et al., 2009; Olmos-Alonso et al., 2016). Also, similar results were found with other mouse models (3xTg, 5xFAD); when microglia numbers were reduced no changes were seen in Aβ levels or plaques in hippocampus, cortex, thalamus and subiculum (Dagher et al., 2015; Spangenberg et al., 2016; Zhong et al., 2019). Our findings are in complete agreement with this, as no changes in Aβ plaque coverage and average plaque size in the hippocampus of APP knock-in mice following microglial elimination were observed (**Figure 4.5, Figure 4.9**). Interestingly, if anything, there are fewer of the smallest plaques, presumably those most recently deposited, when microglia are removed with PLX5622. This is consistent with microglia moderating the initial development of plaques (Spangenberg et al., 2016) but, as we show the same density and coverage of plaques at early stages, microglial cells probably mediate seeding of Aβ plaques. The presence of larger plaques that denominate the overall coverage suggests that there was some level of plaque development before microglia were substantially depleted; those plaques continue to grow normally but there are fewer newly seeded small plaques in the absence of microglia. It was recently proposed that synaptic toxicity imparted by Aβ potentially induces microglia to phagocytose damaged synapses rather than actual Aβ, limiting the spread of damage (Edwards, 2019). Supporting this theory, Tzioras *et al.* (2019) shows adult human microglia containing synaptic proteins and that synapses derived from AD brain are ingested more readily. It can then be suggested that there are alternative roles for microglia in an Aβ environment, including compacting Aβ via TREM2-dependant mechanisms (Wang et al., 2016; Yuan et al., 2016) or clearing Aβ via non-phagocytic mechanisms (Fu et al., 2020). Thus, it can be considered that microglia in the AD brain are not able to cope with the demand of clearing Aβ plaques from the CNS or protect against plaque formation/growth in young pre-pathological mice. The question remains, if microglia attempt to phagocytose Aβ, but they fail to degrade it, then what happens to that engulfed Aβ? Further investigations are necessary to clarify potential explanations.

I also observed that, when microglial numbers were depleted, the remaining Iba-1^{+} microglia were distinctly CD68^{+}, irrespective of the presence of Aβ plaques. It is unclear if those CD68^{+} activated cells were PLX5622-resistant or that blocking the CSF1R shifts the resistant microglia towards a phagocytic phenotype. It is worth considering as well, that microglia are heterogenous, and that different subpopulations have a wide variety of responses to environmental changes (Masuda et al., 2020). For example, in the APP[NL-G-F] mice, the density of CD68^{+} microglia was unaltered by the low-dose of PLX5622 compared to the control mice, despite a halving of the total microglia. Further studies would be required to characterise remaining microglia in our models.

Consistent with the results presented in this thesis, some publications have shown that, following microglia ablation there is a reduction of the amyloid burden in the 5XFAD mice (Sosna et al., 2018; Spangenberg et al., 2019; Son et al., 2020). Supporting that idea, a recent publication describes that, without microglia, Aβ plaque numbers are lowered showing a more diffuse and less compact-like phenotype and additionally inflammatory cytokines associated with microgliosis were supressed by PLX5622 treatments (Casali et al., 2020). Notably, all the previous studies assessing the effect of microglia depletion on amyloid deposition used models overexpressing mutated human *APP*. Amyloid pathology as a result of overexpression together with mutations could trigger a more robust phenotype than the ones seen in the APP knock-in models. Consequently, the overexpression of *APP* artefacts could confer microglia with different signatures, such as the DAM phenotype (Bisht et al., 2016; Keren-Shaul et al., 2017; Pauls et al., 2021), from non-overexpressing models, which then makes our results difficult to compare. Overall, taking together the reports that support or contrast my results, it is clear that there are differences between mouse models, onset of the pathology, duration/efficiency of microglia depletion and techniques for staining/quantifying Aβ plaques that lead to diverse suggestions. This year, a research publication using not just the same microglia depletion approach (PLX5622) but also one of the mouse models used in my project, APP[NL-G-F], showed intriguing results. In contrast to Casali's publication (2020) , Clayton *et al.* (2021) described an increase in

compact, but not diffuse Aβ plaque deposition in the cortex of 6-month-old mice. This is the first report showing an increase in plaque burden after treating mice with PLX5622 and it suggest that microglia are indeed involved in plaque compaction and clearance. This publication aimed to target the peak of the pathology, while my project was focused on the earliest stage of plaque deposition; the difference in age could be triggering different microglial responses. It is at the age of 6 months, when the APP^{NL-G-F} mice start showing AD expression signatures, especially in microglial phagocytosis pathways. Functional enrichment analysis of AD signatures recently revealed that several upregulated pathways correspond exclusively to the activation of the immune system, including phagocytosis or cytokine production pathways in both APP knock-in models. Specifically, in the 6-month-old APP^{NL-G-F} there is a clear upregulation of genes like *Cst7*, *Tyrobp*, *Cx3cr1* and *Trem2* (Pauls et al., 2021), which was absent at 3.5 months of age. Actually, unpublished Edwards' lab data show how those same genes start changing their expression by the age of 4 months, but still no significant differences are found until later ages of the pathology (**Figure 6.1**).
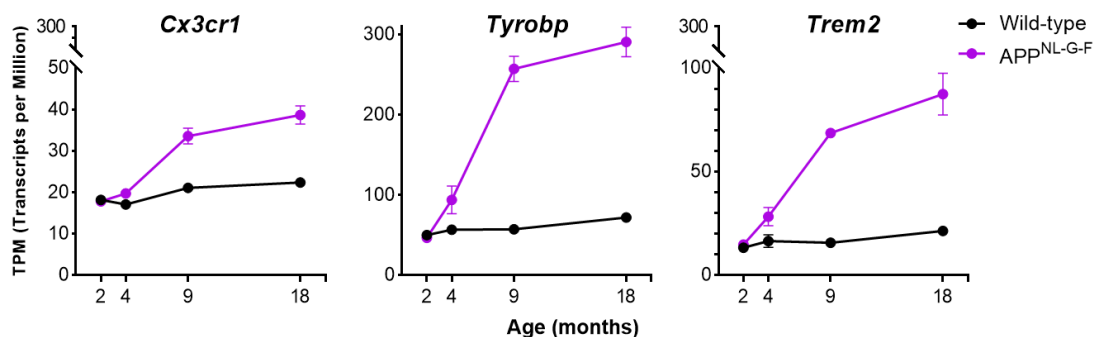
Figure 6.3 APP^{NL-G-F} gene expression at different time points expressed in months. Gene transcripts associated with microglial activation (n=6). Two-way ANOVA revealed a significant main effect of genotype, age and an interaction. Significant differences observed at 9 and 18 months of age (p<0.0001) NS at 2 and 4 months of age. Data soon to be available at http://www.mouseac.org/.

6.4 Synaptic transmission changes in the absence of microglia in healthy mice

Previous studies have shown that microglial depletion by CSF1R inhibitors leads to enhanced dendritic spine densities and synaptic puncta (Elmore et al.,

2014; Rice et al., 2015). Until our article currently in press (Benitez et al., 2021), hippocampal synaptic transmission assessment after ablation of microglia with PLX5622 in AD mouse models has not been reported in the literature. However, a few publications have focused on suggesting how synapses behave in the absence of microglia. A significant decrease in synaptic proteins levels and glutamatergic synaptic function were reported after induction of microglia depletion by diphtheria toxin (Parkhurst et al., 2013); organotypic hippocampal slices treated with clodronate to eliminate microglia results in an increased frequency of excitatory postsynaptic currents, consistent with higher synaptic density or increased release probability (Ji et al., 2013) which suggests that microglia regulate synaptic numbers and/or presynaptic factors. Similarly, both excitatory and inhibitory connectivity were increased in the adult mouse after dramatic PLX-depletion of microglial cells, thus microglia were involved in shaping the cortical synaptic architecture (Liu et al., 2021). Loss-of- function or deletion studies of microglial CD200R or CX3CR1 have shown reduced or enhanced hippocampal LTP (Maggi et al., 2011; Rogers et al., 2011). Nevertheless, it is still unclear how microglia regulate synaptic functions. In this context and given the increasing evidence of microglia role in AD progression, it is crucial to understand how microglial activity regulates synaptic functions under physiological conditions. Thus, apart from assessing Aβ plaque development after depleting ~50 or ~90% of microglial cells in the APP knock-in mice, I also evaluated if microglia were contributing or regulating adult hippocampal synaptic activity in healthy WT mice. Surprisingly, I found that the absence of microglia does not affect basal transmission or synaptic plasticity (**Figure 5.1**, **Figure 5.2**). Processes of astrocytes as well as microglia are in close proximity to synapses (Damisah et al., 2020) and so, potentially astrocytic activity compensates the absence of microglia after PLX5622 treatments and consequently no changes in synapses are seen. For example, it was recently evidenced that in case of microglial dysfunction, the expression of astrocyte marker *Gfap* is significantly increased, and astrocytes display a hypertrophic phenotype (Konishi et al., 2020). Astrocytes can elicit their phagocytic activity to maintain the CNS homeostasis in the absence of microglial inputs.

6.5 Elimination of microglia does not affect synaptic plasticity of APP^{NL-G-F} model

In this study, I was interested in investigating the role of microglia in synaptic communication during the onset of AD pathology in APP knock-in models. We demonstrated that microglial cells do not clear or modulate early Aβ plaque numbers/sizes in the hippocampus, but according to some evidence (Hong et al., 2016a; Spangenberg et al., 2016) microglia could play a role in synaptic damage or neuronal loss in disease. I discovered that in the AD brain of young APP^{NL-G-F}, microglia are not required for the maintenance of hippocampal basal synaptic activity and plasticity. As previously explained, assessment of the I-O relationship in the CA1-CA3 synapses of 3.5-month-old APP^{NL-G-F} mice resulted in an increased fEPSP slope when high stimulation was given (>30V); we proposed that this was an effect of potential hyperexcitability present in this model or a change in background GABA levels. Interestingly, such effect was recovered after partial or almost total depletion of microglia as the fEPSP values went back to control levels (**Figure 5.3A**). Thus, the increase in response in APP^{NL-G-F} is dependent on microglia numbers.

When I assessed short-term and long-term synaptic plasticity, despite a profound effect on microglial numbers, treatments with both drug doses did not affect the PPR or LTP in APP^{NL-G-F} mice (**Figure 5.3B,Figure 5.4**). A similar finding in Trem2 knock-out APP/PS1 mice was reported by Sheng et al., (2019); this model showed impaired microglial functions at an early stage of Aβ plaque deposition. There were not significant impairments in fEPSPs, number of synapses or expression of neurotransmitter receptors at 4 months of age, but synaptic impairments were evident at later disease stages. Supporting my results, preliminary data from Edwards' lab found unchanged dendritic spine numbers in PLX5622 treated mice when comparing WT vs APP^{NL-G-F} groups. The lack of an effect in these animals could mean that microglial cells do not strongly influence the synaptic plasticity phenomenon and removing them does not change it. Also, microglia deficiency has no effect on initial amyloidosis, but potentially at later stages of the pathology, they could become crucial for the progression of the disease.

6.6 Elimination of microglia decreases spontaneous and miniature EPSCs of WT and APP^{NL-F} mice

The role of microglia in excitatory synaptic transmission when plaques are first seen in the APP^{NL-F} mice was also explored in this project. As mentioned before, several soluble factors can regulate neuron-microglia interactions as microglial cells release factors such as chemokines, cytokines and neurotransmitters in response to neuronal signals (Wohleb, 2016). Microglial cytokines are required for normal surface expression of AMPA receptors at synapses. For example, it has been seen that high concentrations of TNF-α causes a rapid exocytosis of AMPA receptors in hippocampal pyramidal neurons (Beattie et al., 2002). Similarly, in young rats engineered to produce human Aβ, an augmented excitatory synaptic transmission at CA3-CA1 synapses carrying the *Trem2*^{R47H} variant was found; such increase was found to be an effect of raised brain concentrations of TNF-α produced by microglial cells (Ren et al., 2020). For this section of my project, I examined the effects of chronic microglial depletion on glutamatergic synaptic transmission in the hippocampal CA1 pyramidal cells of 10-month-old mice. sEPSCs frequency was significantly affected by PLX5622 treatments (**Figure 5.8**). Depleting microglia had a different effect from altering their function with the Trem2^{R47H} variant. In my results, partial or near-total absence of microglia decreased the frequency of spontaneous and miniature EPSCs (**Figure 5.9**), whilst the Trem2^{R47H} rats were reported to show increased mEPSCs without changes in release probability (Ren et al., 2020). It has been established that Trem2^{R47H} alteration decreases the phagocytic CD68$^+$ microglial phenotype in mice (Liu et al., 2020), which is the opposite to what PLX5622 does. After depletion treatments, remaining microglia are mostly CD68$^+$ (**Figure 4.4C,Figure 4.8C**). Taken together, these findings suggest that chronic depletion of microglia could potentially reduce glutamatergic synaptic function in 10 months old APP^{NL-F} and WT mice, possibly by reducing the number of glutamatergic synapses, probability of glutamate release or number of release sites. Then, the reduction in glutamatergic function caused by microglial depletion seems to be independent of the presence of Aβ pathology in the APP^{NL-F} mice and restricted to the presynaptic properties of the cells; microglia depletion does

not affect the postsynaptic transmission of CA3-CA1 synapses, as amplitude, which is dependent on postsynaptic AMPA receptors, was not significantly altered. Additionally, we should consider that there is an increase in release probability as well, especially with the lower dose. This could suggest that there is increased release probability that is compensated by a decrease in synapse numbers or a decrease in axon excitability. This suggestion would endow microglia with a protective role in both WT and APP knock-in mice.

The reduction of EPSCs frequency in spontaneous and miniature currents coincides with the increased microglial activation seen in the hippocampus after 3-month-PLX5622 treatments (**Figure 4.8C**). In partial or near complete depletion groups, the remaining microglial cells were mostly CD68$^+$, this is an indication of phagocytic activity which could be affecting the CA1 synapses. This result supports the publication from Ji et al. (2013) where they propose that microglia are actively mediating changes in synaptic activity by engulfing synaptic components. It seems that remaining microglia could be phagocyting damaged synaptic materials in the effort of keeping homeostasis in the brain and prevent further damage (Edwards, 2019).

6.7 Elimination of microglia effects in evoked synaptic transmission in APP knock-in models.

The results of this project showed that ablation of microglia exacerbated the decrease in PPRs in both APP knock-in models (**Figure 5.7**, **Figure 5.10**). In particular, this phenotype was more pronounced in response to partial removal of microglia than near-complete ablation (at least at the 25 ms inter-stimulus interval), suggesting that the remaining Iba-1$^+$ and mostly CD68$^+$ microglia have a modulating effect, rather than the near-complete absence of microglia being the cause of the change. It can be proposed that, while the loss of microglial cells may be damaging, this is not an amyloid-specific phenomenon but a change in the same direction, exacerbated in disease. The fact that no effect of treatment or genotype on PPR was detected on the 50 ms interstimulus interval, does not invalidate the effect observed at the 25 ms

interval. Any difference in PPR will be less pronounced on longer intervals as a result of calcium being buffered (Zucker and Regehr, 2002).

Taken the results presented in this project together, I suggest that microglial cells may have a direct effect on glutamate release probability rather than, or as well as, Aβ having the effect. While the number of microglia is important, potentially even more important is the level of activation of these cells, as the remaining microglia after PLX5622 treatment tend to be CD68$^+$. It seems that CD68$^+$ cells trigger an increase in neurotransmitter release probability. In the case of the APP^{NL-G-F} treated mice, the high dose of PLX5622 removes more than 90% of microglia and consequently, the few remaining CD68$^+$ cells have little effect on synaptic transmission. In contrast, with the low dose of PLX5622, the remaining CD68$^+$ cells increase the neurotransmitter probability of release, and moreover, this effect is even more striking in the WT mice. In the untreated APP^{NL-F}, the increased probability of release could be a direct effect of the rising Aβ levels when plaques are starting to form or even before plaques are detectable (Benitez et al., 2021). After PLX5622 treatments, in both APP^{NL-F} and WT mice, the decrease in spontaneous and miniature EPSCs may be a homeostatic response to the increased release probability seen in both groups. It is likely that CD68$^-$ microglia help to maintain healthy synapses and in the absence of those cells, a loss of general homeostatic microglial function is triggered. This loss could be reflected in an active increase of release probability from the CA3-CA1 synapses in the presence of only CD68$^+$ cells. This is especially true with the low dose of PLX5622, when there is a substantial number of microglial cells present; no effect in high dose is seen in young 3.5-month-old mice and less effect in older 10-month-old mice.

6.8 Contrasting phenotypes between APP knock-in and transgenic mice

The lack of electrophysiological and microglial phenotypes in the APP^{NL-G-F} mice when plaques first appear is in contrast to the clear effects in both transgenic mice (Cummings et al., 2015; Medawar et al., 2019) and APP^{NL-F}

at an equivalent stage of Aβ pathology. In the case of the APP^{NL-G-F} model, lower soluble Aβ levels due to the higher propensity for Aβ fibrillation imparted by the Arctic mutation may be the cause. So, while the APP^{NL-G-F} model is attractive as it presents with rapid plaque formation, its usefulness as a model for AD is in understanding how folding of Aβ and proximity to plaques affect synaptic phenotypes. On the other hand, the mutations in APP^{NL-F} mice are restricted to the β- and γ-secretase cleavage sites flanking the Aβ sequence and are thus used as a tool to trigger the raise in Aβ levels observed in sporadic AD.

Another consideration in comparing models is the choice of control. Until now the WT mouse has been the best available control, but we have to consider its limitations. The difference in sequence between human and mouse APP alters the affinity for β-secretase. Humanising *APP* increases Aβ levels compared to WT mice (Serneels et al., 2020), suggesting that even with knock-in mice, some of the changes may be exaggerated when compared to WT animals. The humanised APP mouse will be an improved control in future studies.

This second generation of AD mouse models is advantageous over the transgenic models; however, neurofibrillary tangles are never seen in the APP knock-in mice during their lifespan, and therefore the field still lacks a model with a fully AD pathology expressed. The APP knock-in mice seem to be useful as preclinical AD models to study the pathological role of amyloidosis and amyloid-associated neuroinflammation.

6.9 Relationship between amyloid, TREM2 microglia and tau pathology.

Apart from exploring the effects of TREM2 on amyloid pathology, elucidating the mechanisms that link TREM2 and its variants with tau aggregation has become a niche that needs to be further investigated and prioritised within the field. A study using APP/PS1 mice with human tau injections and made to express human TREM2 showed that tau pathology is accelerated and

microglial recruitment to plaques is impaired when the R47H variant is introduced (Leyns et al., 2019). Similarly, it has been shown that in the 5xFAD model both TREM2^{KO} or microglia depletion with PLX3392 results in a faster seeding and spreading of tau around plaques (Gratuze et al., 2021); it is then suggested that TREM2-dependent activation of the DAM phenotype is crucial in delaying Aβ-induced tau pathology. In agreement with Gratuze's group, Lee et. al. (2021) found that tau propagation is exacerbated upon TREM2 deletion, however, this effect is only present when toxic Aβ is expressed in TauPS2APP mice. Taking these publications together it is shown that there are specific pathways through which TREM2-expressing microglia, amyloid and tau pathology interact: TREM2 microglia slows down the progression of the disease by modulating or restricting the amyloid cascade influence towards the spread of tau. It is proposed that during disease, an impaired microglial response contributes to amyloid-induced neuronal damage which eventually results in tangles formation and further neurodegeneration (Hardy and Salih, 2021).

Recently, Delizannis et. al. (2021), further investigated the consequences of not only fully impairing microglial interactions with Aβ and tau by using AD-tau injected 5xFAD×TREM2$^{-/-}$ mice, but also they analysed the effects of a partial impairment with TREM2$^{+/-}$. Heterozygous mice revealed a greater Aβ plaque-associated microglia and a higher but comparable AT8-positive NP tau pathology than the TREM2$^{-/-}$ mice. Additionally, the differences in gene expression and microglial phenotype between TREM2$^{+/-}$ and TREM2$^{-/-}$ mice showed that the former could represent better the single copy loss-of-function TREM2 variants associated with AD risk. The data reported in this thesis agreed with this idea; partial depletion of microglia, by using low dose PLX5622, affects microglial phenotype which may still contribute to the production of Aβ plaques and plaque-associated neuritic damage reflected in electrophysiological impairments with an increased PPR.

6.10 Summary of main findings in APP knock-in mice treated with PLX5622

Figure 6.4 Comparison of synaptic transmission changes in APP knock-in models *vs* Wild-type mice. Summary of synaptic transmission changes in APP knock-in mice with or without microglia depletion using PLX5622. EPSCs based on APP^{NL-F} experiments; LTP data based on APP^{NL-G-F} experiment. PPR results were consistent between both APP knock-in models. Created with BioRender.com

6.11 Microglia CD68$^+$ phenotype increases neurotransmitter release probability with or without the presence of Aβ plaques
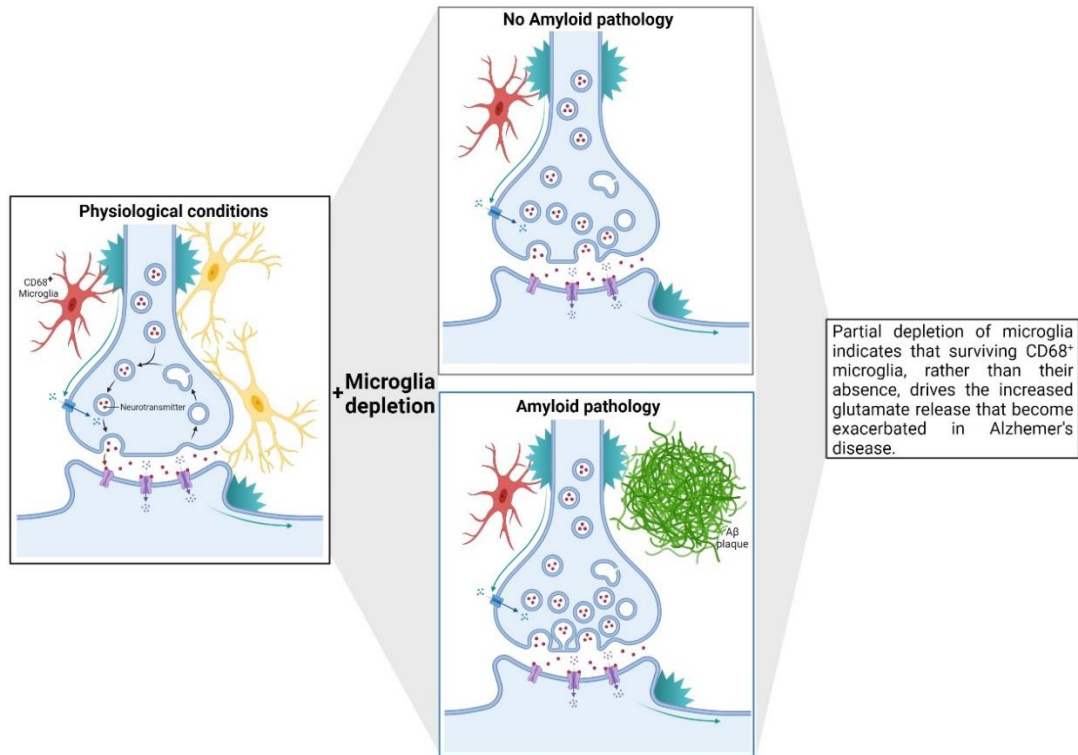
Created with BioRender.com

Figure 6.5 CD68$^+$ microglia is capable of interacting with the synaptic properties of neurons and may be able to influence in the neurotransmitter release probability. Schematic depicting the effect of microglia depletion in the glutamate release probability of neurons with or without Aβ pathology. Electrophysiology and immunohistochemistry data presented in this thesis suggests that surviving phagocytic microglia, and the lack of resting microglia, are triggering an increase in neurotransmitter release (represented by more synaptic vesicles), such effect is more pronounced with the presence of Aβ plaques.

CONCLUDING REMARKS

Within amyloidopathy research, and indeed dementia research in general, the use of mouse models has become crucial in improving our understanding of the aetiology of AD. The availability of models is essential, especially regarding the development and testing of new treatments. Currently, therapies or treatment options for AD are limited to symptomatic relief, rather than targeting early initiating factors that trigger the onset and progression of the disease. Several clinical trials have focused on Aβ with the aim of reducing its production or increasing the clearance, however, such trials have all failed in the clinic, indicating that Aβ is not the sole factor driving the emergence of the disease. Recently, neuroinflammation has gained particular research interest due to the fact that GWAS highlighted variants related to microglial cells that increase the risk of developing AD. Microglia cells are complex and dynamic. For years they have been considered to have important modulatory and management functions during disease, however little is known about their interaction with Aβ or their specific roles/responses during AD.

For the work presented here, I sought to investigate the roles of microglia at an early amyloid pathology stage. In the first chapter of this thesis, I further characterised the phenotype of the APP^{NL-F} and APP^{NL-G-F} mouse models through electrophysiological studies. I carried out experiments to study synaptic function, including basal synaptic transmission and LTP at early stages of Aβ plaques deposition. I found an increased probability of glutamate release at the time plaques start being deposited in the hippocampus of APP^{NL-F} mice; this result is consistent with transgenic models. I next set out to determine the contribution of microglia to plaque formation. I confirmed that microglia in the AD brain are dependent on CSF1R signalling for their survival. Using a CSF1R inhibitor to eliminate microglia for either 1.5 months in 3.5-month-old APP^{NL-G-F} or 3 months in 10-month-old APP^{NL-F}, I discovered no overall changes on Aβ plaque deposition, but a reduction in number of small plaques in both APP knock-in models after microglia depletion. Finally,

removing about half of the proportion of microglial cells indicated that the surviving phagocytic microglia, rather than their absence, were driving an effect on glutamate release that becomes exacerbated in AD.

Collectively, this novel work shows a characterisation and comparison of the relationship between plaques, synaptic transmission and microglial activity in the two APP knock-in mouse lines, in which overexpression and other artefacts associated with transgenic technology are avoided. These data improve our understanding of microglial functions in the AD brain and potentially this information could be used to accelerate the development of disease-modifying therapies to slow or prevent disease progression.

Future directions

In order to understand the implications of CD68$^+$ microglial activity that affect neurotransmitter release probability, it would also be helpful to analyse further surviving microglial gene transcriptional changes after PLX5622 depletion. Transcript levels of genes such as *Trem2*, *Cst7*, *Cstd* or *Tyrobp* could be analysed to determine how inflammatory signalling could be impacted by microglial elimination in APP knock-in mice. Similarly, expression of genes and protein abundance analysis could be useful to find potential defects on synapse membrane proteins (SNAREs) or neurotransmitters signalling systems, such as *Stx1b*, *Snap25*, *Calm* or *Vamp2*. Also, to assess the effect of CD68$^+$ microglial modulation on synaptic transmission properties, the density of dendritic spines could be performed for WT and APP knock-in CA1 pyramidal neurons.

To analyse the differences between PLX5622 surviving microglia and dysfunctional Trem2^{R47H} microglia in synaptic transmission, it would be interesting to perform electrophysiology experiments in CA1 hippocampal cells of APP^{NL-F} mice crossed with TREM2^{R47H} knock-in mice. Additionally, further studies to analyse the heterogeneity or seeding of small Aβ plaques in this

model could be useful to elucidate the potential microglial factors that determine under which conditions Aβ aggregation develops.

As reactive gliosis is one of the features of AD, it would be interesting to assess if microglial elimination affects astrocyte numbers or signalling pathways. Immunostainings for reactive astrocytes using GFAP and S100B with LCO for Aβ plaques in the hippocampus.

Finally, the scope of this thesis was focused on early stages of amyloid pathology where physiological aging aspects are not considered. Neurons are particularly vulnerable to age-associated deterioration and also, it is known that there are microglial inflammatory/phagocytic signalling impairments during ageing. To follow up my work, it would be valuable to assess the effect that PLX5622 could have in the synaptic properties of hippocampal cells of APP^{NL-F} mice at 18-24 months of age.

REFERENCES

Abrahamsson, T., Lalanne, T., Watt, A.J., and Sjostrom, P.J. (2016). In Vitro Investigation of Synaptic Plasticity. Cold Spring Harb Protoc *2016*, pdb top087262.

Abramov, E., Dolev, I., Fogel, H., Ciccotosto, G.D., Ruff, E., and Slutsky, I. (2009). Amyloid-beta as a positive endogenous regulator of release probability at hippocampal synapses. Nat Neurosci *12*, 1567-1576.

Acharya, M.M., Green, K.N., Allen, B.D., Najafi, A.R., Syage, A., Minasyan, H., Le, M.T., Kawashita, T., Giedzinski, E., Parihar, V.K.*, et al.* (2016). Elimination of microglia improves cognitive function following cranial irradiation. Sci Rep *6*, 31545.

Akiyama, H., Barger, S., Barnum, S., Bradt, B., Bauer, J., Cole, G.M., Cooper, N.R., Eikelenboom, P., Emmerling, M., Fiebich, B.L.*, et al.* (2000). Inflammation and Alzheimer's disease. Neurobiol Aging *21*, 383-421.

Akiyama, H., Nishimura, T., Kondo, H., Ikeda, K., Hayashi, Y., and McGeer, P.L. (1994). Expression of the receptor for macrophage colony stimulating factor by brain microglia and its upregulation in brains of patients with Alzheimer's disease and amyotrophic lateral sclerosis. Brain Res *639*, 171-174.

Aladeokin, A.C., Akiyama, T., Kimura, A., Kimura, Y., Takahashi-Jitsuki, A., Nakamura, H., Makihara, H., Masukawa, D., Nakabayashi, J., Hirano, H.*, et al.* (2019). Network-guided analysis of hippocampal proteome identifies novel proteins that colocalize with Abeta in a mice model of early-stage Alzheimer's disease. Neurobiology of disease *132*, 104603.

Alzheimer, A., Stelzmann, R.A., Schnitzlein, H.N., and Murtagh, F.R. (1995). An English translation of Alzheimer's 1907 paper, "Uber eine eigenartige Erkankung der Hirnrinde". Clin Anat *8*, 429-431.

Amit, I., Winter, D.R., and Jung, S. (2016). The role of the local environment and epigenetics in shaping macrophage identity and their effect on tissue homeostasis. Nature immunology *17*, 18-25.

Askew, K., and Gomez-Nicola, D. (2018). A story of birth and death: Insights into the formation and dynamics of the microglial population. Brain, Behavior, and Immunity *69*, 9-17.

Ballard, C., Gauthier, S., Corbett, A., Brayne, C., Aarsland, D., and Jones, E. (2011). Alzheimer's disease. The Lancet *377*, 1019-1031.

Baron, R., Babcock, A.A., Nemirovsky, A., Finsen, B., and Monsonego, A. (2014). Accelerated microglial pathology is associated with Abeta plaques in mouse models of Alzheimer's disease. Aging Cell *13*, 584-595.

Bartels, T., De Schepper, S., and Hong, S. (2020). Microglia modulate neurodegeneration in Alzheimer's and Parkinson's diseases. Science *370*, 66-69.

Beattie, E.C., Stellwagen, D., Morishita, W., Bresnahan, J.C., Ha, B.K., Von Zastrow, M., Beattie, M.S., and Malenka, R.C. (2002). Control of synaptic strength by glial TNFalpha. Science *295*, 2282-2285.

Beauquis, J., Vinuesa, A., Pomilio, C., Pavia, P., and Saravia, F. (2014). [Hippocampal and cognitive alterations precede amyloid deposition in a mouse model for Alzheimer's disease]. Medicina *74*, 282-286.

Bellenguez, C., Grenier-Boley, B., and Lambert, J.C. (2020). Genetics of Alzheimer's disease: where we are, and where we are going. Curr Opin Neurobiol *61*, 40-48.

Benitez, D.P., Jiang, S., Wood, J., Wang, R., Hall, C.M., Peerboom, C., Wong, N., Stringer, K.M., Vitanova, K.S., Smith, V.C.*, et al.* (2021). Knock-in models related to Alzheimer's disease: synaptic transmission, plaques and the role of microglia. Mol Neurodegener *16*, 47.

Bennett, R.E., Bryant, A., Hu, M., Robbins, A.B., Hopp, S.C., and Hyman, B.T. (2018). Partial reduction of microglia does not affect tau pathology in aged mice. J Neuroinflammation *15*, 311.

Benzing, W.C., Wujek, J.R., Ward, E.K., Shaffer, D., Ashe, K.H., Younkin, S.G., and Brunden, K.R. (1999). Evidence for glial-mediated inflammation in aged APPSW transgenic mice. Neurobiology of Aging *20*, 581-589.

Bird, C.M., and Burgess, N. (2008). The hippocampus and memory: insights from spatial processing. Nature reviews Neuroscience *9*, 182-194.

Bisht, K., Sharma, K.P., Lecours, C., Sanchez, M.G., El Hajj, H., Milior, G., Olmos-Alonso, A., Gomez-Nicola, D., Luheshi, G., Vallieres, L.*, et al.* (2016). Dark microglia: A new phenotype predominantly associated with pathological states. Glia *64*, 826-839.

Blennow, K., de Leon, M.J., and Zetterberg, H. (2006). Alzheimer's disease. Lancet *368*, 387-403.

Blennow, K., Zetterberg, H., Rinne, J.O., Salloway, S., Wei, J., Black, R., Grundman, M., Liu, E., and Investigators, A.A.B. (2012). Effect of immunotherapy with bapineuzumab on cerebrospinal fluid biomarker levels in patients with mild to moderate Alzheimer disease. Arch Neurol *69*, 1002-1010.

Bliss, T.V., and Collingridge, G.L. (1993). A synaptic model of memory: long-term potentiation in the hippocampus. Nature *361*, 31-39.

Bliss, T.V., and Lomo, T. (1973). Long-lasting potentiation of synaptic transmission in the dentate area of the anaesthetized rabbit following stimulation of the perforant path. The Journal of physiology *232*, 331-356.

Boche, D., Perry, V.H., and Nicoll, J.A. (2013). Review: activation patterns of microglia and their identification in the human brain. Neuropathol Appl Neurobiol *39*, 3-18.

Bolmont, T., Haiss, F., Eicke, D., Radde, R., Mathis, C.A., Klunk, W.E., Kohsaka, S., Jucker, M., and Calhoun, M.E. (2008). Dynamics of the

microglial/amyloid interaction indicate a role in plaque maintenance. J Neurosci *28*, 4283-4292.

Bornemann, K.D., Wiederhold, K.H., Pauli, C., Ermini, F., Stalder, M., Schnell, L., Sommer, B., Jucker, M., and Staufenbiel, M. (2001). Abeta-induced inflammatory processes in microglia cells of APP23 transgenic mice. Am J Pathol *158*, 63-73.

Braak, E., Griffing, K., Arai, K., Bohl, J., Bratzke, H., and Braak, H. (1999). Neuropathology of Alzheimer's disease: what is new since A. Alzheimer? Eur Arch Psy Clin N *249*, 14-22.

Braak, H., and Braak, E. (1991). Neuropathological stageing of Alzheimer-related changes. Acta Neuropathol *82*, 239-259.

Braskie, M.N., Medina, L.D., Rodriguez-Agudelo, Y., Geschwind, D.H., Macias-Islas, M.A., Thompson, P.M., Cummings, J.L., Bookheimer, S.Y., and Ringman, J.M. (2013). Memory performance and fMRI signal in presymptomatic familial Alzheimer's disease. Hum Brain Mapp *34*, 3308-3319.

Brito-Moreira, J., Paula-Lima, A.C., Bomfim, T.R., Oliveira, F.B., Sepulveda, F.J., De Mello, F.G., Aguayo, L.G., Panizzutti, R., and Ferreira, S.T. (2011). Abeta oligomers induce glutamate release from hippocampal neurons. Curr Alzheimer Res *8*, 552-562.

Busche, M.A., Eichhoff, G., Adelsberger, H., Abramowski, D., Wiederhold, K.H., Haass, C., Staufenbiel, M., Konnerth, A., and Garaschuk, O. (2008). Clusters of hyperactive neurons near amyloid plaques in a mouse model of Alzheimer's disease. Science *321*, 1686-1689.

Busche, M.A., and Konnerth, A. (2016). Impairments of neural circuit function in Alzheimer's disease. Philos Trans R Soc Lond B Biol Sci *371*.

Cagnin, A., Brooks, D.J., Kennedy, A.M., Gunn, R.N., Myers, R., Turkheimer, F.E., Jones, T., and Banati, R.B. (2001). In-vivo measurement of activated microglia in dementia. Lancet *358*, 461-467.

Casali, B.T., MacPherson, K.P., Reed-Geaghan, E.G., and Landreth, G.E. (2020). Microglia depletion rapidly and reversibly alters amyloid pathology by modification of plaque compaction and morphologies. Neurobiology of disease *142*, 104956.

Castillo, E., Leon, J., Mazzei, G., Abolhassani, N., Haruyama, N., Saito, T., Saido, T., Hokama, M., Iwaki, T., Ohara, T*., et al.* (2017). Comparative profiling of cortical gene expression in Alzheimer's disease patients and mouse models demonstrates a link between amyloidosis and neuroinflammation. Sci Rep *7*, 17762.

Chakrabarty, P., Li, A., Ceballos-Diaz, C., Eddy, J.A., Funk, C.C., Moore, B., DiNunno, N., Rosario, A.M., Cruz, P.E., Verbeeck, C*., et al.* (2015). IL-10 alters immunoproteostasis in APP mice, increasing plaque burden and worsening cognitive behavior. Neuron *85*, 519-533.

Chartier-Harlin, M.C., Crawford, F., Houlden, H., Warren, A., Hughes, D., Fidani, L., Goate, A., Rossor, M., Roques, P., Hardy, J*., et al.* (1991). Early-onset Alzheimer's disease caused by mutations at codon 717 of the beta-amyloid precursor protein gene. Nature *353*, 844-846.

Chasseigneaux, S., and Allinquant, B. (2012). Functions of Abeta, sAPPalpha and sAPPbeta : similarities and differences. J Neurochem *120 Suppl 1*, 99-108.

Chen, Y., Fu, A.K.Y., and Ip, N.Y. (2019). Synaptic dysfunction in Alzheimer's disease: Mechanisms and therapeutic strategies. Pharmacol Ther *195*, 186-198.

Cheng, I.H., Palop, J.J., Esposito, L.A., Bien-Ly, N., Yan, F., and Mucke, L. (2004). Aggressive amyloidosis in mice expressing human amyloid peptides with the Arctic mutation. Nat Med *10*, 1190-1192.

Clayton, K., Delpech, J.C., Herron, S., Iwahara, N., Ericsson, M., Saito, T., Saido, T.C., Ikezu, S., and Ikezu, T. (2021). Plaque associated microglia hyper-secrete extracellular vesicles and accelerate tau propagation in a humanized APP mouse model. Molecular Neurodegeneration *16*, 18.

Clayton, K.A., Delpech, J.C., Herron, S., Iwahara, N., Saito, T., Saido, T.C., Ikezu, S., and Ikezu, T. (2020). Amyloid plaque deposition accelerates tau propagation via activation of microglia in a humanized APP mouse model. bioRxiv, 2020.2009.2022.308015.

Condello, C., Yuan, P., and Grutzendler, J. (2018). Microglia-Mediated Neuroprotection, TREM2, and Alzheimer's Disease: Evidence From Optical Imaging. Biol Psychiatry *83*, 377-387.

Condello, C., Yuan, P., Schain, A., and Grutzendler, J. (2015). Microglia constitute a barrier that prevents neurotoxic protofibrillar Abeta42 hotspots around plaques. Nat Commun *6*, 6176.

Cummings, D.M., Liu, W., Portelius, E., Bayram, S., Yasvoina, M., Ho, S.H., Smits, H., Ali, S.S., Steinberg, R., Pegasiou, C.M.*, et al.* (2015). First effects of rising amyloid-beta in transgenic mouse brain: synaptic transmission and gene expression. Brain : a journal of neurology *138*, 1992-2004.

Cummings, J., Lee, G., Ritter, A., Sabbagh, M., and Zhong, K. (2020). Alzheimer's disease drug development pipeline: 2020. Alzheimers Dement (N Y) *6*, e12050.

D'Amelio, M., Cavallucci, V., Middei, S., Marchetti, C., Pacioni, S., Ferri, A., Diamantini, A., De Zio, D., Carrara, P., Battistini, L.*, et al.* (2011). Caspase-3 triggers early synaptic dysfunction in a mouse model of Alzheimer's disease. Nat Neurosci *14*, 69-76.

da Silva, R.P., and Gordon, S. (1999a). Phagocytosis stimulates alternative glycosylation of macrosialin (mouse CD68), a macrophage-specific endosomal protein. Biochem J *338 (Pt 3)*, 687-694.

da Silva, R.P., and Gordon, S. (1999b). Phagocytosis stimulates alternative glycosylation of macrosialin (mouse CD68), a macrophage-specific endosomal protein. The Biochemical journal *338 (Pt 3)*, 687-694.

Dagher, N.N., Najafi, A.R., Kayala, K.M., Elmore, M.R., White, T.E., Medeiros, R., West, B.L., and Green, K.N. (2015). Colony-stimulating factor 1 receptor

inhibition prevents microglial plaque association and improves cognition in 3xTg-AD mice. J Neuroinflammation *12*, 139.

Damisah, E.C., Hill, R.A., Rai, A., Chen, F., Rothlin, C.V., Ghosh, S., and Grutzendler, J. (2020). Astrocytes and microglia play orchestrated roles and respect phagocytic territories during neuronal corpse removal in vivo. Sci Adv *6*, eaba3239.

Davalos, D., Grutzendler, J., Yang, G., Kim, J.V., Zuo, Y., Jung, S., Littman, D.R., Dustin, M.L., and Gan, W.B. (2005). ATP mediates rapid microglial response to local brain injury in vivo. Nat Neurosci *8*, 752-758.

De Strooper, B., and Karran, E. (2016). The Cellular Phase of Alzheimer's Disease. Cell *164*, 603-615.

Delizannis, A.T., Nonneman, A., Tsering, W., De Bondt, A., Van den Wyngaert, I., Zhang, B., Meymand, E., Olufemi, M.F., Koivula, P., Maimaiti, S.*, et al.* (2021). Effects of microglial depletion and TREM2 deficiency on Abeta plaque burden and neuritic plaque tau pathology in 5XFAD mice. Acta Neuropathol Commun *9*, 150.

DiCarlo, G., Wilcock, D., Henderson, D., Gordon, M., and Morgan, D. (2001). Intrahippocampal LPS injections reduce Abeta load in APP+PS1 transgenic mice. Neurobiol Aging *22*, 1007-1012.

Dietrich, K., Bouter, Y., Muller, M., and Bayer, T.A. (2018). Synaptic Alterations in Mouse Models for Alzheimer Disease-A Special Focus on N-Truncated Abeta 4-42. Molecules *23*.

Dissing-Olesen, L., LeDue, J.M., Rungta, R.L., Hefendehl, J.K., Choi, H.B., and MacVicar, B.A. (2014). Activation of neuronal NMDA receptors triggers transient ATP-mediated microglial process outgrowth. J Neurosci *34*, 10511-10527.

Dorszewska, J., Prendecki, M., Oczkowska, A., Dezor, M., and Kozubski, W. (2016). Molecular Basis of Familial and Sporadic Alzheimer's Disease. Curr Alzheimer Res *13*, 952-963.

Edwards, F.A. (2019). A Unifying Hypothesis for Alzheimer's Disease: From Plaques to Neurodegeneration. Trends Neurosci *42*, 310-322.

Efthymiou, A.G., and Goate, A.M. (2017). Late onset Alzheimer's disease genetics implicates microglial pathways in disease risk. Mol Neurodegener *12*, 43.

Elmore, M.R., Lee, R.J., West, B.L., and Green, K.N. (2015). Characterizing newly repopulated microglia in the adult mouse: impacts on animal behavior, cell morphology, and neuroinflammation. PLoS One *10*, e0122912.

Elmore, M.R., Najafi, A.R., Koike, M.A., Dagher, N.N., Spangenberg, E.E., Rice, R.A., Kitazawa, M., Matusow, B., Nguyen, H., West, B.L.*, et al.* (2014). Colony-stimulating factor 1 receptor signaling is necessary for microglia viability, unmasking a microglia progenitor cell in the adult brain. Neuron *82*, 380-397.

Erblich, B., Zhu, L., Etgen, A.M., Dobrenis, K., and Pollard, J.W. (2011). Absence of colony stimulation factor-1 receptor results in loss of microglia, disrupted brain development and olfactory deficits. PLoS One *6*, e26317.

Eyo, U.B., Peng, J., Swiatkowski, P., Mukherjee, A., Bispo, A., and Wu, L.J. (2014). Neuronal hyperactivity recruits microglial processes via neuronal NMDA receptors and microglial P2Y12 receptors after status epilepticus. J Neurosci *34*, 10528-10540.

Fonseca, M.I., Zhou, J., Botto, M., and Tenner, A.J. (2004). Absence of C1q leads to less neuropathology in transgenic mouse models of Alzheimer's disease. J Neurosci *24*, 6457-6465.

Frautschy, S.A., Yang, F., Irrizarry, M., Hyman, B., Saido, T.C., Hsiao, K., and Cole, G.M. (1998). Microglial response to amyloid plaques in APPsw transgenic mice. Am J Pathol *152*, 307-317.

Fu, H., Liu, B., Li, L., and Lemere, C.A. (2020). Microglia Do Not Take Up Soluble Amyloid-beta Peptides, But Partially Degrade Them by Secreting Insulin-degrading Enzyme. Neuroscience *443*, 30-43.

Fuhrmann, M., Bittner, T., Jung, C.K., Burgold, S., Page, R.M., Mitteregger, G., Haass, C., LaFerla, F.M., Kretzschmar, H., and Herms, J. (2010). Microglial Cx3cr1 knockout prevents neuron loss in a mouse model of Alzheimer's disease. Nat Neurosci *13*, 411-413.

Garaschuk, O., and Verkhratsky, A. (2019). Microglia: The Neural Cells of Nonneural Origin. Methods Mol Biol *2034*, 3-11.

Ginhoux, F., Greter, M., Leboeuf, M., Nandi, S., See, P., Gokhan, S., Mehler, M.F., Conway, S.J., Ng, L.G., Stanley, E.R*., et al.* (2010). Fate mapping analysis reveals that adult microglia derive from primitive macrophages. Science *330*, 841-845.

Ginhoux, F., Lim, S., Hoeffel, G., Low, D., and Huber, T. (2013). Origin and differentiation of microglia. Front Cell Neurosci *7*, 45.

Goate, A., Chartier-Harlin, M.C., Mullan, M., Brown, J., Crawford, F., Fidani, L., Giuffra, L., Haynes, A., Irving, N., James, L*., et al.* (1991). Segregation of a missense mutation in the amyloid precursor protein gene with familial Alzheimer's disease. Nature *349*, 704-706.

Gomez-Nicola, D., and Perry, V.H. (2015). Microglial dynamics and role in the healthy and diseased brain: a paradigm of functional plasticity. Neuroscientist *21*, 169-184.

Grathwohl, S.A., Kalin, R.E., Bolmont, T., Prokop, S., Winkelmann, G., Kaeser, S.A., Odenthal, J., Radde, R., Eldh, T., Gandy, S*., et al.* (2009). Formation and maintenance of Alzheimer's disease beta-amyloid plaques in the absence of microglia. Nat Neurosci *12*, 1361-1363.

Gratuze, M., Chen, Y., Parhizkar, S., Jain, N., Strickland, M.R., Serrano, J.R., Colonna, M., Ulrich, J.D., and Holtzman, D.M. (2021). Activated microglia mitigate Abeta-associated tau seeding and spreading. J Exp Med *218*.

Green, K.N., Crapser, J.D., and Hohsfield, L.A. (2020). To Kill a Microglia: A Case for CSF1R Inhibitors. Trends Immunol *41*, 771-784.

Griffin, W.S. (2006). Inflammation and neurodegenerative diseases. Am J Clin Nutr *83*, 470S-474S.

Griffin, W.S., Stanley, L.C., Ling, C., White, L., MacLeod, V., Perrot, L.J., White, C.L., 3rd, and Araoz, C. (1989). Brain interleukin 1 and S-100 immunoreactivity are elevated in Down syndrome and Alzheimer disease. Proc Natl Acad Sci U S A *86*, 7611-7615.

Grundke-Iqbal, I., Iqbal, K., Tung, Y.C., Quinlan, M., Wisniewski, H.M., and Binder, L.I. (1986). Abnormal phosphorylation of the microtubule-associated protein tau (tau) in Alzheimer cytoskeletal pathology. Proc Natl Acad Sci U S A *83*, 4913-4917.

Guerreiro, R., and Hardy, J. (2013). TREM2 and neurodegenerative disease. N Engl J Med *369*, 1569-1570.

Guerreiro, R., Wojtas, A., Bras, J., Carrasquillo, M., Rogaeva, E., Majounie, E., Cruchaga, C., Sassi, C., Kauwe, J.S., Younkin, S.*, et al.* (2013). TREM2 variants in Alzheimer's disease. N Engl J Med *368*, 117-127.

Haass, C., and Selkoe, D.J. (2007). Soluble protein oligomers in neurodegeneration: lessons from the Alzheimer's amyloid beta-peptide. Nat Rev Mol Cell Biol *8*, 101-112.

Hall, A.M., and Roberson, E.D. (2012). Mouse models of Alzheimer's disease. Brain Res Bull *88*, 3-12.

Hama, H., Hioki, H., Namiki, K., Hoshida, T., Kurokawa, H., Ishidate, F., Kaneko, T., Akagi, T., Saito, T., Saido, T.*, et al.* (2015). ScaleS: an optical clearing palette for biological imaging. Nat Neurosci *18*, 1518-1529.

Hamaguchi, T., Tsutsui-Kimura, I., Mimura, M., Saito, T., Saido, T.C., and Tanaka, K.F. (2019). App(NL-G-F/NL-G-F) mice overall do not show impaired motivation, but cored amyloid plaques in the striatum are inversely correlated with motivation. Neurochem Int *129*, 104470.

Hamalainen, A., Pihlajamaki, M., Tanila, H., Hanninen, T., Niskanen, E., Tervo, S., Karjalainen, P.A., Vanninen, R.L., and Soininen, H. (2007). Increased fMRI responses during encoding in mild cognitive impairment. Neurobiol Aging *28*, 1889-1903.

Hamelin, L., Lagarde, J., Dorothee, G., Leroy, C., Labit, M., Comley, R.A., de Souza, L.C., Corne, H., Dauphinot, L., Bertoux, M.*, et al.* (2016). Early and protective microglial activation in Alzheimer's disease: a prospective study using 18F-DPA-714 PET imaging. Brain : a journal of neurology *139*, 1252-1264.

Han, J., Harris, R.A., and Zhang, X.M. (2017). An updated assessment of microglia depletion: current concepts and future directions. Mol Brain *10*, 25.

Hansen, D.V., Hanson, J.E., and Sheng, M. (2018). Microglia in Alzheimer's disease. The Journal of cell biology *217*, 459-472.

Hardy, J., and Salih, D. (2021). TREM2-mediated activation of microglia breaks link between amyloid and tau. Lancet Neurology *20*, 416-417.

Hardy, J., and Selkoe, D.J. (2002). The amyloid hypothesis of Alzheimer's disease: progress and problems on the road to therapeutics. Science *297*, 353-356.

Hark, T.J., Rao, N.R., Castillon, C., Basta, T., Smukowski, S., Bao, H., Upadhyay, A., Bomba-Warczak, E., Nomura, T., O'Toole, E.T.*, et al.* (2021). Pulse-Chase Proteomics of the App Knockin Mouse Models of Alzheimer's Disease Reveals that Synaptic Dysfunction Originates in Presynaptic Terminals. Cell Syst *12*, 141-158 e149.

He, Y., Wei, M., Wu, Y., Qin, H., Li, W., Ma, X., Cheng, J., Ren, J., Shen, Y., Chen, Z.*, et al.* (2019). Amyloid beta oligomers suppress excitatory transmitter release via presynaptic depletion of phosphatidylinositol-4,5-bisphosphate. Nat Commun *10*, 1193.

Hefter, D., Ludewig, S., Draguhn, A., and Korte, M. (2020). Amyloid, APP, and Electrical Activity of the Brain. Neuroscientist *26*, 231-251.

Heneka, M.T., Carson, M.J., El Khoury, J., Landreth, G.E., Brosseron, F., Feinstein, D.L., Jacobs, A.H., Wyss-Coray, T., Vitorica, J., Ransohoff, R.M.*, et al.* (2015). Neuroinflammation in Alzheimer's disease. Lancet Neurol *14*, 388-405.

Heppner, F.L., Greter, M., Marino, D., Falsig, J., Raivich, G., Hovelmeyer, N., Waisman, A., Rulicke, T., Prinz, M., Priller, J.*, et al.* (2005). Experimental autoimmune encephalomyelitis repressed by microglial paralysis. Nat Med *11*, 146-152.

Herber, D.L., Mercer, M., Roth, L.M., Symmonds, K., Maloney, J., Wilson, N., Freeman, M.J., Morgan, D., and Gordon, M.N. (2007). Microglial activation is required for Abeta clearance after intracranial injection of lipopolysaccharide in APP transgenic mice. J Neuroimmune Pharmacol *2*, 222-231.

Hong, S., Beja-Glasser, V.F., Nfonoyim, B.M., Frouin, A., Li, S., Ramakrishnan, S., Merry, K.M., Shi, Q., Rosenthal, A., Barres, B.A.*, et al.* (2016a). Complement and microglia mediate early synapse loss in Alzheimer mouse models. Science *352*, 712-716.

Hong, S., Dissing-Olesen, L., and Stevens, B. (2016b). New insights on the role of microglia in synaptic pruning in health and disease. Curr Opin Neurobiol *36*, 128-134.

Hong, S., and Stevens, B. (2016). Microglia: Phagocytosing to Clear, Sculpt, and Eliminate. Dev Cell *38*, 126-128.

Hopperton, K.E., Mohammad, D., Trepanier, M.O., Giuliano, V., and Bazinet, R.P. (2018). Markers of microglia in post-mortem brain samples from patients with Alzheimer's disease: a systematic review. Mol Psychiatry *23*, 177-198.

Horti, A.G., Naik, R., Foss, C.A., Minn, I., Misheneva, V., Du, Y., Wang, Y., Mathews, W.B., Wu, Y., Hall, A.*, et al.* (2019). PET imaging of microglia by targeting macrophage colony-stimulating factor 1 receptor (CSF1R). Proc Natl Acad Sci U S A *116*, 1686-1691.

Hsia, A.Y., Masliah, E., McConlogue, L., Yu, G.Q., Tatsuno, G., Hu, K., Kholodenko, D., Malenka, R.C., Nicoll, R.A., and Mucke, L. (1999). Plaque-independent disruption of neural circuits in Alzheimer's disease mouse models. Proc Natl Acad Sci U S A *96*, 3228-3233.

Itagaki, S., McGeer, P.L., Akiyama, H., Zhu, S., and Selkoe, D. (1989). Relationship of microglia and astrocytes to amyloid deposits of Alzheimer disease. J Neuroimmunol *24*, 173-182.

Ito, D., Imai, Y., Ohsawa, K., Nakajima, K., Fukuuchi, Y., and Kohsaka, S. (1998). Microglia-specific localisation of a novel calcium binding protein, Iba1. Brain Res Mol Brain Res *57*, 1-9.

Jacobsen, J.S., Wu, C.C., Redwine, J.M., Comery, T.A., Arias, R., Bowlby, M., Martone, R., Morrison, J.H., Pangalos, M.N., Reinhart, P.H.*, et al.* (2006). Early-onset behavioral and synaptic deficits in a mouse model of Alzheimer's disease. Proc Natl Acad Sci U S A *103*, 5161-5166.

Janelsins, M.C., Mastrangelo, M.A., Oddo, S., LaFerla, F.M., Federoff, H.J., and Bowers, W.J. (2005). Early correlation of microglial activation with enhanced tumor necrosis factor-alpha and monocyte chemoattractant protein-1 expression specifically within the entorhinal cortex of triple transgenic Alzheimer's disease mice. J Neuroinflammation *2*, 23.

Jankowsky, J.L., and Zheng, H. (2017). Practical considerations for choosing a mouse model of Alzheimer's disease. Mol Neurodegener *12*, 89.

Jay, T.R., Hirsch, A.M., Broihier, M.L., Miller, C.M., Neilson, L.E., Ransohoff, R.M., Lamb, B.T., and Landreth, G.E. (2017). Disease Progression-Dependent Effects of TREM2 Deficiency in a Mouse Model of Alzheimer's Disease. J Neurosci *37*, 637-647.

Ji, K., Akgul, G., Wollmuth, L.P., and Tsirka, S.E. (2013). Microglia actively regulate the number of functional synapses. PLoS One *8*, e56293.

Jimenez, S., Baglietto-Vargas, D., Caballero, C., Moreno-Gonzalez, I., Torres, M., Sanchez-Varo, R., Ruano, D., Vizuete, M., Gutierrez, A., and Vitorica, J.

(2008). Inflammatory response in the hippocampus of PS1M146L/APP751SL mouse model of Alzheimer's disease: age-dependent switch in the microglial phenotype from alternative to classic. J Neurosci *28*, 11650-11661.

Joel, Z., Izquierdo, P., Salih, D.A., Richardson, J.C., Cummings, D.M., and Edwards, F.A. (2018). Improving Mouse Models for Dementia. Are All the Effects in Tau Mouse Models Due to Overexpression? Cold Spring Harb Symp Quant Biol *83*, 151-161.

Jonsson, T., Stefansson, H., Steinberg, S., Jonsdottir, I., Jonsson, P.V., Snaedal, J., Bjornsson, S., Huttenlocher, J., Levey, A.I., Lah, J.J.*, et al.* (2013). Variant of TREM2 associated with the risk of Alzheimer's disease. N Engl J Med *368*, 107-116.

Jucker, M., Beyreuther, K., Haass, C., Nitsch, C., Cristen, Y., and (Eds) (2006a). Alzheimer: 100 Years and Beyond.

Jucker, M., Beyreuther, K., Haass, C., Nitsch, R.M., Christen, Y., and SpringerLink (2006b). Alzheimer: 100 Years and Beyond (Berlin, Heidelberg: Springer-Verlag Berlin Heidelberg).

Kamphuis, W., Kooijman, L., Schetters, S., Orre, M., and Hol, E.M. (2016). Transcriptional profiling of CD11c-positive microglia accumulating around amyloid plaques in a mouse model for Alzheimer's disease. Biochim Biophys Acta *1862*, 1847-1860.

Karch, C.M., Cruchaga, C., and Goate, A.M. (2014). Alzheimer's disease genetics: from the bench to the clinic. Neuron *83*, 11-26.

Karch, C.M., and Goate, A.M. (2015). Alzheimer's disease risk genes and mechanisms of disease pathogenesis. Biol Psychiatry *77*, 43-51.

Keren-Shaul, H., Spinrad, A., Weiner, A., Matcovitch-Natan, O., Dvir-Szternfeld, R., Ulland, T.K., David, E., Baruch, K., Lara-Astaiso, D., Toth, B.*, et al.* (2017). A Unique Microglia Type Associated with Restricting Development of Alzheimer's Disease. Cell *169*, 1276-1290 e1217.

Kettenmann, H., Hanisch, U.K., Noda, M., and Verkhratsky, A. (2011). Physiology of microglia. Physiol Rev *91*, 461-553.

Kettenmann, H., Kettenmann, H., Ransom, B.R., Allen, N.J., and Ebook Central Academic, C. (2013). Neuroglia (New York: Oxford University Press).

Kierdorf, K., Erny, D., Goldmann, T., Sander, V., Schulz, C., Perdiguero, E.G., Wieghofer, P., Heinrich, A., Riemke, P., Holscher, C.*, et al.* (2013). Microglia emerge from erythromyeloid precursors via Pu.1- and Irf8-dependent pathways. Nat Neurosci *16*, 273-280.

Koffie, R.M., Meyer-Luehmann, M., Hashimoto, T., Adams, K.W., Mielke, M.L., Garcia-Alloza, M., Micheva, K.D., Smith, S.J., Kim, M.L., Lee, V.M.*, et al.* (2009). Oligomeric amyloid beta associates with postsynaptic densities and correlates with excitatory synapse loss near senile plaques. Proc Natl Acad Sci U S A *106*, 4012-4017.

Konishi, H., Okamoto, T., Hara, Y., Komine, O., Tamada, H., Maeda, M., Osako, F., Kobayashi, M., Nishiyama, A., Kataoka, Y.*, et al.* (2020). Astrocytic phagocytosis is a compensatory mechanism for microglial dysfunction. The EMBO journal *39*, e104464.

Kreisl, W.C., Kim, M.J., Coughlin, J.M., Henter, I.D., Owen, D.R., and Innis, R.B. (2020). PET imaging of neuroinflammation in neurological disorders. Lancet Neurol *19*, 940-950.

Lambert, J.C., Ibrahim-Verbaas, C.A., Harold, D., Naj, A.C., Sims, R., Bellenguez, C., DeStafano, A.L., Bis, J.C., Beecham, G.W., Grenier-Boley, B.*, et al.* (2013). Meta-analysis of 74,046 individuals identifies 11 new susceptibility loci for Alzheimer's disease. Nat Genet *45*, 1452-1458.

Landau, S.M., Horng, A., Jagust, W.J., and Alzheimer's Disease Neuroimaging, I. (2018). Memory decline accompanies subthreshold amyloid accumulation. Neurology *90*, e1452-e1460.

Latif-Hernandez, A., Sabanov, V., Ahmed, T., Craessaerts, K., Saito, T., Saido, T., and Balschun, D. (2020). The two faces of synaptic failure in App(NL-G-F) knock-in mice. Alzheimers Res Ther *12*, 100.

Latif-Hernandez, A., Shah, D., Craessaerts, K., Saido, T., Saito, T., De Strooper, B., Van der Linden, A., and D'Hooge, R. (2017). Subtle behavioral changes and increased prefrontal-hippocampal network synchronicity in APP(NL-G-F) mice before prominent plaque deposition. Behav Brain Res.

Latif-Hernandez, A., Shah, D., Craessaerts, K., Saido, T., Saito, T., De Strooper, B., Van der Linden, A., and D'Hooge, R. (2019). Subtle behavioral changes and increased prefrontal-hippocampal network synchronicity in APP(NL-G-F) mice before prominent plaque deposition. Behav Brain Res *364*, 431-441.

Lawson, L.J., Perry, V.H., Dri, P., and Gordon, S. (1990). Heterogeneity in the distribution and morphology of microglia in the normal adult mouse brain. Neuroscience *39*, 151-170.

Lee, S.H., Meilandt, W.J., Xie, L., Gandham, V.D., Ngu, H., Barck, K.H., Rezzonico, M.G., Imperio, J., Lalehzadeh, G., Huntley, M.A.*, et al.* (2021). Trem2 restrains the enhancement of tau accumulation and neurodegeneration by beta-amyloid pathology. Neuron *109*, 1283-1301 e1286.

Lei, F., Cui, N., Zhou, C., Chodosh, J., Vavvas, D.G., and Paschalis, E.I. (2021). Reply to Green and Hume: Nonmicroglia peripheral immune effects of short-term CSF1R inhibition with PLX5622. Proc Natl Acad Sci U S A *118*, e2020660118.

Leyns, C.E.G., Gratuze, M., Narasimhan, S., Jain, N., Koscal, L.J., Jiang, H., Manis, M., Colonna, M., Lee, V.M.Y., Ulrich, J.D.*, et al.* (2019). TREM2 function impedes tau seeding in neuritic plaques. Nat Neurosci *22*, 1217-1222.

Liu, W., Taso, O., Wang, R., Bayram, S., Graham, A.C., Garcia-Reitboeck, P., Mallach, A., Andrews, W.D., Piers, T.M., Botia, J.A.*, et al.* (2020). Trem2 promotes anti-inflammatory responses in microglia and is suppressed under pro-inflammatory conditions. Hum Mol Genet *29*, 3224-3248.

Liu, Y.J., Spangenberg, E.E., Tang, B., Holmes, T.C., Green, K.N., and Xu, X. (2021). Microglia Elimination Increases Neural Circuit Connectivity and Activity in Adult Mouse Cortex. J Neurosci *41*, 1274-1287.

Long, J.M., and Holtzman, D.M. (2019). Alzheimer Disease: An Update on Pathobiology and Treatment Strategies. Cell *179*, 312-339.

Lue, L.F., Brachova, L., Civin, W.H., and Rogers, J. (1996). Inflammation, A beta deposition, and neurofibrillary tangle formation as correlates of Alzheimer's disease neurodegeneration. J Neuropathol Exp Neurol *55*, 1083-1088.

Maggi, L., Scianni, M., Branchi, I., D'Andrea, I., Lauro, C., and Limatola, C. (2011). CX(3)CR1 deficiency alters hippocampal-dependent plasticity phenomena blunting the effects of enriched environment. Front Cell Neurosci *5*, 22.

Malkin, S.L., Kim, K., Tikhonov, D.B., and Zaitsev, A.V. (2014). [Properties of spontaneous and miniature excitatory postsynaptic currents of rat prefrontal cortex neurons]. Zh Evol Biokhim Fiziol *50*, 440-446.

Manabe, T., Wyllie, D.J., Perkel, D.J., and Nicoll, R.A. (1993). Modulation of synaptic transmission and long-term potentiation: effects on paired pulse facilitation and EPSC variance in the CA1 region of the hippocampus. J Neurophysiol *70*, 1451-1459.

Mancuso, R., Fryatt, G., Cleal, M., Obst, J., Pipi, E., Monzon-Sandoval, J., Ribe, E., Winchester, L., Webber, C., Nevado, A.*, et al.* (2019). CSF1R inhibitor JNJ-40346527 attenuates microglial proliferation and neurodegeneration in P301S mice. Brain : a journal of neurology *142*, 3243-3264.

Mango, D., Saidi, A., Cisale, G.Y., Feligioni, M., Corbo, M., and Nistico, R. (2019). Targeting Synaptic Plasticity in Experimental Models of Alzheimer's Disease. Front Pharmacol *10*, 778.

Marchetti, C., and Marie, H. (2011). Hippocampal synaptic plasticity in Alzheimer's disease: what have we learned so far from transgenic models? Rev Neurosci *22*, 373-402.

Marinelli, S., Basilico, B., Marrone, M.C., and Ragozzino, D. (2019). Microglia-neuron crosstalk: Signaling mechanism and control of synaptic transmission. Semin Cell Dev Biol *94*, 138-151.

Marsh, J., and Alifragis, P. (2018). Synaptic dysfunction in Alzheimer's disease: the effects of amyloid beta on synaptic vesicle dynamics as a novel target for therapeutic intervention. Neural Regen Res *13*, 616-623.

Masters, C.L., Simms, G., Weinman, N.A., Multhaup, G., McDonald, B.L., and Beyreuther, K. (1985). Amyloid plaque core protein in Alzheimer disease and Down syndrome. Proc Natl Acad Sci U S A *82*, 4245-4249.

Masuda, A., Kobayashi, Y., Kogo, N., Saito, T., Saido, T.C., and Itohara, S. (2016). Cognitive deficits in single App knock-in mouse models. Neurobiol Learn Mem *135*, 73-82.

Masuda, T., Sankowski, R., Staszewski, O., and Prinz, M. (2020). Microglia Heterogeneity in the Single-Cell Era. Cell Rep *30*, 1271-1281.

Matarin, M., Salih, D.A., Yasvoina, M., Cummings, D.M., Guelfi, S., Liu, W., Nahaboo Solim, M.A., Moens, T.G., Paublete, R.M., Ali, S.S.*, et al.* (2015). A genome-wide gene-expression analysis and database in transgenic mice during development of amyloid or tau pathology. Cell Rep *10*, 633-644.

Matcovitch-Natan, O., Winter, D.R., Giladi, A., Vargas Aguilar, S., Spinrad, A., Sarrazin, S., Ben-Yehuda, H., David, E., Zelada Gonzalez, F., Perrin, P.*, et al.* (2016). Microglia development follows a stepwise program to regulate brain homeostasis. Science *353*, aad8670.

Matsuoka, Y., Picciano, M., Malester, B., LaFrancois, J., Zehr, C., Daeschner, J.M., Olschowka, J.A., Fonseca, M.I., O'Banion, M.K., Tenner, A.J.*, et al.* (2001). Inflammatory responses to amyloidosis in a transgenic mouse model of Alzheimer's disease. Am J Pathol *158*, 1345-1354.

Mattson, M.P. (2004). Pathways towards and away from Alzheimer's disease. Nature *430*, 631-639.

McGeer, E.G., and McGeer, P.L. (1998). The importance of inflammatory mechanisms in Alzheimer disease. Exp Gerontol *33*, 371-378.

Medawar, E., Benway, T.A., Liu, W., Hanan, T.A., Haslehurst, P., James, O.T., Yap, K., Muessig, L., Moroni, F., Nahaboo Solim, M.A.*, et al.* (2019). Effects of rising amyloidbeta levels on hippocampal synaptic transmission, microglial response and cognition in APPSwe/PSEN1M146V transgenic mice. EBioMedicine *39*, 422-435.

Mehla, J., Lacoursiere, S.G., Lapointe, V., McNaughton, B.L., Sutherland, R.J., McDonald, R.J., and Mohajerani, M.H. (2019). Age-dependent behavioral and biochemical characterization of single APP knock-in mouse (APP(NL-G-F/NL-G-F)) model of Alzheimer's disease. Neurobiol Aging *75*, 25-37.

Meilandt, W.J., Ngu, H., Gogineni, A., Lalehzadeh, G., Lee, S.H., Srinivasan, K., Imperio, J., Wu, T., Weber, M., Kruse, A.J.*, et al.* (2020). Trem2 Deletion Reduces Late-Stage Amyloid Plaque Accumulation, Elevates the Abeta42:Abeta40 Ratio, and Exacerbates Axonal Dystrophy and Dendritic Spine Loss in the PS2APP Alzheimer's Mouse Model. J Neurosci *40*, 1956-1974.

Meyer-Luehmann, M., Spires-Jones, T.L., Prada, C., Garcia-Alloza, M., de Calignon, A., Rozkalne, A., Koenigsknecht-Talboo, J., Holtzman, D.M., Bacskai, B.J., and Hyman, B.T. (2008). Rapid appearance and local toxicity of amyloid-beta plaques in a mouse model of Alzheimer's disease. Nature *451*, 720-724.

Monasor, L.S., Müller, S.A., Colombo, A., König, J., Roth, S., Liesz, A., Berghofer, A., Saito, T., Saido, T.C., Herms, J.*, et al.* (2019). Fibrillar Aβ triggers microglial proteome alterations and dysfunction in Alzheimer mouse models. bioRxiv, 861146.

Murphy, M.P., and LeVine, H., 3rd (2010). Alzheimer's disease and the amyloid-beta peptide. J Alzheimers Dis *19*, 311-323.

Naj, A.C., Jun, G., Beecham, G.W., Wang, L.S., Vardarajan, B.N., Buros, J., Gallins, P.J., Buxbaum, J.D., Jarvik, G.P., Crane, P.K., *et al.* (2011). Common variants at MS4A4/MS4A6E, CD2AP, CD33 and EPHA1 are associated with late-onset Alzheimer's disease. Nat Genet *43*, 436-441.

Najafi, A.R., Crapser, J., Jiang, S., Ng, W., Mortazavi, A., West, B.L., and Green, K.N. (2018). A limited capacity for microglial repopulation in the adult brain. Glia *66*, 2385-2396.

Nakagawa, Y., and Chiba, K. (2015). Diversity and plasticity of microglial cells in psychiatric and neurological disorders. Pharmacol Ther *154*, 21-35.

Nandi, S., Gokhan, S., Dai, X.M., Wei, S., Enikolopov, G., Lin, H., Mehler, M.F., and Stanley, E.R. (2012). The CSF-1 receptor ligands IL-34 and CSF-1 exhibit distinct developmental brain expression patterns and regulate neural progenitor cell maintenance and maturation. Dev Biol *367*, 100-113.

Neves, G., Cooke, S.F., and Bliss, T.V. (2008). Synaptic plasticity, memory and the hippocampus: a neural network approach to causality. Nature reviews Neuroscience *9*, 65-75.

Nicoll, R.A. (2017). A Brief History of Long-Term Potentiation. Neuron *93*, 281-290.

Nilsson, P., Saito, T., and Saido, T.C. (2014). New mouse model of Alzheimer's. ACS Chem Neurosci *5*, 499-502.

Nimmerjahn, A., Kirchhoff, F., and Helmchen, F. (2005). Resting microglial cells are highly dynamic surveillants of brain parenchyma in vivo. Science *308*, 1314-1318.

Obata, Y., Murakami, K., Kawase, T., Hirose, K., Izuo, N., Shimizu, T., and Irie, K. (2020). Detection of Amyloid beta Oligomers with RNA Aptamers in App(NL-G-F/NL-G-F) Mice: A Model of Arctic Alzheimer's Disease. ACS Omega *5*, 21531-21537.

Olmos-Alonso, A., Schetters, S.T., Sri, S., Askew, K., Mancuso, R., Vargas-Caballero, M., Holscher, C., Perry, V.H., and Gomez-Nicola, D. (2016). Pharmacological targeting of CSF1R inhibits microglial proliferation and prevents the progression of Alzheimer's-like pathology. Brain : a journal of neurology *139*, 891-907.

Pan, X.D., Zhu, Y.G., Lin, N., Zhang, J., Ye, Q.Y., Huang, H.P., and Chen, X.C. (2011). Microglial phagocytosis induced by fibrillar beta-amyloid is attenuated by oligomeric beta-amyloid: implications for Alzheimer's disease. Mol Neurodegener *6*, 45.

Paolicelli, R.C., Bisht, K., and Tremblay, M.E. (2014). Fractalkine regulation of microglial physiology and consequences on the brain and behavior. Front Cell Neurosci *8*, 129.

Paolicelli, R.C., Bolasco, G., Pagani, F., Maggi, L., Scianni, M., Panzanelli, P., Giustetto, M., Ferreira, T.A., Guiducci, E., Dumas, L.*, et al.* (2011). Synaptic pruning by microglia is necessary for normal brain development. Science *333*, 1456-1458.

Paolicelli, R.C., Jawaid, A., Henstridge, C.M., Valeri, A., Merlini, M., Robinson, J.L., Lee, E.B., Rose, J., Appel, S., Lee, V.M.*, et al.* (2017). TDP-43 Depletion in Microglia Promotes Amyloid Clearance but Also Induces Synapse Loss. Neuron *95*, 297-308 e296.

Paresce, D.M., Chung, H., and Maxfield, F.R. (1997). Slow degradation of aggregates of the Alzheimer's disease amyloid beta-protein by microglial cells. The Journal of biological chemistry *272*, 29390-29397.

Park, D., Na, M., Kim, J.A., Lee, U., Cho, E., Jang, M., and Chang, S. (2017). Activation of CaMKIV by soluble amyloid-beta1-42 impedes trafficking of axonal vesicles and impairs activity-dependent synaptogenesis. Sci Signal *10*, eaam8661.

Parkhurst, C.N., Yang, G., Ninan, I., Savas, J.N., Yates, J.R., 3rd, Lafaille, J.J., Hempstead, B.L., Littman, D.R., and Gan, W.B. (2013). Microglia promote

learning-dependent synapse formation through brain-derived neurotrophic factor. Cell *155*, 1596-1609.

Parodi, J., Sepulveda, F.J., Roa, J., Opazo, C., Inestrosa, N.C., and Aguayo, L.G. (2010). Beta-amyloid causes depletion of synaptic vesicles leading to neurotransmission failure. The Journal of biological chemistry *285*, 2506-2514.

Pauls, E., Bayod, S., Mateo, L., Alcalde, V., Juan-Blanco, T., Saido, T.C., Saito, T., Berrenguer-Llergo, A., Attolini, C.S.-O., Gay, M*., et al.* (2021). Identification and drug-induced reversion of molecular signatures of Alzheimer's disease onset and progression in App^{NL-G-F}, App^{NL-F} and 3xTg-AD mouse models. bioRxiv, 2021.2003.2017.435753.

Petrache, A.L., Rajulawalla, A., Shi, A., Wetzel, A., Saito, T., Saido, T.C., Harvey, K., and Ali, A.B. (2019). Aberrant Excitatory-Inhibitory Synaptic Mechanisms in Entorhinal Cortex Microcircuits During the Pathogenesis of Alzheimer's Disease. Cereb Cortex *29*, 1834-1850.

Pfeiffer, T., Avignone, E., and Nagerl, U.V. (2016). Induction of hippocampal long-term potentiation increases the morphological dynamics of microglial processes and prolongs their contacts with dendritic spines. Sci Rep *6*, 32422.

Piaceri, I., Nacmias, B., and Sorbi, S. (2013). Genetics of familial and sporadic Alzheimer's disease. Front Biosci(EliteEd) *5*, 167-177.

Pickett, E.K., Koffie, R.M., Wegmann, S., Henstridge, C.M., Herrmann, A.G., Colom-Cadena, M., Lleo, A., Kay, K.R., Vaught, M., Soberman, R*., et al.* (2016). Non-Fibrillar Oligomeric Amyloid-beta within Synapses. J Alzheimers Dis *53*, 787-800.

Posfai, B., Cserep, C., Orsolits, B., and Denes, A. (2019). New Insights into Microglia-Neuron Interactions: A Neuron's Perspective. Neuroscience *405*, 103-117.

Priller, C., Bauer, T., Mitteregger, G., Krebs, B., Kretzschmar, H.A., and Herms, J. (2006). Synapse formation and function is modulated by the amyloid precursor protein. J Neurosci *26*, 7212-7221.

Prinz, M., Jung, S., and Priller, J. (2019). Microglia Biology: One Century of Evolving Concepts. Cell *179*, 292-311.

Prokop, S., Miller, K.R., and Heppner, F.L. (2013). Microglia actions in Alzheimer's disease. Acta Neuropathol *126*, 461-477.

Quiroz, Y.T., Budson, A.E., Celone, K., Ruiz, A., Newmark, R., Castrillon, G., Lopera, F., and Stern, C.E. (2010). Hippocampal hyperactivation in presymptomatic familial Alzheimer's disease. Ann Neurol *68*, 865-875.

Quon, D., Wang, Y., Catalano, R., Scardina, J.M., Murakami, K., and Cordell, B. (1991). Formation of beta-amyloid protein deposits in brains of transgenic mice. Nature *352*, 239-241.

Rademakers, R., Baker, M., Nicholson, A.M., Rutherford, N.J., Finch, N., Soto-Ortolaza, A., Lash, J., Wider, C., Wojtas, A., DeJesus-Hernandez, M.*, et al.* (2011). Mutations in the colony stimulating factor 1 receptor (CSF1R) gene cause hereditary diffuse leukoencephalopathy with spheroids. Nat Genet *44*, 200-205.

Ransohoff, R.M. (2016a). How neuroinflammation contributes to neurodegeneration. Science *353*, 777-783.

Ransohoff, R.M. (2016b). A polarizing question: do M1 and M2 microglia exist? Nat Neurosci *19*, 987-991.

Rasmussen, J., Mahler, J., Beschorner, N., Kaeser, S.A., Hasler, L.M., Baumann, F., Nystrom, S., Portelius, E., Blennow, K., Lashley, T.*, et al.* (2017). Amyloid polymorphisms constitute distinct clouds of conformational variants in different etiological subtypes of Alzheimer's disease. Proc Natl Acad Sci U S A *114*, 13018-13023.

Ren, S., Yao, W., Tambini, M.D., Yin, T., Norris, K.A., and D'Adamio, L. (2020). Microglia TREM2(R47H) Alzheimer-linked variant enhances excitatory transmission and reduces LTP via increased TNF-alpha levels. Elife *9*.

Report, A.s.A. (2020). 2020 Alzheimer's disease facts and figures. Alzheimers Dement.

Ricciarelli, R., and Fedele, E. (2018). cAMP, cGMP and Amyloid beta: Three Ideal Partners for Memory Formation. Trends Neurosci *41*, 255-266.

Rice, H.C., Marcassa, G., Chrysidou, I., Horre, K., Young-Pearse, T.L., Muller, U.C., Saito, T., Saido, T.C., Vassar, R., de Wit, J.*, et al.* (2020). Contribution of GABAergic interneurons to amyloid-beta plaque pathology in an APP knock-in mouse model. Mol Neurodegener *15*, 3.

Rice, R.A., Spangenberg, E.E., Yamate-Morgan, H., Lee, R.J., Arora, R.P., Hernandez, M.X., Tenner, A.J., West, B.L., and Green, K.N. (2015). Elimination of Microglia Improves Functional Outcomes Following Extensive Neuronal Loss in the Hippocampus. J Neurosci *35*, 9977-9989.

Ries, M., and Sastre, M. (2016). Mechanisms of Abeta Clearance and Degradation by Glial Cells. Front Aging Neurosci *8*, 160.

Rogers, J., Webster, S., Lue, L.F., Brachova, L., Civin, W.H., Emmerling, M., Shivers, B., Walker, D., and McGeer, P. (1996). Inflammation and Alzheimer's disease pathogenesis. Neurobiol Aging *17*, 681-686.

Rogers, J.T., Morganti, J.M., Bachstetter, A.D., Hudson, C.E., Peters, M.M., Grimmig, B.A., Weeber, E.J., Bickford, P.C., and Gemma, C. (2011). CX3CR1 deficiency leads to impairment of hippocampal cognitive function and synaptic plasticity. J Neurosci *31*, 16241-16250.

Russell, C.L., Semerdjieva, S., Empson, R.M., Austen, B.M., Beesley, P.W., and Alifragis, P. (2012). Amyloid-beta acts as a regulator of neurotransmitter release disrupting the interaction between synaptophysin and VAMP2. PLoS One *7*, e43201.

Sacher, C., Blume, T., Beyer, L., Peters, F., Eckenweber, F., Sgobio, C., Deussing, M., Albert, N.L., Unterrainer, M., Lindner, S*., et al.* (2019). Longitudinal PET Monitoring of Amyloidosis and Microglial Activation in a Second-Generation Amyloid-beta Mouse Model. J Nucl Med *60*, 1787-1793.

Saifullah, M.A.B., Komine, O., Dong, Y., Fukumoto, K., Sobue, A., Endo, F., Saito, T., Saido, T.C., Yamanaka, K., and Mizoguchi, H. (2020). Touchscreen-based location discrimination and paired associate learning tasks detect cognitive impairment at an early stage in an App knock-in mouse model of Alzheimer's disease. Mol Brain *13*, 147.

Saito, T., Matsuba, Y., Mihira, N., Takano, J., Nilsson, P., Itohara, S., Iwata, N., and Saido, T.C. (2014). Single App knock-in mouse models of Alzheimer's disease. Nat Neurosci *17*, 661-663.

Saito, T., and Saido, T.C. (2018). Neuroinflammation in mouse models of Alzheimer's disease. Clinical & experimental neuroimmunology *9*, 211-218.

Sakakibara, Y., Sekiya, M., Saito, T., Saido, T.C., and Iijima, K.M. (2018). Cognitive and emotional alterations in App knock-in mouse models of Aβ amyloidosis. BMC Neurosci *19*, 46.

Sanchez-Mejias, E., Navarro, V., Jimenez, S., Sanchez-Mico, M., Sanchez-Varo, R., Nunez-Diaz, C., Trujillo-Estrada, L., Davila, J.C., Vizuete, M., Gutierrez, A*., et al.* (2016). Soluble phospho-tau from Alzheimer's disease hippocampus drives microglial degeneration. Acta Neuropathol *132*, 897-916.

Sasaguri, H., Nilsson, P., Hashimoto, S., Nagata, K., Saito, T., De Strooper, B., Hardy, J., Vassar, R., Winblad, B., and Saido, T.C. (2017). APP mouse models for Alzheimer's disease preclinical studies. The EMBO journal *36*, 2473-2487.

Sassi, C., Nalls, M.A., Ridge, P.G., Gibbs, J.R., Lupton, M.K., Troakes, C., Lunnon, K., Al-Sarraj, S., Brown, K.S., Medway, C*., et al.* (2018). Mendelian adult-onset leukodystrophy genes in Alzheimer's disease: critical influence of CSF1R and NOTCH3. Neurobiol Aging *66*, 179 e117-179 e129.

Schafer, D.P., Lehrman, E.K., Kautzman, A.G., Koyama, R., Mardinly, A.R., Yamasaki, R., Ransohoff, R.M., Greenberg, M.E., Barres, B.A., and Stevens, B. (2012). Microglia sculpt postnatal neural circuits in an activity and complement-dependent manner. Neuron *74*, 691-705.

Schedin-Weiss, S., Nilsson, P., Sandebring-Matton, A., Axenhus, M., Sekiguchi, M., Saito, T., Winblad, B., Saido, T., and Tjernberg, L.O. (2020). Proteomics Time-Course Study of App Knock-In Mice Reveals Novel Presymptomatic Aβ42-Induced Pathways to Alzheimer's Disease Pathology. J Alzheimers Dis *75*, 321-335.

Schulz, C., Gomez Perdiguero, E., Chorro, L., Szabo-Rogers, H., Cagnard, N., Kierdorf, K., Prinz, M., Wu, B., Jacobsen, S.E., Pollard, J.W.*, et al.* (2012). A lineage of myeloid cells independent of Myb and hematopoietic stem cells. Science *336*, 86-90.

Sebastian Monasor, L., Muller, S.A., Colombo, A.V., Tanrioever, G., Konig, J., Roth, S., Liesz, A., Berghofer, A., Piechotta, A., Prestel, M.*, et al.* (2020). Fibrillar Abeta triggers microglial proteome alterations and dysfunction in Alzheimer mouse models. Elife *9*.

Selkoe, D.J., and Hardy, J. (2016). The amyloid hypothesis of Alzheimer's disease at 25 years. EMBO Mol Med *8*, 595-608.

Serneels, L., T'Syen, D., Perez-Benito, L., Theys, T., Holt, M.G., and De Strooper, B. (2020). Modeling the beta-secretase cleavage site and humanizing amyloid-beta precursor protein in rat and mouse to study Alzheimer's disease. Mol Neurodegener *15*, 60.

Sevenich, L. (2018). Brain-Resident Microglia and Blood-Borne Macrophages Orchestrate Central Nervous System Inflammation in Neurodegenerative Disorders and Brain Cancer. Front Immunol *9*, 697.

Sheng, L., Chen, M., Cai, K., Song, Y., Yu, D., Zhang, H., and Xu, G. (2019). Microglial Trem2 induces synaptic impairment at early stage and prevents amyloidosis at late stage in APP/PS1 mice. FASEB J *33*, 10425-10442.

Shi, Q., Chowdhury, S., Ma, R., Le, K.X., Hong, S., Caldarone, B.J., Stevens, B., and Lemere, C.A. (2017). Complement C3 deficiency protects against neurodegeneration in aged plaque-rich APP/PS1 mice. Sci Transl Med *9*.

Sierra, A., Paolicelli, R.C., and Kettenmann, H. (2019). Cien Anos de Microglia: Milestones in a Century of Microglial Research. Trends Neurosci *42*, 778-792.

Sobue, A., Komine, O., Hara, Y., Endo, F., Mizoguchi, H., Watanabe, S., Murayama, S., Saito, T., Saido, T.C., Sahara, N.*, et al.* (2021). Microglial gene signature reveals loss of homeostatic microglia associated with neurodegeneration of Alzheimer's disease. Acta Neuropathol Commun *9*, 1.

Son, Y., Jeong, Y.J., Shin, N.R., Oh, S.J., Nam, K.R., Choi, H.D., Choi, J.Y., and Lee, H.J. (2020). Inhibition of Colony-Stimulating Factor 1 Receptor by PLX3397 Prevents Amyloid Beta Pathology and Rescues Dopaminergic Signaling in Aging 5xFAD Mice. Int J Mol Sci *21*.

Sos, K.E., Mayer, M.I., Takacs, V.T., Major, A., Bardoczi, Z., Beres, B.M., Szeles, T., Saito, T., Saido, T.C., Mody, I.*, et al.* (2020). Amyloid beta induces interneuron-specific changes in the hippocampus of APPNL-F mice. PLoS One *15*, e0233700.

Sosna, J., Philipp, S., Albay, R., 3rd, Reyes-Ruiz, J.M., Baglietto-Vargas, D., LaFerla, F.M., and Glabe, C.G. (2018). Early long-term administration of the CSF1R inhibitor PLX3397 ablates microglia and reduces accumulation of intraneuronal amyloid, neuritic plaque deposition and pre-fibrillar oligomers in 5XFAD mouse model of Alzheimer's disease. Mol Neurodegener *13*, 11.

Spangenberg, E., Severson, P.L., Hohsfield, L.A., Crapser, J., Zhang, J., Burton, E.A., Zhang, Y., Spevak, W., Lin, J., Phan, N.Y.*, et al.* (2019). Sustained microglial depletion with CSF1R inhibitor impairs parenchymal plaque development in an Alzheimer's disease model. Nat Commun *10*, 3758.

Spangenberg, E.E., and Green, K.N. (2017). Inflammation in Alzheimer's disease: Lessons learned from microglia-depletion models. Brain Behav Immun *61*, 1-11.

Spangenberg, E.E., Lee, R.J., Najafi, A.R., Rice, R.A., Elmore, M.R., Blurton-Jones, M., West, B.L., and Green, K.N. (2016). Eliminating microglia in Alzheimer's mice prevents neuronal loss without modulating amyloid-beta pathology. Brain : a journal of neurology *139*, 1265-1281.

Spies, P.E., Verbeek, M.M., van Groen, T., and Claassen, J.A. (2012). Reviewing reasons for the decreased CSF Abeta42 concentration in Alzheimer disease. Front Biosci (Landmark Ed) *17*, 2024-2034.

Stalder, M., Phinney, A., Probst, A., Sommer, B., Staufenbiel, M., and Jucker, M. (1999). Association of microglia with amyloid plaques in brains of APP23 transgenic mice. Am J Pathol *154*, 1673-1684.

Stevens, B., Allen, N.J., Vazquez, L.E., Howell, G.R., Christopherson, K.S., Nouri, N., Micheva, K.D., Mehalow, A.K., Huberman, A.D., Stafford, B.*, et al.* (2007). The classical complement cascade mediates CNS synapse elimination. Cell *131*, 1164-1178.

Stratoulias, V., Venero, J.L., Tremblay, M.E., and Joseph, B. (2019). Microglial subtypes: diversity within the microglial community. The EMBO journal *38*, e101997.

Szepesi, Z., Manouchehrian, O., Bachiller, S., and Deierborg, T. (2018). Bidirectional Microglia-Neuron Communication in Health and Disease. Front Cell Neurosci *12*, 323.

Takeuchi, T., Duszkiewicz, A.J., and Morris, R.G. (2014). The synaptic plasticity and memory hypothesis: encoding, storage and persistence. Philos Trans R Soc Lond B Biol Sci *369*, 20130288.

Tang, J., Huang, H., Patel, S., DeFelice, J., Zhou, Y., Gentleman, S., Matthews, P. (2021). Characterization of glial and neuronal pathology associated with Amyloid-beta proteins in an Alzheimer's Disease model. In British Neuroscience Association Festival of Neuroscience 2021 (UK).

Thal, D.R., Rub, U., Orantes, M., and Braak, H. (2002). Phases of A beta-deposition in the human brain and its relevance for the development of AD. Neurology *58*, 1791-1800.

Tondo, G., Iaccarino, L., Caminiti, S.P., Presotto, L., Santangelo, R., Iannaccone, S., Magnani, G., and Perani, D. (2020). The combined effects of microglia activation and brain glucose hypometabolism in early-onset Alzheimer's disease. Alzheimers Res Ther *12*, 50.

Toniolo, S., Sen, A., and Husain, M. (2020). Modulation of Brain Hyperexcitability: Potential New Therapeutic Approaches in Alzheimer's Disease. Int J Mol Sci *21*.

Torres, L., Danver, J., Ji, K., Miyauchi, J.T., Chen, D., Anderson, M.E., West, B.L., Robinson, J.K., and Tsirka, S.E. (2016). Dynamic microglial modulation of spatial learning and social behavior. Brain Behav Immun *55*, 6-16.

Town, T., Laouar, Y., Pittenger, C., Mori, T., Szekely, C.A., Tan, J., Duman, R.S., and Flavell, R.A. (2008). Blocking TGF-beta-Smad2/3 innate immune signaling mitigates Alzheimer-like pathology. Nat Med *14*, 681-687.

Tozzi, A., Sclip, A., Tantucci, M., de Iure, A., Ghiglieri, V., Costa, C., Di Filippo, M., Borsello, T., and Calabresi, P. (2015). Region- and age-dependent reductions of hippocampal long-term potentiation and NMDA to AMPA ratio in a genetic model of Alzheimer's disease. Neurobiol Aging *36*, 123-133.

Tremblay, M.E., Lowery, R.L., and Majewska, A.K. (2010). Microglial interactions with synapses are modulated by visual experience. PLoS Biol *8*, e1000527.

Tzioras, M., Daniels, M.J.D., King, D., Popovic, K., Holloway, R.K., Stevenson, A.J., Tulloch, J., Kandasamy, J., Sokol, D., Latta, C.*, et al.* (2019). Altered synaptic ingestion by human microglia in Alzheimer's disease. bioRxiv *ID795930*, 1-25.

Unger, M.S., Schernthaner, P., Marschallinger, J., Mrowetz, H., and Aigner, L. (2018). Microglia prevent peripheral immune cell invasion and promote an anti-

inflammatory environment in the brain of APP-PS1 transgenic mice. J Neuroinflammation *15*, 274.

Van Dam, D., and De Deyn, P.P. (2011). Animal models in the drug discovery pipeline for Alzheimer's disease. Br J Pharmacol *164*, 1285-1300.

Van Hoeymissen, E., Philippaert, K., Vennekens, R., Vriens, J., and Held, K. (2020). Horizontal Hippocampal Slices of the Mouse Brain. J Vis Exp, e61753.

Wake, H., Moorhouse, A.J., Jinno, S., Kohsaka, S., and Nabekura, J. (2009). Resting microglia directly monitor the functional state of synapses in vivo and determine the fate of ischemic terminals. J Neurosci *29*, 3974-3980.

Walsh, D.M., and Selkoe, D.J. (2007). A beta oligomers - a decade of discovery. J Neurochem *101*, 1172-1184.

Wang, Y., Cella, M., Mallinson, K., Ulrich, J.D., Young, K.L., Robinette, M.L., Gilfillan, S., Krishnan, G.M., Sudhakar, S., Zinselmeyer, B.H.*, et al.* (2015). TREM2 lipid sensing sustains the microglial response in an Alzheimer's disease model. Cell *160*, 1061-1071.

Wang, Y., Ulland, T.K., Ulrich, J.D., Song, W., Tzaferis, J.A., Hole, J.T., Yuan, P., Mahan, T.E., Shi, Y., Gilfillan, S.*, et al.* (2016). TREM2-mediated early microglial response limits diffusion and toxicity of amyloid plaques. J Exp Med *213*, 667-675.

Wegiel, J. (2001). The role of microglial cells and astrocytes in fibrillar plaque evolution in transgenic APPSW mice. Neurobiology of Aging *22*, 49-61.

Wegiel, J., Imaki, H., Wang, K.C., Wegiel, J., Wronska, A., Osuchowski, M., and Rubenstein, R. (2003). Origin and turnover of microglial cells in fibrillar plaques of APPsw transgenic mice. Acta Neuropathol *105*, 393-402.

Whyte, L.S., Hemsley, K.M., Lau, A.A., Hassiotis, S., Saito, T., Saido, T.C., Hopwood, J.J., and Sargeant, T.J. (2018). Reduction in open field activity in the absence of memory deficits in the AppNL−G−F knock-in mouse model of Alzheimer's disease. Behavioural Brain Research *336*, 177-181.

Wittenberg, R., Hu, B., Barraza-Araiza, L., and Rehill, A. (2019). Projections of older people with dementia and costs of dementia care in the United Kingdom, 2019–2040 (Care Policy and Evaluation Centre, London School of Economics and Political Science).

Wohleb, E.S. (2016). Neuron-Microglia Interactions in Mental Health Disorders: "For Better, and For Worse". Front Immunol *7*, 544.

Yang, T., Li, S., Xu, H., Walsh, D.M., and Selkoe, D.J. (2017). Large Soluble Oligomers of Amyloid beta-Protein from Alzheimer Brain Are Far Less Neuroactive Than the Smaller Oligomers to Which They Dissociate. J Neurosci *37*, 152-163.

Yang, Y., Kim, J., Kim, H.Y., Ryoo, N., Lee, S., Kim, Y., Rhim, H., and Shin, Y.K. (2015). Amyloid-beta Oligomers May Impair SNARE-Mediated Exocytosis by Direct Binding to Syntaxin 1a. Cell Rep *12*, 1244-1251.

Yeh, F.L., Hansen, D.V., and Sheng, M. (2017). TREM2, Microglia, and Neurodegenerative Diseases. Trends Mol Med *23*, 512-533.

Yuan, P., Condello, C., Keene, C.D., Wang, Y., Bird, T.D., Paul, S.M., Luo, W., Colonna, M., Baddeley, D., and Grutzendler, J. (2016). TREM2 Haplodeficiency in Mice and Humans Impairs the Microglia Barrier Function Leading to Decreased Amyloid Compaction and Severe Axonal Dystrophy. Neuron *90*, 724-739.

Zhan, Y., Paolicelli, R.C., Sforazzini, F., Weinhard, L., Bolasco, G., Pagani, F., Vyssotski, A.L., Bifone, A., Gozzi, A., Ragozzino, D.*, et al.* (2014). Deficient neuron-microglia signaling results in impaired functional brain connectivity and social behavior. Nat Neurosci *17*, 400-406.

Zhang, C., Browne, A., Divito, J.R., Stevenson, J.A., Romano, D., Dong, Y., Xie, Z., and Tanzi, R.E. (2010). Amyloid-beta production via cleavage of amyloid-beta protein precursor is modulated by cell density. J Alzheimers Dis *22*, 683-984.

Zhang, H., Wu, L., Pchitskaya, E., Zakharova, O., Saito, T., Saido, T., and Bezprozvanny, I. (2015). Neuronal Store-Operated Calcium Entry and Mushroom Spine Loss in Amyloid Precursor Protein Knock-In Mouse Model of Alzheimer's Disease. J Neurosci *35*, 13275-13286.

Zhao, R., Hu, W., Tsai, J., Li, W., and Gan, W.B. (2017). Microglia limit the expansion of beta-amyloid plaques in a mouse model of Alzheimer's disease. Mol Neurodegener *12*, 47.

Zhong, L., Xu, Y., Zhuo, R., Wang, T., Wang, K., Huang, R., Wang, D., Gao, Y., Zhu, Y., Sheng, X.*, et al.* (2019). Soluble TREM2 ameliorates pathological phenotypes by modulating microglial functions in an Alzheimer's disease model. Nat Commun *10*, 1365.

Zhou, T., Huang, Z., Sun, X., Zhu, X., Zhou, L., Li, M., Cheng, B., Liu, X., and He, C. (2017). Microglia Polarization with M1/M2 Phenotype Changes in rd1 Mouse Model of Retinal Degeneration. Front Neuroanat *11*, 77.

Zucker, R.S., and Regehr, W.G. (2002). Short-term synaptic plasticity. Annu Rev Physiol *64*, 355-405.